Electron traps in cadmium sulphide

Nicholas, K. H.

Electron Traps in Cadmium Sulphide

by

K. H. Nicholas B.Sc.

Presented in canditure for the degree of Doctor of Philosophy of the University of Durham.

August 1963

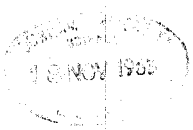

ACKNOWLEDGMENTS.

The author wishes to thank the Department of Scientific and Industrial Research for the financial assistance that made this work possible. He is indebted to Professor D. A. Wright for the use of his laboratory facilities; to Dr. J. Woods for his supervision and unfailing guidance; to Miss R. Noble, Mr. G. A. Marlor and Mr. L. Clark in connection with the crystal growing; to the Technical Staff of the Department of Applied Physics headed by Mr. F. Spence and to Miss A. Kelly who typed the thesis.

CONTENTS

INTRODUCTION

Photoconductivity can be defined as the increase in electrical conductivity of a substance when radiation is incident upon it. Photoconductivity was first reported by Willoughby Smith in 1873.[1] He observed a decrease in the resistance of a bar of selenium when it was illuminated. For many years selenium remained the most studied photoconductor though several other substances were found to possessthis property.

By 1925 photoconductivity was shown to be a bulk property of most materials, due to an increase in the number of charge carriers, rather than to a change in their mobilities. This was concluded from Hall effect measurements[2]. Other mechanisms are also possible, and in lead sulphide in particular it has been argued that the photoconductive effect in chemically prepared films might be due to inter-granular potential barriers. According to this mechanism an increase in conduction occurs when the barrier heights are reduced by illumination.[3]

Gudden and Pohl in the 1920's were the first to make systematic observations of the effect in cadmium and zinc sulphides.[4,5] They also showed that a decrease in resistance could be produced by radiation other than visible light. In particular they studied the effects of X-rays and high speed electrons. Bergmann and Hansler,[6] using the Dember

effect, showed that an increase in free electrons caused the increase in conductivity in cadmium sulphide. They also measured the wavelength of maximum sensitivity.

Since then considerable advances have been made in the understanding of photoconductivity. The importance of contacts was realised, and it was found necessary to assume that several carriers passed between the cathode and anode for each incident photon absorbed. To explain these results photocurrents were divided into primary and secondary currents. With primary currents, carriers are produced in the crystal and drift in the applied field towards the appropriate electrode and are either lost from the crystal or trapped within it. Carriers are not replenished via the electrodes. If "ohmic" contacts are applied to the crystal, a carrier can enter the crystal at one electrode for each carrier which leaves at the other (see section 1.16). The current is then a secondary current. The transit of carriers between the contacts will continue until a carrier is lost by recombination within the crystal. Ohmic contacts were used throughout the work described in this thesis.

The detailed properties of cadmium sulphide photoconductors are largely determined by various crystal defects. The study of these defects dominates the present investigations.

For many years the uses of photoconductors were limited by their comparatively low sensitivity. Photovoltaic cells in the optical region, photographic plates in the X-ray region, and thermal detectors in the infra red were superior to photoconductive cells. With improved performances there is an increasing number of applications for photoconductors. Cadmium sulphide is being developed for use in optical, X-ray, Gamma ray and electron beam devices. Thus cadmium sulphide could be used in image converters and intensifiers, and also in furnace controllers, relay circuits, electron and X-ray diffraction experiments for example.

Photoconductive cadmium sulphide cells are already available commercially. The main practical difficulties preventing a wide scale application of cadmium sulphide in many devices is its slow response at low light levels, coupled with the problem of preparing the material with controlled and reproducible properties. A proper understanding of electron trapping phenomena would greatly assist the resolution of both these problems. The work described in this thesis forms a contribution to this end.

CHAPTER I.

The Theory of Conduction in Crystals.

1.1 Introduction.

Though photoconductivity is not confined to crystalline solids most of the modern theoretical and practical developments have been made on such substances. It is necessary first of all therefore to understand conduction processes in a crystal.

A crystal is a periodic array of atoms or ions in three dimensions. The three main types of bonding holding the atoms in place are metallic, covalent and ionic.

Metallic bonding relies on a sea of shared electrons to bind the ions together. As a result a large increase in the number of free electrons would be needed to cause an appreciable fractional change in the number of free electrons, and consequently the conductivity. Due to the large concentration of free carriers and their ready access to unfilled energy bands (see section 1.8), free carrier absorption is the dominant mechanism of optical absorption in metals. This process is not associated with any appreciable change in conductivity.

With the lower electron densities which are possible with covalent and ionic bonded crystals, greater photoconductive sensitivity can be obtained. Photosensitivity is defined as the fractional change in conductivity per

unit incident photon. With covalent bonding one or more electrons are shared by an atom with other adjacent atoms forming paired bonding forces. In ionic bonding an atom loses one or more electrons while neighbouring atoms gain electrons. The Coulombic attraction between the charged atoms provides the basis of the bonding.

With all the kinds of bonding the repulsive forces between the atoms balancing those of attraction are due to the repulsion of the tightly bound electrons forming the ion cores. Most non-metallic crystals exhibit a mixture of part ionic-part covalent bonding. The proportion of ionic to covalent bonding present in a crystal can be determined by the effect of the electron clouds on X-ray diffraction experiments[7], piezoelectric effects[8] and luminescence[9]. A guide to the degree of ionicity can be obtained from the electronegativity (affinity for electron attraction) of the atoms in the crystal. The greater the difference between the electronegativity of the different elements present the more ionic the bonding. Perhaps the most satisfactory way of determining the degree of ionicity is to study Restrahlen absorption and apply the Szigeti relations.

1.2 Band Theory

To discover the distribution of allowed quantum mechanical electron states in a crystal within what is

called the 'one electron approximation' there are two methods of approach. The first is to consider an isolated atom and its electronic states and then study the effects of bringing other atoms into its vicinity to form a crystal. This is called the valence bond model and is based on the Heitler and London model of molecular bonding. The other method where the electrons are regarded as belonging to the whole crystal was proposed by Bloch[10].

1.3 The Valence Bond Model or Tight Binding Approximation.

Allowed energies for a completely free electron are given by the solution of the Schrodinger equation

$$\frac{-h^2}{8\pi^2 m} \times \nabla^2 \psi = E\psi \qquad (1.1)$$

where h is Planck's constant, m is the electron mass, E is its energy and ψ its wave function. $|\psi|^2 dv$ is the probability of finding an electron in the volume element dv.

It can be shown that E can have any value greater or equal to zero, under the necessary conditions that ψ is finite over all space and not identically zero, and that ψ and $\nabla\psi$ are continuous over real space.

If we consider the outermost electron bound to an isolated ion, the Schrodinger equation becomes

$$\frac{-h^2}{8\pi^2 m} \times \nabla^2 \psi - V(x,y,z) = E\psi \qquad (1.2)$$

where V(x,y,z) is the potential energy of the electron in

the field due to the nucleus. For a Coulomb field $V(x,y,z)$ is $\frac{Ze^2}{4\pi\epsilon_o r}$ where Z is the effective charge on the nucleus, e the charge on an electron, ϵ_o the permittivity of free space and r the distance of the electron from the nucleus. Solution of equation (1.2) leads to the result that the electron can take on only certain discrete values of energy E.

If we no longer consider the atom as isolated but consider two similar atoms gradually brought together, their electrical potentials will interact with each other and V in equation 1.2 will be modified. The electron energy levels in the isolated atoms are degenerate (indistinguishable). They are split by the interaction between the electron clouds as the atoms approach one another. The degree of splitting will depend on the degree of interaction. This will be increased by bringing the atoms closer, and the effect will be greatest for the outermost electrons of an atom which are nearest the equivalent electrons in the other atom and not electrically shielded from them. In this way the degeneracy will be removed.

If now we consider a regular lattice of atoms being brought together, the energy levels will show N fold splitting, where N is the total number of atoms. The splitting will increase as the atoms are brought together, and a band of levels will be set up, each band containing

a level corresponding to a discrete level in each of the separate atoms. The degree of splitting will be least for the innermost electrons in levels which are shielded from the corresponding electrons in neighbouring atoms. Figure 1.1 illustrates the effects on the discrete energy levels as the atoms approach each other.

This model assumes that an electron sees a potential due to all the other electrons, which together with the potential of the positive ions comprises a network of potential wells. This assumption is typical of the one electron approximation. The Bloch model is also based on the one electron approximation.

1.4 The Bloch or Weak Binding Model.

In this model the crystal is regarded as an infinite solid. First consider a one dimensional field with a periodic potential of period a. Then $V_x = V(x + ar)$ where r is an integer. Using Bloch's theorem the Schrodinger equation can be solved to give a solution

$$\psi_k(x) = U_k(x)\exp(ikx) \qquad (1.3)$$

where $U_k(x)$ is a periodic function of x with the same period a, and k is called the wave number vector. Wave packets comprised of waves of this form are required to describe localised electrons. The electron velocity is equivalent to a group velocity of the waves dw/dk where w is the angular frequency $w = 2\pi\nu$, ν is the wave

frequency. Then since $E_k = h\nu$ the electron velocity

$$\frac{dw}{dk} = \frac{2\pi}{h} \frac{dE}{dk} \qquad (1.4)$$

From equation 1.3

$$\psi(x) = U_k(x)\exp(\frac{-2\pi rx}{a}) \qquad (1.5)$$

$$\therefore \quad \exp i(k + 2\pi r/a)x = U_{k'}(x)\exp(ik'x)$$

where $k' = k + 2\pi r/a$, and $U_{k'}(x)$ is a periodic function of a. Thus E is a periodic function of k, and k can be restricted to the range $-\pi/a \leqslant k \leqslant \pi/a$. As V(x) is usually an even function of x only the $0 \leqslant k \leqslant \pi/a$ range need be used. This is called a reduced representation.

In three dimensions the same argument can be followed with the vector $\underline{r}$ replacing x and ra being replaced by $\underline{ra} = n_1a_1\underline{i} + n_2a_2\underline{j} + n_3a_3\underline{k}$ where n_1, n_2, n_3 are integers, a_1, a_2, a_3 are the lattice spacings and $\underline{i}, \underline{j}, \underline{k}$ are unit vectors in the directions of the crystal axes.

Thence the electron velocity

$$\underline{V} = \frac{2\pi}{h} \nabla_k E_k \qquad (1.6)$$

Kronig and Penney[11] discussed a model in which atoms formed square potential wells in a one dimensional lattice. They showed that the distribution of electron levels in energy:-

(1) Consists of a series of allowed energy bands separated by forbidden regions.

(2) The width of the bands increases with increasing crystal binding energy.

(3) The width of the band decreases with increasing electron binding energy.

(4) Discontinuities in allowed energy as a function of wave vector occur at $k = n\pi/a$ where $n = 1,2,3,.....$

(5) The reduced representation is applicable.

(6) The total number of wave functions (allowed energy levels) in each band is equal to the number of unit cells in the crystal, which is equal to the number of atoms, N, in the crystal.

The first, third and last conclusions had been arrived at in the tight binding theory. As the binding energy of a crystal increases with decreasing lattice spacing (2) also follows from the tight binding model. Figure 1.2 shows a reduced representation of a typical set of energy bands.

1.5 Number of Electrons per Level.

According to the concept of electron spin and the Pauli exclusion principle two electrons can occupy one quantum state as a result of the two allowed spin orientations. A level can therefore accommodate two electrons, and if there are N atoms in a crystal, the crystal can have 2N electrons in each band of levels.

1.6 Effective Mass

If an electric field F is applied to a crystal which contains a free electron, its subsequent motion in the field is described by the following equations

$$\frac{dE}{dt} = eFv = 2\left(\frac{eF\pi}{h}\right)\left(\frac{dE}{dk}\right) \qquad \therefore \frac{dk}{dt} = \frac{2\pi eF}{h}$$

where t is the time and e is the charge on an electron. From equation 1.4 it follows that the electron experiences an acceleration

$$\frac{dv}{dt} = \frac{2\pi}{h}\left(\frac{d^2E}{dk^2}\right)\left(\frac{dk}{dt}\right) = \left(\frac{4\pi^2 eF}{h^2}\right)\frac{d^2E}{dk^2} \qquad (1.7)$$

Comparison with the motion of a free particle of mass m according to classical mechanics where the acceleration equals eF/m leads to the definition of effective mass, m^x, of an electron, so that the classical formula can still be used to describe the motion of an electron in a solid. Thus

$$m^x = \frac{h^2}{4\pi^2 \frac{d^2E}{dk^2}} \qquad (1.8)$$

Clearly m^x varies with the wave vector $\underline{k}$. The concept of effective mass applies only to charge transport properties of the crystal. In three dimensions

$$\frac{1}{m^x} = \frac{4\pi^2}{h^2} \; \mathrm{grad}_k \; \mathrm{grad}_k \; E(k) \qquad (1.9)$$

where $\mathrm{grad}_k \mathrm{grad}_k E(k)$ is a tensor quantity rather than the scalar defined by equation (1.8).

For comparison with the classical case the effective number of free electrons will be $N_{eff} = \Sigma\left(\frac{m}{m^x}\right)$ summed over

all occupied states in the band. For a one dimensional lattice the number of levels is $a\delta k/2$ in the range k to $k + \delta k$ where a is the lattice parameter. With two electrons per level the effective number of electrons in the band is

$$N_{eff} = \left(\frac{8\pi am}{h^2}\right) \left(\frac{dE}{dk}\right)_{k = k_1}$$

Thus for a full band the effective number of conduction electrons is zero as dE/dk is zero at the top of the band, see figure 1.2. The maximum number will occur when $(dE/dk)_k$ is a maximum, that is at the point of inflection in the E(k) curve.

1.7 Positive Holes

The current, i, due to an electron passing from one contact to another separated by a distance d is given by its charge, -e, divided by the transit time, t_t.

$$i = -\frac{e}{t_t} = -\frac{ev}{d}$$

where v is the electron velocity. For all the electrons present

$$I = -\frac{e}{d} \Sigma v$$

with a full band this is zero and there is no conduction. If one electron is missing from an otherwise full band

$$I = -\frac{e}{d} \sum_{band}^{full} v + \frac{e}{d} Vp = \frac{e}{d} Vp$$

where Vp is the velocity the missing electron would have

had in the crystal. The resulting current is clearly equal to that carried by a positive charged electron with the same velocity as the missing electron would have had. This effective positive electron is referred to as a positive hole, or simply a hole.

1.8 Electric Conduction in Crystals.

In a full band no conduction can take place as the effective number of free electrons is zero. This means that the conductivity depends on the degree of filling of the uppermost bands with electrons. The diagrams in figure 1.3 show four simple cases.

In the first 1.3(a) the lower band is full and cannot lead to conduction. The next band is empty with a large energy gap between the two allowed bands. The effective number of free electrons in each band is zero and the substance is an insulator.

If, however, the energy gap between the bands is small, as in figure 1.3(b), at temperatures above absolute zero, some electrons will be thermally excited into the empty band from the highest full band, so that neither band will be completely full nor empty. Conduction will now take place in both bands. The temperature at which conduction will become appreciable depends on the energy gap and to a lesser extent on the mobilities and densities of states in the bands concerned. Where this temperature is

experimentally obtained the crystal is classed as an intrinsic semiconductor.

If a band is only half full as in the figure 1.3(c) conduction will be very high and the crystal behaves as a metal. With a three dimensional crystal lattice it is possible for two bands to overlap in energy. In this way a crystal which would have been an insulator or semiconductor becomes a metal. This is shown for the example of magnesium in figure 1.3(d).

These four examples comprise the main conduction mechanisms found in pure(intrinsic) crystals to which band theory can be applied.

1.9 Semiconductors.

The highest full band (at absolute zero) is called the valence band (V.B. in figure 1.3) and the lowest empty or partially empty band is called the conduction band(C.B. in figure 1.3). The energy gap between these bands is called the forbidden gap.

If there are localised energy levels between the conduction and valence bands due to impurities or imperfections in the crystal, they can affect the number of free electrons. In particular a centre with a level near the conduction band which is filled with an electron can lose it to the conduction band by thermal excitation and so help to increase conductivity. Such a level is called

a donor.

Similarly any centres with empty levels near the valence band will be capable of capturing electrons leaving a hole in the valence band. This type of centre is called an acceptor.

A crystal with donors and predominantly electron conduction is referred to as n-type. In a crystal in which holes are the main means of conduction the crystal is said to be p-type. If impurities are responsible for the production of donors and acceptors the specimen is called an impurity semiconductor.

1.10 Distribution of Electrons

In this discussion all energies are measured from the bottom of the conduction band unless otherwise stated.

Electrons are Fermions and obey Fermi-Dirac statistics. The probability of occupancy of an allowed quantum state at energy E is

$$F(E) = \frac{1}{e^{\frac{(E - E_F)}{kT}} + 1} \qquad (1.10)$$

where E_F is the Fermi energy, and is the energy at which the probability of occupancy is one half. If the density of ~~states~~ levels with energies between E and E + dE is Z(E)dE The density of electrons in the range E to E + dE will be N(E) = F(E)Z(E)dE. If the electrons are g-fold spin

degenerate, but obey Pauli's exclusion principle there will be g possible electron states per level.

For an intrinsic semiconductor the number of electrons in the conduction band with energies in the range E to E + dE is $n_e(E)dE = Z(E)F(E)dE = gN_c(E)F(E)dE$. Integrating over the conduction band, the total number of electrons in the conduction band becomes

$$n_i = g \int_o^{E_t} N_c(E)F(E)dE \qquad (1.11)$$

where E_t is the energy at the top of the conduction band. Similarly for holes in the valence band where the probability of occurrence of a hole is that of finding an empty electron state.

$$p(E)dE = gN_v(E)(1-F(E))dE \qquad (1.12)$$

and the total number of holes in a band

$$p_i = g \int_{Eb}^{-\Delta E} N_v(E)\,(1-F(E))dE \qquad (1.13)$$

where the energy is $-\Delta E$ at the top and E_b at the bottom of the valence band.

For spherical constant energy surfaces in $\underline{k}$ space

$$N_c(E)dE = 2\pi(2m_e)^{3/2}\left(\frac{h}{2\pi}\right)^{-3} E^{1/2}\,dE \qquad (1.14)$$

$$N_v(E)dE = 2\pi(2m_h)^{3/2}\left(\frac{h}{2\pi}\right)^{-3}(-\Delta E - E)^{1/2}dE \qquad (1.15)$$

where m_e and m_h are the effective masses of electrons and holes respectively.

Assuming that the carriers fill only states near the band edges so that the semiconductor is non-degenerate and $E - E_F \gg kT$, it follows that

$$n_i = 2\left(\frac{2\pi m_e kT}{h^2}\right)^{3/2} \exp\left(\frac{E_F}{kT}\right) = N_c \exp\left(\frac{E_F}{kT}\right) \qquad (1.16\ a\ \&\ b)$$

$$p_i = 2\left(\frac{2\pi m_h kT}{h^2}\right)^{3/2} \exp\left(\frac{-E_F + \Delta E}{kT}\right) = N_v \exp\left[\left(\frac{E_F + \Delta E}{kT}\right)\right.$$

$$(1.17\ a\ \&\ b)$$

For an intrinsic semiconductor $p_i = n_i$. Then from the above equations

$$E_F = -\frac{\Delta E}{2} + \frac{3kT}{4} \ln\left(\frac{m_h}{m_e}\right) \qquad (1.18)$$

In an impurity semiconductor the number of intrinsic carriers is small compared with those originating from impurities. For donors equation 1.16b still holds, as does equation 1.17b for acceptors

Thus $$n_p = N_c N_v \exp\left(\frac{-\Delta E}{kT}\right) = n_i^2 \qquad (1.19)$$

This means that the product np is independent of the addition of impurities (doping) but the depth of the Fermi level will vary, e.g. with variations of n in equation 1.19.

Often in an impurity semiconductor the impurities are closer than kT in energy to the edges of the bands in which they produce carriers. The reason for this can be

seen from a calculation of the ionisation energy of impurities assuming a hydrogen like model. Then the ionisation energy is given by

$$\delta E = \frac{13.6}{\epsilon^2} \left(\frac{m^*}{m}\right) \text{ eV}$$

where ϵ is the dielectric constant of the material and m^*/m the effective mass ratio. For high dielectric materials where the electron orbit is large the crystal dielectric constant can be used. The $1/\epsilon^2$ factor leads to the shallowness of impurities mentioned above for materials of large dielectric constant such as cadmium sulphide, germanium, silicon etc.

When the impurity depths are within an energy kT of the appropriate band nearly all the donors will have lost their electrons to the conduction band and all acceptors will have gained electrons from the valence band. The impurities are then said to be fully ionised or exhausted.

If N_d is the number of donors and N_a the number of acceptors and they are both fully ionised, then there will be $N_d - N_a + n_i$ electrons in the conduction band (If $N_d > N_a$). If n_i is negligible the crystal is n-type and $N_d - N_a = N_c \exp(E_F/kT)$ (1.20). For $N_a > N_d$ and n_i the crystal will be p-type and $N_a - N_d = N_v \exp(-(E_F + \Delta E)/kT)$. The donors and acceptors in such a crystal are said to be compensated.

If a semiconductor is at a sufficiently low temperature

the impurities will not be ionised and the carrier concentration is low. As the temperature is increased some impurities are ionised and the carrier concentration increases until they are all ionised. The density of carriers will remain constant as the temperature rises further. At higher temperatures the carrier concentration increases with temperature again due to intrinsic excitation across the band gap. Whether or not the intrinsic region is reached will depend mainly on the band gap, the magnitude of the impurity conductivity and the temperature attainable without destroying the crystal.

1.11 Defects

Any form of crystal defect or chemical impurity may produce an electron level in the forbidden gap of the crystal. One common method for producing n-type and p-type material is to use chemical doping.

If an atom in the crystal lattice is replaced by one of an element in the next higher group in the periodic table this new atom will have one too many electrons to satisfy bonding in covalent crystals. The extra electron, as a result, will only be loosely bound to the atom and the atom acts as a donor level. In this way the crystal can be made n-type. Atoms of elements more than one group higher may also be usable in this way forming double donors.

To produce p-type semiconductors a replacement atom

of an element one group lower than the original atom is used. The impurity is deficient of one electron for bonding requirements and readily accepts one. An element more than one group lower than the original one can also be used if it will go substitutionally into the lattice.

1.12 Relaxation Time and Carrier Mobility

Following Sommerfeld's theory of free electron conduction in metals, let the density of occupied states in thermal equilibrium in an element dp_x, dp_y, dp_z of phase space be $(2/h^3)F_o(p)dp_x dp_y dp_z$ where F_o is the Fermi distribution function and p the momentum. When an electric field E_x is applied in the x direction the distribution function is disturbed and the density of filled states per unit volume in the range dp_x, dp_y, dp_z becomes $(2/h^3)$ $F(p)dp_x dp_y dp_z$. Thence the current density is

$$J_x = -\left(\frac{2}{h^3}\right) e \iiint V_x (F-F_o) dp_x dp_y dp_z \qquad (1.21)$$

where V_x is the x component of velocity of the electrons with momentum p.

In the steady state the rate of change of distribution due to the field must be balanced by that due to scattering processes.

$$\left(\frac{\delta F}{\delta t}\right)_{coll} = - e E_x \left(\frac{\delta F}{\delta p_x}\right) \qquad (1.22)$$

It is assumed that a relaxation time (τ_r) can be defined such

that

$$\left(\frac{\delta F}{\delta t}\right)_{coll} = - \frac{(F - F_o)}{\tau_R} \qquad (1.23)$$

As the energy of electrons $E = (p_x^2 + p_y^2 + p_z^2)/2m$ and from equations 1.23 and 1.22

$$\frac{F - F_o}{\tau_R} = e \; V_x \; F_x \left(\frac{\delta F_o}{\delta E}\right) \qquad (1.24)$$

Here it is assumed that the applied field, E_x, is small and $\frac{\delta F}{\delta p_x}$ in (1.22) can be replaced by $\delta F_o / \delta p_x$. Substituting (1.24) in equation 1.21, and assuming τ_R is a function of energy but independent of direction it can be shown that

$$\frac{J_x}{E_x} = \sigma = - \frac{16\pi e^2 (2m)^{\frac{1}{2}}}{3h^3} \tau_F = \frac{ne^2 \tau_F}{m} \qquad (1.25)$$

where τ_F is the value of τ_R for the electron energy at the Fermi level.

The same result can be obtained from band theory with the effective mass replacing the electron mass. Then $\frac{e \tau_{Fe}}{m_e}$ is then referred to as the electron mobility (μ_e).
A similar result applies to semiconductors with degenerate statistics. In non-degenerate semiconductors the mobility depends on the mean relaxation time $\langle \tau \rangle$ averaged over all electron energies and $\mu = \frac{e\langle \tau \rangle}{m}$.

1.13 Scattering Processes.

The relaxation time depends on the mechanism of carrier

scattering. The carriers can be scattered by the lattice vibrations (acoustical and optical modes), charged or neutral impurities, and other carriers. Each mode of scattering leads to a different temperature dependence of mobility. In cadmium sulphide for instance the mobility varies as $T^{-\frac{3}{2}}$ indicating the dominant scattering mechanism is by longitudinal acoustical mode vibrations of the lattice, despite the ionic component in its bonding.

1.14 Conductivity.

The conductivity of a semiconductor is given by the sum of the electron and hole conductivities. Thus from equation 1.25 and equivalent equation for holes

$$\sigma = ne\mu_e + pe\mu_p \qquad (1.26)$$

where n and p are the densities of electrons and holes in the conduction band and valence band respectively.

1.15 The Hall Effect.

One method of evaluating mobilities is by measuring the Hall effect which can be done in metals as well as in semiconductors.

An electric field E_x is applied to the crystal in the x direction, as shown in figure 1.4. This causes a current density J_x to flow. A magnetic field B_z is applied in the z direction and contacts are placed on the crystal to measure a voltage in the mutually perpendicular y direction.

The carriers accumulate at the surface of the sample and set up an electric field E_y which opposes further deflection of carriers by the Lorentz forces. E_y is called the Hall field and $E_y = RJ_xB_z$ where R is called the Hall constant.

In equilibrium under open circuit conditions the force on charged carriers due to B_z in the y direction, must balance the force on the charges due to E_y. Thus with electrons in an n-type specimen

$$e\,E_y = -\,e\,B_z\,\bar{V}_x = -\,\frac{B_zJ_x}{n}, \text{ since } \bar{V}_x = \frac{J_x}{n_e}$$

where $\bar{V}_x$ is the average drift velocity.

If Θ is the Hall angle, that is the angle between the resultant electric field direction and the applied electric field then

$$\tan\Theta = \frac{E_y}{E_x} = -\,B_z\mu_e \qquad (1.27)$$

It follows therefore that the Hall voltage

$$V_H = \frac{IB_z}{tne} = -\,B_z\mu_eE_xw \qquad (1.28)$$

where I is the total current, t is the crystal thickness, w is the width of the specimen and n is the electron density. This simple analysis also shows that $R = -\,1/ne$.

The analysis assumes among other things that τ, the relaxation time is independent of electron velocity. Since this is only true of metals and degenerate semiconductors a factor r varying between 1 and 2 should be introduced.

As a result the Hall constant becomes

$$R = - r/ne \qquad (1.29).$$

The product of Hall constant and electrical conductivity, $R\sigma$, is defined as the Hall mobility, since

$$R\sigma = r\mu \qquad (1.30).$$

It must be remembered that the Hall mobility is not necessarily equal to the conductivity mobility, μ. The factor $r = \frac{\langle \tau^2 \rangle}{\langle \tau \rangle^2}$, where the averaging is done over all electron energies, and cannot be calculated unless the scattering mechanism is known.

Carrier mobilities can also be determined in experiments in which the drift velocities of either minority or majority carriers are measured.[12] The drift mobility is not necessarily identical with either the Hall or conductivity mobility, except in highly extrinsic, trap free material.

1.16 Electrical Contacts.

In order to measure the electrical properties of a crystal it is usually necessary to make electrical contacts to the crystal. Consider a crystal in vacuo. The diagram in figure 1.5 shows the energy level situation at the surface. ϕ_s is the work function and χ_s the electron affinity. The depth of the Fermi level below the conduction band

$$E_F = \phi_s - \chi_s \qquad (1.31)$$

Placing metal contacts on the crystal may form a metal semiconductor barrier. Ignoring surface effects on the semiconductor, the situation for an n-type semiconductor

is shown in figure 1.5 for contacts formed with metals of (a) high and (b) low work function ϕ_m.

If with the metal and semiconductor separated the Fermi level in the metal is lower than in the semiconductor, i.e. $\phi_m > \phi_s$, electrons will diffuse from the semiconductor into the metal. This process continues until a large enough field is set up to prevent any further net diffusion of electrons. The loss of electrons from the semiconductor produces an insulating layer near the surface of the semiconductor containing a net positive charge due to ionised donors. Such a layer is called a depletion layer. The contact possesses rectifying properties and may well limit the current flow when an electric field is applied.

When the Fermi level of the isolated metal is higher than that of the semiconductor i.e. $\phi_m < \phi_s$ no barrier is set up and the admission of electrons into the crystal is governed by the bulk properties of the crystal. Such a contact is called an ohmic contact and is suitable for the determination of the bulk properties of the semiconductor. On this argument the condition for ohmic contacts is that the work function of the metal must be less than that of the semiconductor.

For a p-type semiconductor where an ohmic contact requires the injection of holes into the semiconductor the work function of the metal must be greater than that

of the semiconductor. If it is not a depletion layer forms a barrier and complicates the measurement of bulk properties.

1.17 Surface States.

Even if the work function of the contact metal is matched to the semiconductor, crystal surface states may introduce a barrier and a depletion layer. An oxide film on the surface is one of several such sources of surface states. If the film is conducting it will effectively short circuit the bulk of the crystal. In the absence of an oxide layer, surface states known as Tamm levels which are due to the disruption of the periodicity of the crystal lattice can still act as acceptors on an n-type semiconductor or donors on a p-type semiconductor. In this way an 'inversion' barrier is set up at the surface.

Surface properties are affected by mechanical damage as well as mechanical and chemical polishing techniques. Diffusion of the metal of the contact into the crystal can also assist the production of an ohmic contact if this tends to form a localised n^+ or p^+ conducting region at the contact, or if it neutralises the surface states. Clearly a metal that tends to form an insulating layer if it diffuses in, is unsuitable as a contact as it will always form a surface barrier.

CHAPTER 2.

Optical Properties

2.1 Radiation

Electromagnetic radiation of frequency ν can be regarded as composed of photons with energy $E = h\nu$ (2.1) where h is Planck's constant. Except for very high energy photons ($\sim$ 1MeV) where the Compton effect is appreciable, each photon gives up all its energy in one interaction. Electromagnetic radiation can be absorbed by semiconductors in several ways. Considering absorption by electrons only, the radiation can be absorbed by inner shell electrons, valence band electrons, free carriers, and electrons bound to localised impurity and defect centres (see figure 2.2).

Inner shell electrons require large photons to excite them to higher empty states as the lower energy states are full. This is beyond the range of optical or near optical radiations and will not be considered in detail.

In a semiconductor free carrier absorption will take place at low photon energies. At higher photon energies, usually near the visible region, absorption by excitation of electrons from the valence to the conduction band is possible. Absorption involving exciton states near the conduction band occurs at slightly lower energies.

The selection rules of quantum mechanics require that

the wave vector $\underline{k}$ must be conserved in absorption for the process to be allowed and have a high probability of taking place. As the wave vector of radiation in the near visible region is small compared with that of electrons in the crystal, the wave vector of the electron must be almost unchanged by its transfer from the valence to conduction band when a photon is absorbed. Since most energy level diagrams of semiconductors have the wave vector plotted as the abscissa and the energy as the ordinate, transitions of constant wave vector are called vertical transitions.

If the structure of the energy bands is simple and the minimum of the conduction band and the maximum of the valence band occur at $\underline{k} = 0$ (see figure 2.1(a)), the minimum energy transition of an electron between the bands is vertical (direct) and there is a sharp increase in absorption when the photon energy is increased through this minimum value. If the bands are such that the minimum energy transition between the bands is not vertical there will still be an increase in absorption as the photon energy passes through this minimum value (see figure 2.1 (b)). This is because non vertical (indirect) transitions have a finite probability of occurring. Momentum is conserved by the emission or absorption of a phonon. When the energy of the incident photon is increased still more there will

be a further increase in absorption when direct transitions at $\underline{k} = 0$ can occur.

The density of phonons increases with temperature, causing absorption by indirect transitions to increase. If a phonon is absorbed in the interaction the threshold for band to band absorption can be slightly less than the indirect forbidden gap, by an amount equal to the phonon energy. The situation theoretically is further complicated by the fact that indirect or direct transitions can be "allowed" or "forbidden" depending on the parity of the initial and final wave functions. This however is important quantitatively rather than qualitatively.

Direct or indirect transitions from the valence to conduction band due to irradiation will both lead to an increase in conductivity as a result of the increased concentration of free electrons and holes in the conduction and valence bands. This is the first stage of the photo-conductive process.

Absorption by free carriers in a band is limited by the width of the band and usually only occurs at wavelengths greater than 1 micron. The absorption increases with wavelength and depends strongly on the density of free carriers. It is only significant for semiconductors with high carrier concentrations. Optical absorption in crystals can be complicated by the production of excitons. Excitons can

be regarded as electrons orbiting round atoms in the tight binding model or electrons orbiting round holes in the loose binding model. Thus they can be regarded as electrons occupying bound excited states. The excitation levels form a hydrogen like series just below the conduction band (see figure 2.2). Though an electron in such a state does not contribute to conduction directly, the electrons can be excited thermally into the conduction band if the temperature is high enough for lattice vibrations to supply the exciton binding energy. In this way exciton absorption can lead at sufficiently high temperatures to an increase in the free electron concentration and thus to photoconductivity.

Turning to impure crystals, electrons in bound impurities can be excited to higher levels within the impurity or into the conduction band. Excitation within a bound impurity cannot lead to photoconductivity. If the electron, however, is excited into the conduction band it can then contribute to conduction. Impurity absorption appears either as a continuum or a separate absorption band on the long wavelength side of the absorption edge. The higher the crystal temperature the nearer the spectrum approaches to a continuum. This effect is due to phonon interactions.

2.2 Continuity Equations

Once an electron-hole pair has been produced the

carriers diffuse by thermal agitation, and are influenced by any fields present. Thus we have the continuity equations describing production, diffusion, drift in an electric field, and recombination of electrons and holes.

$$\frac{\delta p}{\delta t} = q - \left(\frac{p-p_o}{\tau}\right) - \frac{1}{e}\,\mathrm{div}\,\bar{J}^{+} \qquad (2.2) \qquad \frac{\delta n}{\delta t} = q - \left(\frac{n-n_o}{\tau}\right) + \frac{1}{e}\,\mathrm{div}\,\bar{J}^{-} \qquad (2.3)$$

$$\bar{J}^{+} = e\mu_h p\bar{E} - eD_h\,\mathrm{grad}\,p \qquad (2.4)$$

$$\bar{J}^{-} = be\mu_h n\bar{E} + beD_h\,\mathrm{grad}\,n \qquad (2.5) \qquad \bar{J} = \bar{J}^{+} + \bar{J}^{-} \qquad (2.6)$$

$$\mathrm{div}\,\bar{E} = e\,(\Delta p - \Delta n)/\epsilon \qquad (2.7)$$

where p stands for the density of holes and n for the density of electrons; o as a suffix denotes the density in the absence of illumination. q is the rate of generation of electron-hole pairs by the illumination, τ is their free life time and $\bar{J}^{+}$ and $\bar{J}^{-}$ are the hole and electron currents, μ_h is the hole mobility and D_h is the hole diffusion constant. $b = \frac{\mu_e}{\mu_h} = \frac{D_e}{D_h}$ is the mobility ratio and μ_e and D_e are the electron mobility and diffusion coefficient. $\bar{E}$ is the applied electric field and ϵ the dielectric constant of the material, $\Delta p = p - p_o$, $\Delta n = n - n_o$ and the net current $\bar{J} = \bar{J}^{+} + \bar{J}^{-}$.

For a more conducting type of semiconductor it can be assumed that at any point there is charge neutrality.

$\therefore \Delta p = \Delta n$ and in the low illumination case $\Delta p \ll p$ or n.

Then $$\frac{\delta \Delta p}{\delta t} = q - \frac{\Delta p}{\tau} + D \text{ div grad } \Delta p + \mu \bar{E} \text{ grad } \Delta p \quad (2.8)$$

where the ambipolar diffusion constant $D = D_e \left[\frac{n_o + p_o}{bn_o + p_o}\right]$ and effective mobility $\mu = \mu_e \left[\frac{p_o - n_o}{bn_o + p_o}\right]$.

For more insulating materials where charge neutrality does not occur but assuming intrinsic material and a small signal, the equations are again soluble. For irradiation with I photons per unit area of a solid with a coefficient of absorption K, the rate of generation of electron-hole pairs assuming one pair is produced per absorbed photon is $q = KI \exp(-Ky)$ (2.9) where y is the depth below the surface on which the radiation is incident.

From the above assumptions and assuming $\frac{e\mu_h n_i}{\epsilon D_h}$ is very large it follows that

$$\frac{L^2 d^2 \Delta p}{dy^2} - \Delta p = KI\tau \exp(-Ky) \quad (2.10)$$

where $L = (D\tau)^{\frac{1}{2}}$ is the ambipolar diffusion length. If we assume that the surface recombination velocity (s) is the same for both the front and back surfaces $J^+ = -es\,\Delta p$ at the top surface ($y = 0$) and $J^+ = es\,\Delta p$ at the bottom ($y = t$) surface, and

$$\Delta p = P_1 \cosh \frac{y}{L} + P_2 \sinh \frac{y}{L} + \frac{KI\tau \exp(-Ky)}{1 - K^2L^2}$$

$$0 < y < t \quad (2.11)$$

2.3 Photoconductivity in Intrinsic Semiconductors.

If electrodes are applied to the specimen in the x

direction (see figure 2.3) and the distribution of carriers in the y direction is neglected then the photocurrent for a crystal with thickness t is

$$\Delta i = \frac{e(b+1)\mu_h}{t} E_x \int \Delta p dy. \quad \text{Let} \quad \Delta P = \int_o^t \Delta p dy, \text{ then } \Delta i \propto \Delta P.$$

from equation (2.11) if $\alpha = \frac{\tau s}{L}$,

$$\Delta P \frac{(1-K^2L^2)}{\tau} = 1 - \exp(-Kt) + KL \left(\alpha \cosh \frac{t}{L} + \sinh \frac{t}{L} - \alpha\right) x$$

$$\frac{(KL-\alpha)\exp(-Kt)-KL-\alpha}{(1+\alpha^2)\sinh \frac{t}{L} + 2\alpha \cosh \frac{t}{L}} \qquad (2.12)$$

Now consider some special cases.

(1) If surface recombination is neglected

$$\Delta P = \tau(1 - \exp(-Kt)) = \tau(\text{total absorbed quanta})$$

(2) For thick samples where $t \gg L$ and if $\alpha \sim 1$, (i.e. the recombination velocity is small) and $KL\alpha \gg 1$ (surface absorption of the radiation), as $K \to \infty$

$$\Delta P_\infty = I \tau_{eff} \qquad (2.13)$$

where $\frac{1}{\tau_{eff}} = \frac{1}{\tau} + \frac{s}{L}$

(3) If α and t are large but $\alpha \ll KL$ e.g. at short wave lengths $\Delta P = \frac{I\tau}{\alpha}$

(4) If $\alpha \to \infty$ i.e. total recombination at the surface

$$\Delta P(1-K^2L^2)/I\tau = 1-KL \tanh \frac{t}{2L} - (1+KL \tanh \frac{t}{2L})\exp(-Kt) \quad (2.14)$$

This has a maximum $\Delta P_{max} = 0.51\tau I$ at $KL = 0.54$ for $\frac{t}{L} = 5$

K and therefore KL can be varied by varying the wavelength of radiation falling on the crystal. In practice

the surface recombination velocity can be obtained from equations (2.13) and (2.14) since $\frac{\Delta P_{max}}{\Delta P_{\infty}} = 0.51\alpha$ (2.15) (see figure 2.4).

Photoconductivity in certain more insulating semiconductors will be discussed later in this thesis.

2.4 Dember Effect.

Another effect observed in a homogeneous semiconductor is the Dember effect.[13] The crystal is illuminated as shown in the diagram in figure (2.5).

Radiation strongly absorbed at the surface of the crystal produces electron-hole pairs. The electrons and holes in the absence of a field diffuse away from the surface. The rate of diffusion for electrons is different from that for holes and as a result charge separation will take place in the crystal. This sets up an e.m.f. opposing the charge separation and as a result equilibrium is established with a voltage difference between the top and bottom surfaces of the crystal.

With surface absorption of the radiation, charge neutrality, and a thick specimen, the open circuit voltage $V_D = \frac{(b-1)\, q\, L}{\mu_h (n_o + p_o)(1+\alpha_1)}$ (2.16) where α_1 refers to recombination in the illuminated surface.

As might have been expected the voltage is proportional to the difference between the mobilities of electrons and holes, to the rate of excitation and the ambipolar diffusion

length. The voltage also decreases for higher surface recombination velocities and the $(n_o + p_o)$ factor means that the Dember voltage is highest in an intrinsic sample (as $n_o p_o = n_i^2 = \text{constant}$).

2.5 Photoelectromagnetic Effect (P.E.M.)[14,15,16].

A magnetic field is applied to the crystal parallel to the surface of the crystal in say the z direction. Illumination is still considered to be incident normally on the crystal surface and to be absorbed at the surface. Electrons and holes will diffuse away from the surface as in the Dember effect, but now they will be deflected in the magnetic field as shown in the diagram in figure (2.6). As the electrons and holes are deflected in opposite directions a voltage will be set up between contacts at the ends of the crystal in the x direction. For a low density of photoexcited carriers, and a small magnetic field, the diffusion lengths of the carriers must be equal as no current flows in the y direction $\therefore L_n = L_p = \sqrt{\tau D}$.

If the contacts are short circuited the charge transfer per electron-hole pair between the contacts is $\frac{(D\tau)^{\frac{1}{2}} e(\tan \theta_n + \tan \theta_p)}{X}$ where θ_p and θ_n are the Hall angles for the holes and electrons and X is the length of the specimen between the electrodes. The short circuit current is then

$$J_x = q\ e\ (D\tau)^{\frac{1}{2}} B(\mu_n + \mu_p) = q\ B[2kT\tau e\mu_n\mu_p(\mu_n + \mu_p)]^{\frac{1}{2}} \qquad (2.17)$$

and the open circuit voltage $E_{oc} = \left(\frac{qB}{tn_i}\right)(D\tau)^{\frac{1}{2}}$ (2.18)

2.6 Photo Hall Effect.[17]

This is the Hall effect measured under illumination where most of the carriers are photoexcited. It has been found that under illumination the mobility varies with illumination and temperature in certain substances including cadmium sulphide. The variation of temperature and illumination changes the occupancy and so charges in the defects. In this way the scattering and so mobility is altered. Interpretation of the results can give information about the parameters of defects in the crystal.(see figure 2.7).

2.7 Photovoltaic Effect.

If the crystal is not homogeneous but contains a p-n junction, photo generated minority carriers will diffuse across the junction. This causes a photovoltage to develop between contacts on the crystal. The process is called the photovoltaic effect. It can be used to convert radiant energy into electrical energy. This is utilised in solar batteries.

2.8 Luminescence.

If an electron is excited to a higher energy state it may return to the original state with the emission of radiation. According to the Franck-Condon principle (see figure 2. 8) electron excitation transitions take place so rapidly (10^{-13}sec) that the transitions are vertical (constant

radius) and the high frequency dielectric constant must be used for calculations concerning the transition. With the electron in the excited state relaxation of the system takes place more slowly. During this process the effective dielectric constant is the low frequency one. The relaxation process involves a loss in energy by the electron to the lattice. As a result the energy emitted when de-excitation takes place is less than that absorbed during excitation. This is the explanation of Stoke's law of fluorescence. The Franck-Condon principle also shows that optical and thermal activation energies will be different in crystals with any component of ionicity in their bonding.

If the emission follows the excitation within 10^{-8} seconds it is called fluorescence but if the emission is delayed longer than this it is called phosphorescence. 10^{-8} secs is chosen somewhat arbitrarily as a dividing line. It is of the order of the life of an excited state of an isolated atom.

In some phosphor systems excitation can take place from one state to another within an impurity atom and not contribute to conductivity. On the other hand in many phosphors including the sulphide types an electron can (1) be excited from an impurity level into the conduction band, (2) from the valence band to an impurity level or (3) from the valence to conduction band. Each of these processes

can lead eventually to luminescent emission accompanied by photoconductivity. In general however radiative emission must take place before non-radiative thermal de-excitation can occur. It is necessary therefore for the electron to have only a short life time in the excited state and this leads to low photoconductive sensitivity.

As most non-radiative de-excitations are at least partly thermal they tend to increase with temperature causing the luminescence to decrease with increasing temperature. This is known as thermal quenching. For some radiative recombination processes, however, thermal excitation from a metastable excited level is needed prior to emission. This causes a peak in emission at a particular temperature as the crystal temperature is increased. Study of these peaks will be discussed later under thermal glow curves.

CHAPTER 3.

Cadmium Sulphide and Related Compounds.

3.1 Semiconductors and Semi-insulators.

Several assumptions made in chapter 2 during the discussion of photoconductivity in semiconductors will no longer be valid when they are applied to semi-insulators such as undoped cadmium sulphide.

One such assumption is that charge neutrality will be observed in the crystal as far as free carriers are concerned. This is not true for a semi-insulator. One reason for this is that the number of trapping states is appreciable compared with the number of free carriers in the crystal in the dark. Another result of the large number of traps is to make the life time of holes in the valence band different from that of electrons in the conduction band. It was assumed for semiconductors that under illumination the increase in the concentration of carriers would be much less than thermal equilibrium concentrations of carriers in the crystal. In semi-insulators the density of photoexcited carriers is often several orders of magnitude greater than the dark density of carriers.

These differences between semi-insulators and semiconductors though they affect several formulae derived above for semiconductors do not affect the basic concepts of energy

bands, mobility, effective mass or ohmic contacts in semi-insullators. The differences in properties of semi-insulators alter the various effects discussed above for intrinsic semiconductors quantitatively rather than qualitatively. For this reason only photoconductivity, and to a lesser extent luminescence, will be considered again specifically in semi-insulators.

Semi-insulators are characterised by having forbidden band gaps of 1.5 - 5.0 eV and dark conductivities of the order of 10^{10} ohm. cm. Cadmium sulphide will be taken as an example because the practical work discussed in this thesis is confined to this substance.

3.2 Cadmium Sulphide.

Cadmium sulphide is a II-VI compound since cadmium is an element in group II of the periodic table and sulphur is an element of group VI. In general the compounds of zinc and cadmium with sulphur, selenium and tellurium are wide band gap semiconductors or semi-insulators. The values of band gap[18] of these compounds are shown in figure (3.1).

Cadmium sulphide has a forbidden band gap width of 2.4 eV.[19] Substitutional impurities from group IIIB and VII can increase the conductivity from 10^{-10} mhos/cm. for pure specimens, to 1mho/cm. for highly doped specimens ($\sim$ 10 parts per million). Donors lie within 1/10 eV of the bottom of the conduction band and are therefore fully ionised at

room temperature. Acceptor levels are usually of the order of 1 eV[20] above the valence band and as a result the concentration of free holes is very small. Thermoelectric and Hall effect measurements on highly doped samples always indicate n-type conduction. The mobility of free electrons is about 200 cm/volt. sec.[21] at room temperature and is proportional to $T^{-\frac{3}{2}}$[22] where T is the absolute temperature. This would suggest that the acoustic mode lattice vibrations provide the dominant scattering mechanism which is surprising in a compound with an appreciable polar component in its bonding. The refractive index of cadmium sulphide is 2.6[23] at a wavelength of 5000Å and its low frequency dielectric constant is 11.6.[24] The effective electron mass as measured by cyclotron resonance has several values[25] associated with ellipsoidal equal energy surfaces. An average value of electron effective mass from these measurements and others on the thermoelectric power of cadmium sulphide is 0.25 m.

3.3 General Assumptions.

Unless otherwise stated certain conditions will be assumed throughout the rest of this thesis.

(1) It is assumed that the crystals under investigation are homogeneous. This was /~~confirmed~~ implied for crystals on which the work for this thesis was done, by the agreement between calculated energy depths from formulae both involving and independent of the crystal dimensions.

(2) Ohmic behaviour at the contacts with no rectification is assumed. The fact that these properties were experimentally observed in the crystals measured also lent support to the assumption that the crystals were homogeneous.

(3) It is assumed all crystal are n-type. This is almost certainly correct as p-type cadmium sulphide is only found in highly doped specimens, where the conduction probably occurs in an impurity band.[26]

(4) Non degenerate statistics are used. This follows from the low density of electrons involved, compared with the density of states in the conduction band.

(5) Measurements made are of steady state values except for, (i) the thermally stimulated measurements which are taken at a constant rate of rise of temperature and (ii) the measurements on the rate of rise and decay of photocurrent. To some extent this assumption is only valid by definition of steady state values since in some cases general deterioration of the crystal took place at an appreciable rate. "Steady state" values were usually taken as those reached within a few minutes, except under low illuminations.

(6) Values of various constants in cadmium sulphide were taken from the scientific literature and will be discussed where they are used.

(7) The effects of free holes are neglected except where they are specifically discussed. No evidence of conduction by holes was found during the present measurements.

(8) The energy levels of electron capturing defects (traps) are assumed to lie in groups at discrete energy depths. Evidence of this will be introduced later.

(9) The effects of the anisotropy of the crystal are neglected. These are not in general important. This was demonstrated by the experimental fact that the energy depths of defect levels are independent of the direction of current flow.

(10) A single value scalar effective mass is assumed. This is incorrect in cadmium sulphide,[25] but as an average value was used, errors involved in its use can be neglected, particularly as most calculations did not require its absolute value.

(11) The crystal stays electrically neutral. That is no appreciable build up of space charge occurs in the crystal. The net electric charge, including charges in defect centres, is zero for the whole crystal. This does not necessarily mean that the number of free carriers of each sign in the crystal is the same. It does mean that an electron must have been removed from the crystal at the positive (anode) contact to

the crystal before another electron can enter the crystal at the negative (cathode) contact.

(12) Direct recombination between an electron in the conduction band and a hole in the valence band is negligible except under intense illumination when all other recombination paths are saturated.

(13) It is assumed that the density of carriers freed by illumination is much greater than the dark density of carriers.

(14) The density of defect states is assumed to be greater than the density of carriers except under intense illumination.

(15) As band theory is used the substance is assumed to be a single crystal.

(16) Other specific assumptions for different theories will be introduced as the theories are developed.

CHAPTER 4.

Photoconductive and Luminescent Processes in Cadmium Sulphide and Related Materials.

4.1 Excitation Processes.

As stated earlier when light shines on a crystal the density of carriers increases and as a result the conductivity increases by $\Delta\sigma = e(\Delta n\mu_n + \Delta p\mu_p)$ (4.1) where $\Delta n(\Delta p)$ is the increase in the density of electrons (holes) in the conduction (valence) band. The density of carriers is the product of their rate of excitation and their average life time as free carriers. Part of the time between the excitation of a carrier and its capture by a centre leading to its recombination is spent in traps with energy levels which lie near the band in which the carrier is mobile. As a result the time during which the carrier is free to participate in conduction, which time is called the free carrier life time, is less than the time between its excitation and recombination (the excited life time). As the carrier can remain in a recombination centre for a long time before recombining with a charge of the opposite sign both the excited life time and the free life time for electrons differ from the corresponding values for holes.

When appreciable numbers of traps are present the decay time of the photocurrent will be determined by the rate of thermal excitation of carriers from the traps and

will not be equal to any of the life times mentioned above.

If the illumination creates f electron-hole pairs per unit time per unit volume

$$f\tau_{nc} = \Delta n, \quad f\tau_{pc} = \Delta p,$$

$$\therefore \quad \Delta\sigma = f\, e(\mu_n \tau_{nc} + \mu_p \tau_{pc}) \qquad (4.2)$$

where τ_{nc} and τ_{pc} are the free life times of electrons and holes. In highly photosensitive cadmium sulphide virtually all the photocurrent is carried by electrons so that $\Delta p = 0$, and

$$\Delta\sigma = fe\mu_n \tau_{nc} \qquad (4.3)$$

This is a result of the presence of fast hole trapping states which are described below.

4.2 Definition of Photoconductivity and Photoconductive Gain.

Photoconductivity can be defined as the increase in electrical conductivity per unit change of intensity of illumination, or more conveniently as the increase in conductivity per electron-hole pair produced by the radiation.

Photoconductive gain can be defined for the crystal as a whole by the expression

$$\frac{\Delta I}{e} = GF \qquad (4.4)$$

where ΔI is the total increase in the photocurrent and F is the total rate of production of electron-hole pairs in the whole crystal. Thus G times the rate of photon production equals

the number of carriers passing through the crystal per second. From equation (4.3) $G = \tau_{nc} \mu_n \frac{V}{L^2}$ (4.5) but since the electron transit time $T = \frac{L^2}{\mu V}$ (4.6), $G = \frac{\tau_{nc}}{T}$ (4.7).

Highly photo-sensitive cadmium sulphide is characterised by having such a low dark current that even at comparatively low illuminations the dark current is small compared with the photocurrent ($\sim$ 1000x dark current for 20ft. candles). Both the dark conduction and photoconduction are controlled by defects and impurities.

4.3 Lattice Defects and Impurities.

For a defect or impurity to be important in the electronic processes taking place in a semi-insulator it must have an electronic energy level or levels situated between the conduction and valence bands. It is assumed that the relaxation energy after such a centre captures or emits an electron is small.

With a defect which has an empty electronic level, and can therefore capture a free electron, a cross section S $cm.^2$ can be defined such that the rate of capture of carriers is $SvnN_t$, where v is the average thermal velocity of the electrons and n and N_t are the densities of free electrons and empty defect states respectively. Thus S has the dimensions of area. The cross section is a mean cross section to take account of the distribution of carrier velocities. v is therefore the mean thermal velocity of the carriers.

Thus $v = \left(\frac{8kT}{\pi m^*}\right)^{\frac{1}{2}}$ (4.8) where m^* is the effective mass of the carriers. It should be noted that S can vary with velocity and consequently with the temperature.

4.4 Fermi Levels.

The rate of thermal release of carriers from defects with levels at a depth E eV below the conduction band is $n_t \nu \exp(^{-E}/_{kT})$ (4.9) where n_t is the density of filled defects, and ν is called the attempt to escape frequency. If the Fermi level coincides with the position of the defect levels their occupancy will be $\frac{1}{2}$ and $n_t = n$. In equilibrium the rate of filling and the rate of emptying of the defects must be equal. Substituting these conditions in equation (4.9) and comparing the resulting equation with that defining the Fermi level $(\frac{n}{N_c} = \exp(^{-E}/_{kT}))$ (4.10) it can be seen that $N_c \nu = \frac{\nu}{s}$ (4.11) where N_c is the effective density of states in the conduction band.

The Fermi level is defined on the basis of thermal generation and recombination in the dark where thermal equilibrium prevails. When optical excitation forms an additional means of increasing the free electron population the Fermi level as defined by equation (4.10) is raised towards the conduction band. A Fermi level defined in this way for non-thermal equilibrium conditions is called a quasi or steady state Fermi level. Similarly there will be more holes in the valence band. Under illumination the electron

and hole quasi Fermi levels must separate from the equilibrium Fermi level in a photoconducting semi-insulator.

4.5 Demarcation Levels.

What part a defect centre plays in recombination or trapping processes depends on the position of its energy level within the forbidden gap, and on the temperature. For example, a defect that has captured an electron can either return the electron to the conduction band, or the electron can recombine with a hole from the valence band. If the electron is re-excited into the conduction band by a thermal process the defect is called a trap, but if recombination with a free or trapped hole takes place the defect is called a recombination centre.

In steady state conditions an electron demarcation level can be defined in such a way that an electron occupying a defect level at that depth has equal probabilities of thermal excitation to the conduction band and of recombining with a hole. Then $\nu e \exp(\frac{-E_{Dn}}{kT}) = p \nu Sp$ where Sp is the capture cross section of the defect for holes. Thence $E_{Dn} = E_{Fn} + kT\ln\frac{Sn}{Sp}$ (4.12) where E_{Dn} is the electron demarcation level and Sn and Sp are the cross section of the defects for holes and electrons. Similarly the hole demarcation level $E_{Dp} = E_{Fp} + kT\ln\frac{Sn}{Sp}$ (4.13) where E_{Fp} is the hole Fermi level.

As the demarcation levels are separated from the quasi Fermi levels by an amount which is independent of the illumination, they approach the conduction and valence bands as the illumination increases, in the same way as the quasi

Fermi levels. The diagram in Figure (4.1) shows the position of the quasi Fermi and demarcation levels under illumination.

The ideas developed above, which are due to Rose,[27] show that most of the levels above the electron demarcation level will act as traps, and those below the hole demarcation level will act as hole traps. Levels lying between the electron and hole demarcation levels will act predominantly as recombination centres for electrons and holes.

~~The demarcation level is sharply defined in cadmium sulphide crystals. 99% of the levels which lie 0.1 eV above the demarcation level will act as traps. The remaining 1% act as recombination centres.~~

4.6 Sensitisation Centres.

The free life time of a carrier is the reciprocal of the probability of capture of the free carrier by a recombination centre. Consider one set of recombination centres (type I in Figure (4.2)) with equal probability for capture of holes and electrons. In the absence of any other recombination centres the free life time for electrons will be $\tau_{nc} = \frac{1}{N_R v S_n}$ (4.14) where N_R is the density of such centres.

Consider what happens when a second set of recombination centres are introduced (type II in figure (4.2)) with the same hole cross section as type I centres but much smaller subsequent cross section for electron capture. The holes will accumulate in these type II centres so that there will

be an excess of electrons elsewhere in the crystal. The excess electrons will tend to fill the type I centres. As a result the number of empty type I centres will be much decreased. Recombination via the type II centres, called the sensitising centres, is slow because of their very small cross section for electrons. The high photosensitivity of cadmium sulphide is due to the presence of such sensitising centres, which increase the free carrier life time by rendering type I centres ineffective.

4.7 Infra Red and Thermal Quenching

The levels associated with the sensitising centres in cadmium sulphide are only about 1 eV [28] above the valence band. If the crystal is simultaneously illuminated with infra red radiation with photon energy equal to the energy difference between the levels in the sensitising centres and the valence band, electrons are excited into these centres from the valence band. The holes produced recombine with the electrons already occupying the type I centres. This means that the electron occupancy of type I centres is reduced so that they are more effective in promoting free electron capture. This results in a decrease in photosensitivity. The infra red radiation is said to have quenched the photoconductivity.

As it requires only a relatively small amount of energy to excite electrons from the valence band into type II centres, the excitation can take place thermally at high temperatures.

Thus the photosensitivity will also decrease at elevated temperatures. This is called thermal quenching. Another way of looking at thermal quenching is to observe that when the crystal is heated the hole Fermi level rises above the levels in the sensitising centres, which means they can no longer retain an excess of holes. As a result there will no longer be excess electrons to fill the type I centres and the sensitivity falls.

If the hole demarcation level lies just above the levels in the sensitising centres in the dark, the centres will act as traps. On illuminating the crystal more carriers are produced, and the hole Fermi level and hole demarcation level will fall. As the illumination is increased the demarcation level will pass through the sensitising centres which will start to act as sensitising centres instead of traps. In other words the illumination has brought about an increase in sensitivity. Photoconductivity will therefore increase faster than linearly with illumination in this region. This phenomenon is called supralinearity.

4.8 Conductivity and Photosensitivity.

"Pure" ~~stoichiometric~~ cadmium sulphide is highly resistive and a poor photoconductor. When donors are introduced in the form of a group IIIB or group VII substitutional impurity or of excess cadmium, photoconductivity increases much faster than the dark conductivity at first producing a

good photoconductor (see figure 4.3). As the donor density is increased further the rise in photoconductivity becomes less and less rapid while the dark current begins to increase more rapidly. The sensitivity falls as a result and highly doped specimens are poor photoconductors.

When semiconducting cadmium sulphide is compensated by increasing the concentration of acceptors by introducing copper or excess sulphur, the conductivity of the specimen decreases again. To begin with the dark conductivity decreases more rapidly than the photoconductivity and as a result the crystal becomes highly photosensitive again at about the same dark conductivity as in the absence of compensation.

The density of impurities necessary to produce these large changes of conductivity is of the order of parts per million.

When doping with a halogen and copper for example charge compensation takes place. That is the density of copper ions accepted into the lattice is approximately equal to the density of halogen ions in the lattice. As the copper acceptor levels are separated from the valence band by an energy which is much larger than that between the donors and the conduction band, more of the donors are ionised than the acceptors. As a result there is an effective excess of donors in the crystal. This is the situation which

prevails in the highly photosensitive region for temperatures between that of liquid air and 100°C. It is within this range of temperatures that the crystal is most likely to be studied and used.

4.9 Types of Defects.

The most important types of defects found in a crystal are (1) impurities (substitutional and interstitial), (2) vacancies in the lattice, (3) constituents of the compound held interstitially in the lattice, (4) complexes of all these and (5) other lattice defects such as dislocations.

4.10 Impurities.

Group III or group VII elements can substitute for cadmium and sulphur respectively to form donors. Indium and Chlorine are examples of elements commonly used.

Group I or group V elements replacing cadmium or sulphur in the lattice act as acceptors. Copper is typical of this kind of impurity though there is some evidence that it can enter the crystal non-substitutionally.

The impurities may either be added to the crystal by growing the crystal in a vapour containing the impurities, or it can be added later using a diffusion technique.

4.11 Vacancies.

Cadmium and sulphur vacancies will be produced during the growth of the crystal and the density of vacancies of one constituent can be increased by heating the crystals

in the vapour of the other. Vacancies can capture either electrons or holes thus varying their charge, but cadmium vacancies generally act as acceptors, while sulphur vacancies act as donors.

If an impurity is introduced substitutionally into the crystal lattice replacing an atom or ion of different charge some form of "charge compensation" is necessary to maintain electro-neutrality. The compensation may take several forms (1) by another impurity of opposite effective charge, (2) by vacancies or (3) by production or capture of free carriers. A fourth method of compensation equivalent to the last mentioned above is that an ion of one of the constituents of the crystal changes its valency. This is called controlled valency compensation.

Kroger and Vink and van den Boomgaard[65] have used the methods of physical chemistry to predict the density of defects in cadmium sulphide. They assume the distribution of atomic defects is determined by the growth conditions, and that the electrons which are mobile down to room temperature are distributed over the various defects according to Fermi Dirac statistics.

4.12 Photoconductive Decay.

If the intensity of illumination incident on a photo-

conductive cadmium sulphide crystal is changed, transient conditions prevail until a new equilibrium conductivity is reached. The steady state theory discussed above is based on the assumption of thermal equilibrium between the defect states and the conduction bands and this does not necessarily apply under transient conditions.

Consider the results of suddenly removing a source of illumination from the vicinity of a cadmium sulphide crystal. If there were no states above the electron demarcation level in the dark, the decay will be that of free electrons in the conduction band recombining with holes trapped in recombination centres. If however there are defect levels above the electron demarcation level these defects will act as electron traps, and after the illumination is switched off electrons will be excited thermally into the conduction band from traps. The lifetime of an electron in a trap is usually much greater than the free electron life time, so that the decay in photoconductivity is wholly or partly determined by the excitation from these traps, depending on the magnitudes of the two lifetimes.

Care should be taken in using the concept of the demarcation level under transient conditions as it only has full meaning under steady state conditions. As the energy depth of the demarcation level depends on the ratio of hole to electron cross sections of the defects, its position will

be different for different sets of defects. The difference in energy depth of the various demarcation levels due to the cross section factor is usually small and the qualitative arguments used are still valid.

Although the decay time at low illuminations does not yield information on the free electron life time it can give information about the trapping or recombination levels. This is especially true if there are defect levels near the electron demarcation level in the dark causing a slow decay. At high illuminations, however, the traps are saturated and the initial decay gives the free carrier lifetime.

4.13 Thermally stimulated currents.

If a crystal is cooled to 77°K the Fermi levels and demarcation levels approach their free carrier bands. In cadmium sulphide at 77°K only the very shallow electron levels will lie above the electron Fermi level.

If the crystal is strongly illuminated electrons excited into the conduction band will be captured by the defects. As most levels lie below the electron Fermi level at low temperature, electrons will not be returned to the conduction band when the light is removed. If the crystal is heated in the dark, electrons will be thermally excited out of deeper and deeper defect levels as the Fermi

level falls.

Any set of defects with levels at a certain depth will empty their electrons into the conduction band in a burst around a particular temperature. Each electron excited into the conduction band from a defect takes part in conduction until it is annihilated by recombination. As a result a plot of current against temperature will show peaks corresponding to discrete sets of defect levels. The curve is called a thermally stimulated current or conductivity glow curve.

If the electrons excited into the conduction band recombine with holes radiatively a plot of radiation emission against temperature also will show peaks corresponding to the discrete sets of levels. The curve is then called a thermal glow or thermoluminescent curve. From the peaks, information about defect levels and sometimes the recombination centres can be obtained.

Of the two methods the thermal glow technique was first used in 1930 by Urbach[29] for crystals of sodium chloride. Randall and Wilkins[30] rediscovered and applied the method to various phosphors in 1946. The thermally stimulated current measurements were made soon after this.

Conductivity and thermal glow curves are closely connected quantitatively as well as qualitatively. At

any temperature T during a glow curve run, let there be n_c electrons cm^{-3} in the conduction band with a free life time of τ_{nc}. If the luminescent efficiency is unity the thermoluminescent emission (in photons/unit time cm^3) $L(T) = n_c/\tau_{nc}$. The conductivity $\sigma(T) = n_c e\mu = L(T)\tau_{nc}\, e\mu$. Thus the shape of the peaks differ only insofar as $\mu\tau_{nc}$ varies with temperature.

4.14 Comparison of Photoconductive Decay and Thermally Stimulated Current Measurements.

Evaluation of the properties of defects from measurements of decay of photoconductivity and thermally stimulated current curves, both rely mainly on the thermal emptying of defect levels. During this emptying the electron Fermi and demarcation levels move from one position to another. The depth of the electron Fermi level under steady state conditions is $E_{Fn} = kT \log_e(\frac{N_c}{n})$ where T is the absolute temperature, and n is the density of free electrons. The movement of the Fermi level on changing the incident illumination is caused by the variation in the density of free electrons. As the term $\frac{N_c}{n}$ is of the order of

10^{10} for photosensitive cadmium sulphide, the variation of the Fermi level for a variation of several orders of magnitude in illumination is only of the order of 0.1eV in 0.5eV depth. Some information can be obtained about levels above the electron Fermi level from the decay measurements, but the range of information obtainable at fixed temperature is limited. Using the thermally stimulated current measurements in conjunction with decay measurements at various temperatures, a much wider range of information can be obtained.

4.15 Luminescence.

As mentioned earlier there are two basic types of phosphor in which luminescence occurs.

In the first type (type I), excitation of the electron and the emission of radiation as the electron returned to a lower energy state is confined to a localised impurity. No free carriers are produced during the process and there is no photoconductive effect.

In the second type (type II), the excited state is not localised and free carriers are produced directly or indirectly causing an increase in conductivity. The photoconductivity produced is often small since to obtain high luminescent efficiency the recombination must occur before

the thermal, non-radiative, decay can occur.

With most activators cadmium sulphide is a phosphor of type II and shows several phenomena analogous to photo-conductive phenomena. Excitation from the traps responsible for long decays in photoconductivity can also lead to phosphorescence if the recombination process of the free electrons is radiative.

The connection between conductivity and thermal glow curves was described in section (4.13) There are however several differences between the luminescent and photoconductive glow mechanisms. As the processes in competition with luminescent recombination are mainly thermal in origin, the luminescent efficiency usually falls more sharply as the temperature rises than does the photoconductive gain.

In type I phosphors luminescent emission can be obtained without any accompanying increase in photoconductivity. In these phosphors a thermal glow experiment will detect centres which cannot be detected from measurements of the electrical properties of the crystals.

The energy of the photons absorbed in excitation and emitted in recombination processes can be determined from measurements of the wavelengths of the radiation involved. In addition, the infra-red quenching spectrum has been used to find the energies involved in the quenching processes. Little agreement has been found so far between the values

of defect parameters in cadmium sulphide calculated from measurements on the luminescent and photoconductive properties. This may be due to incorrect evaluation of defect level energy depths, or because of inherent differences either in the centres involved or the energies lost in relaxation processes.

Better agreement between values of energy depth and capture cross section determined from luminescent and photoconductive measurements may be apparent when more carefully calculated values have been obtained.

CHAPTER 5.

Evaluation of Defect Properties

5.1 Introduction.

The information concerning defects which it is necessary to know in order to exercise some measure of control over the properties of photoconducting cadmium sulphide is (1) the nature of a defect (2) the density of such defects (3) the electron (and hole) capture cross sections of the defect and (4) the position of the defect energy levels within the band scheme.

(1) The nature of defects.

If the defect is an impurity, chemical methods would appear to be the best form of detection. In cadmium sulphide however the impurity densities in undoped specimens are so low or of such a nature (e.g. oxygen) that spectro-chemical analysis is not often of great value.

The best methods of investigating defects are probably those which involve changing the composition in a controlled way, followed by measurements of the change in electrical and optical properties. The composition of a crystal can be changed by diffusing in an impurity, or by heating in an excess of cadmium or sulphur vapour to produce non-stoichiometric crystals. Radiation damage, particularly electron bombardment or γ-radiation, can be used to produce

vacancies and interstitials.

The situation is still complicated as an impurity or vacancy can exist in different states of ionisation within the crystal. Measured values of the energy depths and cross sections of the defect levels can then help to distinguish between the possible atomic configurations which constitute the defect. In this context electron-spin resonance measurements would be invaluable.

(2) Density of Defects.

The chief problem in evaluating the density of defects from photo conduction measurements lies in the difficulty of determining either the gain or the free carrier life time in the crystal.

The total charge passing through the crystal due to the excitation of one electron is, according to equation (4.7),

$$\Delta q = \frac{\tau_{nc}^{e}}{T} = Ge \qquad (5.1)$$

where τ_{nc} is the electron life time and T is its transit time from cathode to anode. Thus the area under a photo-conductive decay curve, or a thermally stimulated current curve, plotted against time is

$$\int_{t_1}^{t_2} I\,dt = N_t \Delta q = N_t Ge \qquad (5.2)$$

where I is the current excess over the dark current, and N_t

is the number of electrons released from traps between times t_1 and t_2.

To use this method to obtain the density of defects it is necessary to determine the gain. Also a value for gain is needed if calculations based on the steady state photoconductivity are to be used. The transit time can be obtained from equation (4.6) if the applied voltage, crystal thickness and electron mobility are known.

The free electron life time is often difficult to measure and depends on the temperature and intensity of illumination, although the variation due to the latter is often ignored. One of the more common methods of determining the life time is to measure the initial decay when illumination of high intensity is removed. Under these conditions the defect levels capturing electrons are saturated and the initial decay gives the free electron life time directly. This needs intense ($\sim$ 1000ft. candles) illumination. The variation of life time with illumination intensity can then be determined from the photocurrent versus intensity curve. Another equivalent method is to study the rate of response to pulsed illumination on top of a high intensity bias illumination. As an alternative two other methods can be used to avoid the necessity of measuring the life time of free electrons directly.

(a) Under certain circumstances after illuminating

a crystal at low light levels, the rise of photocurrent with time shows plateaux(see figure 5.1) of constant current before the steady state conductivity is reached.[31] Each plateau is due to the filling of a set of electron trapping defect levels. The length of a plateau is approximately equal to the number of defect levels divided by the rate of production of electron-hole pairs. If one electron-hole pair is produced by each incident photon the number of defects can be estimated. Values of the energy depth of the various trapping levels are not obtainable with this method.

(b) The second method of evaluation of defect densities without the direct measurement of gain does permit a correlation with energy depths of trapping levels obtained from thermally stimulated current curves. The crystal is illuminated using a source of low variable intensity with wavelength close to the absorption edge. The same voltage is applied to the crystal as in the thermally stimulated current measurement. The intensity of illumination is adjusted, until under steady state conditions, the current flowing through the crystal is the same as the thermally stimulated current at that temperature. This is repeated over the temperature range of the peak being studied.

The rate of excitation of electrons into the conduction band by the incident illumination must then be the same as

that when the thermally stimulated current is flowing. Assuming one electron is excited per incident photon, the rate of excitation of electrons into the conduction band can be calculated, and by integrating this value over the thermally stimulated current peak the number of defects releasing electrons can be found.

The main disadvantage of this method is that the time taken to reach steady state conditions at the low light levels required is several hours. This means it would take about 24 hours to find the correct illumination and this would have to be repeated at numerous temperatures, each temperature being held constant to within a degree or two. Such an experiment is obviously impracticable.

An approximate method has been used in which the light intensity required to produce a current equal to one half the maximum current of the thermally stimulated peak under investigation[32] is measured at the temperature of the current maximum. A value of gain can be calculated from such measurements. This value of gain is assumed to be constant throughout the range of temperatures covered by the thermally stimulated current curve ($\sim 50^{\circ}$). This assumes that the gain is independent of temperature and illumination. For the gain to be constant the photoconductivity must be temperature independent, and proportional to the intensity of illumination over a range of about $50^{\circ}C$. This is unlikely

under conditions where a set of defects change from acting as recombination centres to acting as traps.

(3) Electron Capture Cross Section for Carriers.

The calculation of cross sections using measurements of photoconductive decay and thermally stimulated currents will be discussed when those phenomena are described in detail in chapter 7.

If the plateau of constant current in the low light level photoconductive rise measurements mentioned above, is at a measurable current value, the cross section of the defect levels being filled with electrons can be calculated. It is necessary to know the constant value of the photocurrent, the voltage applied, the crystal dimensions and the intensity of illumination. In the present measurements the plateau often formed before the photocurrent had risen to a value which was measurable with the apparatus available ($\frac{1}{100}$ μA with 100v applied to the crystal).

Analysis of the Photo Hall [17] measurements leads to a value of the product of the density of defects and their cross section as shown in figure (2.7). These results can be combined with the values of the density of defects obtained from other methods to give the cross section values.

Knowledge of the value of the cross section for electron capture is important as it gives a strong indication of the charge on the defect. The cross section is about

10^{-12} cm^2 for strong coulomb attraction, 10^{-15} cm^2 for a neutral centre and 10^{-22} cm^2 for strongly repulsive centres.[33]

(4) Energy depth of defect levels.

Thermally stimulated current curves and photoconductive decay curves which are among the commonest methods used to obtain the energy depth of defect levels will be discussed in chapter (6). Other direct current methods which can be used employ a knowledge of the position of the electron Fermi level under conditions where:- (1) sharp changes in photoconductivity occur with variations in temperature[34], (2) supralinearity is observed,[34] and (3) rapid changes in mobility of electrons as a function of temperature are detected by photo Hall measurements.[17]

Energy depths can also be calculated from luminescent decay and glow effects, as well as from emission and excitation spectra. Spectral response and optical absorption can only be used to measure defect level energy depths at high defect densities in cadmium sulphide.

CHAPTER 6.

Evaluation of Defect Parameters using Thermally Stimulated Current Curves

6.1 Introduction

The technique of determining thermally stimulated currents has already been described, but before discussing the quantitative analysis of the curves obtained, it will be convenient to define various experimental values used in calculations on a single current peak. See the diagram in figure 6.1. The crystal is heated so that the temperature increases linearly with time at a rate $\beta\,^{o}K$ per second. The temperature at the current maximum, I^{*}, is $T^{*o}K$. The temperature at which the current is half its maximum value on the low temperature (rise) side is T' and on the high temperature (fall) side is T".

6.2 Discussion of Assumptions Common to all Theories.

In addition to the assumptions listed in section (3.3) additional ones are made in all the theories used to evaluate thermally stimulated current curves. The assumption that the defect levels form groups at a few discrete depths in the energy level scheme is extended to assume there is a negligible relaxation energy when the defect captures an electron. That is the energy released when the defect captures an electron from the conduction band is approximately

equal to the energy absorbed from the lattice when the electron is excited back into the conduction band.

Defect-defect interactions and band to band recombinations are neglected, except for the latter at high intensity illumination. It is assumed further that there are no discontinuous changes in mobility, gain, or effective mass, as the temperature is increased through the range of the thermally stimulated current peak. In some circumstances these last assumptions might be expected to lead to some inaccuracy but with the small temperature ranges involved ($\sim 50^{o}$) no inconsistency was observed. This fact is inferred from the agreement between values of energy depths of defect levels obtained by measurements on different parts of each peak. The results will be described in chapter 11.

If there is an appreciable dark current it is assumed that it has the same value at any particular temperature whether there is a thermally stimulated current present or not. This may be incorrect due to the defect levels being full during the thermally stimulated current run, but empty during any subsequent measurement in the dark when the defects will act as recombination centres. There was one sample in which the dark current was different after a thermally stimulated current curve had been obtained. In this crystal new donors were created by heating the crystal

above 50°C in the dark.

An important assumption is that the electron recombination life time is small compared with the time for appreciable changes to occur in the rate of thermal excitation of electrons into the conduction band. That is the shape of the thermally stimulated current curve is controlled by the variation in the rate of excitation of electrons to the conduction band, and is not distorted by the finite time they spend there.

The rate of rise of temperature during a thermally stimulated current run is maintained constant. This simplifies the theories used to analyse the peaks as well as being comparatively easily obtainable experimentally. It is also assumed that the temperature is constant throughout the crystal. Any temperature differences present within the crystal would distort the shape of the peak and produce thermoelectric e.m.f.'s. No such e.m.f.'s were found in the absence of an applied field.

6.3 General Theory.

Consider a crystal containing one set of shallow trapping levels, one set of deep traps, and one set of recombination centres. Let us examine the effect of the shallow traps on the thermally stimulated current curve produced by electrons being emptied from the deep traps.

Much less energy is required to excite an electron into the conduction band from shallow trapping levels than from the deeper levels. As a result the rate of thermal excitation into the conduction band of electrons retrapped in the shallow levels is much faster than the rate at which the deeper traps are emptied. Thus the position, shape and size of the current peak associated with the deeper traps are independent of the shallow trapping levels.

If an electron is excited into the conduction band it may be captured by a recombination centre, or recaptured by one of the set of defects being emptied. Three cases are often considered:-

(1) The probability of capture of a free electron by a recombination centre is much greater than that of recapture by one of the defects being emptied. These conditions lead to monomolecular kinetics.

(2) Electrons in the set of traps being thermally emptied are excited into, and recaptured from, the conduction band several times before they finally disappear via the recombination centres. This situation is usually referred to as fast retrapping.

(3) There is equal probability of an electron in the conduction band being captured by a recombination centre or one of the traps being emptied. This situation was first studied by Garlick and Gibson[35].

The cases (2) and (3) both lead to bimolecular kinetics.

If there is a set of traps (a) with large cross sections which is empty before the traps (b) being studied start emptying, then electrons excited from (b) will be captured immediately by the large cross section traps (a). If the time between the excitation of an electron from (b) and its annihilation via a recombination centre is increased by the presence of the large cross section traps (a), the shape of the thermally stimulated peak will be affected. The shape of the curve will be characteristic of the large cross section traps (a) under fast retrapping conditions.

The origin of the terms monomolecular and bimolecular kinetics arises from the similarity between the equations for the rates of rise and decay of photoconductivity which they lead to, and the rate equations obtained for the monomolecular and bimolecular chemical reactions of gases. The fast retrapping situation is also bimolecular, but will be referred to here as the case of fast retrapping to avoid confusion.

6.4 Kinetics of Recombination

The probability of an electron at depth E being thermally excited into the conduction band is given by

$$f = \nu e^{-E/kT} \qquad (6.0)$$

where ν is the attempt to escape frequency. If there are n_t filled traps at any instant the rate of excitation of electrons into the conduction band is

$$\frac{dn}{dt} = -\frac{dn_t}{dt} = n_t \nu e^{-E/kT} \qquad (6.1)$$

The change in conductivity due to the resulting thermally excited electrons is $\Delta\sigma = \frac{dn}{dt} e \tau \mu$ where τ is the free electron life time. With a constant heating rate

$$dT = \beta\, dt \qquad (6.2)$$

where dT is the rise in temperature and dt is the increase in time.

(i) Monomolecular kinetics. Here retrapping is neglected. From equations 6.1 and 6.2, and neglecting the temperature variation of $N_c v S$ where S is the capture cross section for electrons

$$\frac{dn_t}{dt} = n_{to} \exp(-E/kT) \exp\left[-\int \frac{\nu}{\beta} \exp(E/kT)dT\right] \qquad (6.3)$$

where n_{to} is the density of traps which are filled initially, and

$$\Delta\sigma = n_{to} e\mu N_c v S \tau \exp(-E/kT) \exp\left[-\frac{N_c v S}{\beta} \exp(-E/kT)dT\right] \qquad (6.4)$$

since $\nu = N_c v S$ (equation 4.11).

Equation (6.4) is equivalent to the expression obtained by Randall and Wilkins [30] to describe thermo-luminescent emission. It will be referred to in this thesis as the Randall and Wilkins equation.

(ii) Bimolecular kinetics. In this case it is assumed that there is equal probability of capture of electrons by the

recombination centres and the "emptying" centres. The expression for thermally stimulated conductivity under these conditions[35] is

$$\Delta\sigma = \frac{e\mu\tau n_{to}^2 \exp(-E/kT)}{N_t\left[1 + \frac{n_{to}}{N_t}\int_{T_o}^{T}\frac{N_c v S}{\beta}\exp(-E/kT)dT\right]^2} \qquad (6.5)$$

where n_{to} is the density of defects initially full and N_t is the total density of these defects.

The monomolecular case (i) leads to an asymmetrical peak with a slower rise of current on the low temperature side, than fall on the high temperature side. The bimolecular case (ii) leads to a more symmetrical peak showing the same asymmetry but to a lesser extent.

Certain features are common to peaks with either of the recombination mechanisms

(1) For the same electron capture cross section of the defects, heating rate and density of filled defects, the temperature at which the current is a maximum is proportional to the energy depth.

(2) For a constant density of filled defects with levels at a constant energy depth, the temperature of the maximum current varies slowly if the cross section or heating rate is altered.

(3) The area under the current peak is proportional to the

density of defects which were filled initially. However for bimolecular kinetics the shape of the peak is affected by the initial occupancy of the defects.

(4) The initial rise of current with temperature as the defects begin to empty is given (i) for monomolecular kinetics by

$$\Delta\sigma = N_{to} N_c v S \mu \tau e \exp(-E/kT) \qquad (6.6)$$

and (ii) for bimolecular kinetics by

$$\Delta\sigma = \frac{n_{to}^2}{N_t} N_c v S \mu \tau e \exp(-E/kT) \qquad (6.7)$$

Thus if the set of traps is saturated with electrons by the illumination at low temperature there will be no difference between the equations for the different kinetics.

Although there are some similarities between the glow curves which result from the two types of kinetics considered so far ((1) to (4) above), there are some differences even if the trap parameters and heating rate are the same.

(1) The bimolecular curve is more symmetrical and wider than the monomolecular one (see figure 6.2).

(2) With bimolecular kinetics the shape of the curve and the temperature of the maximum current T^* vary as the initial occupancy of the traps is varied. With mono-

molecular kinetics $T^{\star}$ and the shape of the curve are independent of the initial degree of trap filling.

The probability of thermal excitation of an electron from a trap, f, is given by

$$f = N_c v S \exp(-E/kT) \qquad (6.8)$$ (see equation 6.0).

The rate of change of the density of occupied traps with monomolecular kinetics (no retrapping) and monomolecular recombination is

$$\frac{dnt}{dt} = - n_t f \qquad (6.9)$$

The density of free electrons n during the decay is $- \frac{dnt}{dt} \tau$. If τ is constant, then

$$n = n_{to} \tau f \exp(-ft) \qquad (6.10)$$

i.e. the decay is exponential with time constant equal to 1/f.

When retrapping is significant only a fraction of the excited electrons will return to recombination centres. The rest will be retrapped. The probability that a free electron will recombine is a function of the total cross section of the recombination centres for electron capture divided by the total cross section for recombination centres plus that for empty traps. Thus the fraction of free electrons which recombine and are anihilated is $\frac{S_R N_R}{S_R N_R + S(N_t - n)}$, where S_R and

N_R are the cross section and density of recombination centres. Under these conditions the rate of trap emptying is

$$\frac{dn}{dt} = - \frac{S_R N_R n_t f}{S_R N_R + S(N_t - n_t)} \qquad (6.11)$$

If $S_R = S$, $N_R = n + n_t$, $n >> n_t$, and the traps are initially saturated then

$$n = \frac{N_t \tau f}{(1 + ft)^2} \qquad (6.12)$$

Equation (6.12) represents a typical bimolecular type of photoconductive decay.

CHAPTER 7.

Discussion of the Methods of Evaluating Glow Curves.

7.1 Initial Rise Methods.

(i) Garlick and Gibson.[35]

The equations (6.6) and (6.7) for the initial rise of thermally stimulated current under monomolecular and bimolecular conditions are both of the form $\Delta\sigma = \text{const.} \exp(-E/kT)$. Since the conductivity is proportional to the current under ohmic conditions, $\Delta I \propto \exp(-E/kT)$, where ΔI is the thermally stimulated current. Thus for both monomolecular and bimolecular kinetics a plot of $\log_e \Delta I$ against $1/T$ for the initial rise of the thermally stimulated current peak should yield a straight line of slope $-E/k$, where E is the depth of the trapping levels.

This method of calculating energy depths will be referred to as the Garlick and Gibson method and the value so obtained will be denoted by E_{GG}. The method is also valid for fast retrapping kinetics. Haake[36] has investigated how far up the rise side of the peak the equations are valid.

An extension of this theory to allow for the temperature variation of the cross section of the defects leads to the equation

$$\log \Delta I = b \log T - E/kT + \text{constant} \qquad (7.1)$$

where the cross section

$$S = S_o T^{(2-b)} \qquad (7.2)$$

S_o and b are constants (see next section).

The extra term bln(T) decreases the value of energy depth by an amount E_1 depending on the temperature. Let $b \frac{\delta(\ln T)}{\delta(1/T)} = E_1/k$ since $\frac{\delta(\ln T)}{\delta(1/T)}$ varies only slowly with T and $\frac{\delta(\ln I)}{\delta(1/T)} = E_2/k$ so that $E_2 - E_1 = E$. ln(T) is plotted as a function of (1/T), the slope of the line is E_1/b. Values of E_1/b for different temperatures are given in table (7.1).

7.2 Monomolecular Methods.

(i) Keating's Analysis.[37]

The Randall and Wilkins theory assumes $N_c vS$ is independent of temperature. As the effective density of states in the conduction band, N_c, is proportional to $T^{3/2}$, and the thermal velocity of electrons is proportional to $T^{1/2}$, the assumption is equivalent to assuming $S \propto T^{-2}$.

The cross-section of a defect for capture of an electron usually varies with temperature, and with Coulomb attraction the electron capture cross section does vary as T^{-2}. However with repulsive and neutral centres, cross sections which change as rapidly as T^{-4} have been found in silicon.[38]

Keating avoids the assumption that $S \propto T^{-2}$ by putting $S \propto T^{-a}$ so that $N_c vS \propto T^{-b}$ where $a = 2 - b$. It is still assumed that the cross section is proportional to some power of T but there are experimental and theoretical reasons for expecting such a variation.[38]

Following Randall and Wilkins argument for monomolecular kinetics, and putting $N_c vS = BT^b$ Keating shows that

$$\ln\left(\frac{\Delta\sigma}{\sigma_o}\right) = b \ln T - E/kT - \frac{B}{\beta} \int_{T_o}^{T} T^b \exp(-E/kT)dT \qquad (7.3)$$

TABLE 7.1

E_1/b eV	$T^{o}K$
0.033	355
0.023	285
0.019	220
0.016	180
0.013	150

$$E_1 = bk \frac{\delta \log_e T}{\delta (\frac{1}{T})}$$

E_1/b VALUES AT VARIOUS TEMPERATURES.

When the traps first begin to lose their electrons to the conduction band the final term in equation (7.3) is small, (7.3 therefore reduces to (7.1) which describes the initial rise of the stimulated current.

Keating makes an approximation to the integral in equation (7.3) which is valid provided $E/kT^{*} > 10$. The resulting equation is evaluated in terms of the temperatures T' and T" at which the conductivity is equal to one half its maximum value on the rise and decay sides of the peak respectively. Assuming $E/kT \gg b + 2$, and neglecting the difference between T' and T" and T^{*} in a small correction term, the equation can be solved for different values of b and E/kT^{*}. For values of E/kT^{*} between 10 and 35 and $\frac{T" - T^{*}}{T^{*} - T'}$ between 0.75 and 0.9 the following result is obtained

$$\frac{kT^{*}}{E} = \frac{T" - T'}{T^{*}}\left(1.2\left(\frac{T" - T^{*}}{T^{*} - T'}\right) - 0.54\right) + 5.5 \times 10^{-3} - \left(\frac{\frac{T" - T^{*}}{T^{*} - T'} - 0.75}{2}\right)^{2} \qquad (7.4)$$

Experimental curves usually yield values of E/kT^{*} and $\frac{T" - T^{*}}{T^{*} - T'}$ which lie within the range of validity of the assumptions made in deriving this equation. Using (7.4) the trap depth E_{FK} can be obtained from measured values of T', T" and T^{*}. In principle it is also possible to evaluate the cross section and the temperature dependence of the cross section from a

single glow curve.

(ii) Grossweiner's Method.[39]

The Grossweiner method is based on a simplification of the Randall and Wilkins equation and therefore assumes monomolecular kinetics. The possibility of a temperature dependence of the various crystal properties is neglected.

The values $I^{*}/2$ and T', where the current reaches half its maximum value, on the low temperature side of the maximum, are substituted in equation (6.4). The resulting equation is then divided by the equation obtained for the maximum current when I^{*} and T^{*} are substituted in equation (6.4). Assuming $E/kT^{*} > 20$, to justify a series approximation, and that $N_c vS/\beta > 10^7$, Grossweiner shows that the trap depth is given by

$$E_G = \frac{1.51kT^{*}T'}{T^{*} - T'} \qquad (7.5)$$

By deriving and substituting from equation (7.8) in (7.5) Grossweiner showed that the electron capture cross section of the defects is

$$S_G = \frac{3T'\beta \exp \frac{E}{kT^{*}}}{2N_c vT^{*}(T^{*} - T')} \qquad (7.6)$$

A further conclusion is that the photoconductive decay time due to traps emptying at the temperature T^{*} is

$$\tau^{*} = \frac{2T^{*}}{3T'} \left(\frac{T^{*} - T'}{\beta}\right) \qquad (7.7)$$

7.3 Methods which are Independent of the Recombination Kinetics.

(i) Haering and Adams Theory.[40]

Haering and Adams consider the conditions appropriate to both monomolecular and fast retrapping kinetics. With monomolecular kinetics they use Randall and Wilkins equation (equation 6.4). Differentiating $\log_e \sigma(T)$ with respect to T and equating the result to zero to find the conditions for maximum conductivity, the following equation is obtained

$$\exp\left(\frac{E}{kT^*}\right) = \frac{N_c v S k T^{*2}}{\beta E} \qquad (7.8)$$

(7.8) is valid for E/kT large and $N_c \mu v e S n_{to} \tau$ independent of temperature. From equations (7.8) and (6.4) with E/kT large, an asymptotic expansion gives

$$\sigma(T^*) = \sigma_o \exp\left(-\frac{E}{kT^*} - 1\right), \text{ where } \sigma_o = N_c S v e \mu \tau n_{to} \qquad (7.9)$$

Under fast retrapping conditions it is assumed that the defect levels are in thermal equilibrium with the conduction band. With fast retrapping the Randall and Wilkins equation is no longer applicable and is replaced by

$$\sigma(T) = ne\mu = \frac{N_c \mu}{N_t} e\, n_{to} \exp\left(-E/kT - \frac{1}{N_t \beta \tau} \int_{T_o}^{T} N_c \exp(-E/kT)dT\right)$$

Maximising $\ln\sigma(T)$ with respect to T and assuming $\frac{N_c \mu}{N_t} n_{to} e$ is constant Haering and Adams showed that

$$\exp(E/kT^{*}) = \frac{N_c k T^{*2}}{N_t \beta \tau E} \qquad (7.10)$$

Using an asymptotic expansion for large E/kT again they conclude that $\sigma(T^{*}) = \sigma_o \exp(- E/kT^{*} - 1)$. This equation is of the same form as (7.9) for monomolecular recombination, the only difference being that the constant σ_o is changed to

$$\frac{N_c \mu}{N_t} n_{to} e \qquad (7.11)$$

If the crystal is heated at different heating rates in a series of thermally stimulated current runs I^{*} and T^{*} will vary. Since the current and conductivity are proportional to one another, equations (7.10) and (7.11) indicate that a plot of $\ln(I^{*})$ against $1/T^{*}$ should be a straight line. The slope of the line will be equal to $-E_{HA}/k$. The subscripts HA are used in the later part of this thesis to denote the trap depth, E_{HA}, calculated using this method.

For successful application, Haering and Adams' technique requires that with all the thermally stimulated current runs made at the different heating rates, the initial density of filled defects (n_{to}) and the free electron life time (τ) remain unchanged.

(ii) The Method of Different Heating Rates.

The temperature, T^{*}, at which the maximum thermally

stimulated current is obtained varies with the heating rate, β. With monomolecular recombination the dependence of T^* on β is given by equation (7.8) of the previous section. Under fast retrapping conditions the variation of T^* with is given by equation (7.10). Both equations are of the form

$$\frac{kT^{*2}}{\beta} = \text{const } \exp(E/kT^*) \qquad (7.12)$$

Booth[41] used two heating rates β_1 and β_2 in his experiments and from the resulting two simultaneous equations obtained values for the trap depth.

$$E = k \frac{T_1^* T_2^*}{T_1^* - T_2^*} \ln \left(\frac{\beta_1 T_2^{*2}}{\beta_2 T_1^{*2}} \right) \qquad (7.13)$$

Hoogenstraaten[42] used several heating rates and plotted $\ln(T^{*2}/\beta)$ against $1/T^*$ to obtain a straight line of slope E_{HR}/k. E_{HR} is used subsequently in this thesis to denote trap depths calculated in this way.

Clearly calculations based on the variations of T^* with heating rate are independent of retrapping[37] but as with (i) above it is necessary to assume (a) the same initial electron occupancy of the traps and (b) that the life time as a function of T is unchanged during the recording of each of the different thermally stimulated current curves. For monomolecular recombination equation (7.8) can be used to obtain a value of electron capture

cross section S when the value of E has been determined. It is however incorrect to obtain a value of E using analysis strictly limited to fast retrapping and then use this value in equation (7.8) to find the capture cross section S. This is the procedure adopted by Bube[43]. For fast retrapping equation (7.8) is not applicable and (7.10) must be used instead. Since (7.10) does not contain the term S, no information concerning cross-sections can be obtained in this way.

7.4 Methods Utilising Different Formulae for Different Kinetics.

(i) Schon's Theory

The main difference between Schon's[44] approach and others discussed in this thesis is that Schon includes transitions to the valence band in his considerations. His work was concerned solely with thermoluminescent glow curves, but if a temperature independence of τ is assumed, the thermally stimulated current will be proportional to the thermoluminescence.

The theory follows that of Klasens and Hoogenstraaten.[45] Schon extended it, and considered three sets of conditions in photoconducting phosphors.

(1) Assuming that the recombination process is radiative and that $n_t(1-\frac{S_R}{S})<N_t$ (i.e. bimolecular kinetics) he shows that the trap depth can be obtained from measure-

ments at two different heating rates. In fact

$$E = k \frac{T_1^* T_2^*}{T_1^* - T_2^*} \ln \frac{\beta_1 T_2^{*\,7/2}}{\beta_2 T_1^{*\,7/2}} \qquad (7.14)$$

His analysis also suggests that the thermoluminescence (J) is such that plots of $\frac{\delta(\ln J)}{\delta T}$ against T for glow curves obtained at different heating rates differ only in the region of the maximum glow. A theoretical plot of $\frac{\delta(\ln J)}{\delta T}$ against temperature is shown in figure 7.1(a).

Assuming (a) that the recombination is radiative, (b) that retrapping is negligible ($S_R/S \gg 1$, i.e. monomolecular recombination), and (c) that the traps are not appreciably empty ($\frac{S_R}{S} N_t > N_t$) he obtains the same equation (7.14) for the trap depth. Now however the $\frac{\delta(\ln J)}{\delta T}$ v T plot is different and is shown in figure 7.1 (b).

With his third special case Schon assumes that radiationless recombination is dominant, the traps are initially saturated with electrons, fast retrapping kinetics applies and there are less traps than recombination centres. Under these conditions the right hand side of (7.14) yields the height of the recombination centres above the valence band

$$E_A = \frac{k T_1^* T_2^*}{T_1^* - T_2^*} \ln \frac{\beta_1 T_2^{*\,7/2}}{\beta_2 T_1^{*\,7/2}} \qquad (7.15)$$

instead of the trap depth. The $\frac{\delta(\ln J)}{\delta T}$ v T curves are somewhat similar to those in figure 7.1 (a) but follow the

functions $\frac{E - E_A}{kT^2}$ on the ascending side and $-\frac{2E_A - E}{kT^2}$ on the descending side of the glow curve. He concludes that the initial assumptions are equivalent to assuming $E_A < E < 2E_A$.

In general the difference between the curves in figures 7.1(a) and 7.1(b) can be used as a means of determining whether the recombination process is monomolecular or bimolecular. Application of this method does however suffer from one serious disadvantage. The critical part of the curve involves the measurement of small currents on the high temperature side of the maximum. This is very difficult, as the fall side of the peak cannot be thermally cleaned (see section 10.2).

Since Schon calculates the rate of radiative recombination (J), in the presence of radiationless transitions, it might be thought to be inaccurate to apply the results to a conductivity glow curve. In all the theories of conductivity glow considered so far the variation of τ with temperature has been neglected. This is equivalent to assuming that the recombination probability is temperature independent. With this assumption the conductivity is proportional to the radiative transitions for which the cross section is also temperature independent. The possibility of radiationless transitions occurring within the recombination centre is usually excluded. This does however

spotlight the fact that the assumption of a temperature independent life time of free carriers is not valid under conditions where radiationless transitions occur, though the variation is small over the width of a thermally stimulated current peak.

Equation (7.14) which applies to Schon's first two special cases (and in numerical value to the third) is similar to that of Booth (equation 7.13). According to (7.12) a plot of $\ln\left(\frac{T^{*}{}^{y}}{\beta}\right)$ v $1/T^{*}$ ($y = 2$) from measurements made at a variety of heating rates should give a straight line of slope E/k. Now however $y = \frac{7}{2}$ instead of 2. The effect of the factor $T^{*}{}^{3/2}$ is to add a term $\ln(T^{*}{}^{3/2})$ to the ordinate of the graph which will lower the slope by $\frac{3}{2}\frac{(T)}{(1/T)}$ i.e. the b factor in table 7.1 is $\frac{3}{2}$. Thus values of trap depth obtained using Schon's method will be less than those calculated using the arguments of section 7.3(ii) by an amount varying from 0.02eV at 160°K to 0.05eV at 350°K. Except for the very shallowest traps this was found to be less than other errors inherent in evaluating energy depths by these methods.

(ii) Halperin and Braner's approximation

Halperin and Braner[46] studied several recombination mechanisms and conditions of retrapping with different distributions of electron and hole states. In the case of a single set of trapping levels at a discrete energy depth

(as has been assumed in all the theories described so far) they distinguish between 1st order (monomolecular) and 2nd order (bimolecular) kinetics.

For both mechanisms they assume that $E/kT^{*} > 10$ and $N_c vS$ is independent of temperature. By making the geometrical approximation that the thermally stimulated current curve can be represented by a triangle the following equations were derived for the respective kinetics:-

1st order kinetics $$E_{HB_1} = \left(\frac{1.72}{T^{*} - T^{1}}\right) kT^{*2} (1-2.58\,\Delta)$$

where $$\Delta = \frac{2kT^{*}}{E_{HB}}$$

2nd order kinetics $$E_{HB_2} = \left(\frac{2}{T^{*} - T^{1}}\right) kT^{*2} (1-3\,\Delta)$$

They also derived the following rules to show which kind of kinetics is applicable.

If $\frac{T'' - T^{*}}{T^{*} - T'} \leqslant e^{-1} \left(1 + \frac{2kT^{*}}{E_{HB}}\right)$ the kinetics are first order.

If $\frac{T'' - T^{*}}{T'' - T'} > e^{-1} \left(1 + \frac{2kT^{*}}{E_{HB}}\right)$ the kinetics are second order.

The application of these criteria to our results would indicate that nearly all the peaks in the crystals examined were formed under recombination mechanisms that were second order. That this was so, even when traps with cross-sections as small as $10^{-24} cm^2$ were involved, throws some doubt on

this method of determining the recombination kinetics.

The magnitude of the trap depth, E_{HB}, appears on the right hand side of each of the two sets of formulae which are needed to determine the trap depth and the type of recombination mechanism. In both sets of formulae the term involving E_{HB} on the right hand side of the equation appears as a small correction. In consequence E_{HB} is calculated by successive approximation.

7.5 Fast retrapping theories.

The basis of the theories concerned with thermally stimulated currents under fast retrapping conditions is that the defect levels are at all times in thermal equilibrium with the conduction band. As a result steady state theories are applicable. All the theories discussed below assume that $N_c v S \mu \tau$ is independent of temperature.

(i) The Theory of Boer, Oberlander and Voigt.

The authors consider a two level scheme with emptying traps, and recombination centres which have a much lower probability of capture of the free electrons than the trapping levels.

They show that

$$E_{BOV} = kT^{*} \log_e \frac{N_c}{n^{*}} \frac{\eta}{1-\eta} \qquad (7.15)$$

where n^{*} is the density of electrons in the conduction band when the stimulated current reaches a maximum and η is the

fraction of filled traps at the corresponding temperature T^{*}. Boer et al then assume that η is largely independent of the heating rate. This has been demonstrated theoretically and practically.

Equation (7.15) for constant η is equivalent to that derived by the Haering and Adams equation (7.11) since the conductivity is proportional to the density of carriers in the conduction band. The same method of curve analysis can then be used as described in section (7.3(i)), and the disadvantages described there also apply.

With fast retrapping it can also be shown that the cross section of the recombination centres is given by

$$S_R v = \gamma = \frac{E_{BOV}}{kT^{*2}} \times \frac{\beta}{n^{*}T^{*}} \qquad (7.16)$$

If fast retrapping occurs no information concerning the trap cross sections can be obtained from a thermally stimulated current curve.

(ii) Bube's Approximation.

Bube assumes that the defect levels are approximately half full at the current maximum. This is equivalent to requiring that at the current maximum the electron Fermi level coincides with the defect levels, i.e. that the occupancy at maximum current η is one half. With this assumption Boer et al's equation reduces to

$$E_B = kT^{*} \log_e \frac{N_c}{n^{*}} \qquad (7.17)$$

(7.17) has been shown to be a good approximation for very fast retrapping but to give incorrect results for slow retrapping. Boer et al [47] have shown the occupancy at the peak maximum is less than $\frac{1}{2}$ and is of the order of $\frac{1}{10}$ to $\frac{1}{100}$ at the current maximum.

(iii) Lushchik.[48] Lushchik makes a geometrical approximation in deriving a formula appropriate to fast retrapping and obtains the expression

$$E_L = \frac{kT^{*2}}{T'' - T^*} \qquad (7.18)$$

His method therefore utilises the high temperature side of the thermally stimulated current curve. This is a disadvantage as it is more difficult to make accurate measurements on this part of the curve (see section(10.2)).

7.6 Comparison of Methods.

A detailed comparison of the above methods will be made in the discussion after the experimental work and the results obtained in the present work have been described. In this way a coherent discussion of the practical and theoretical problems is possible.

7.7 Photoconductive Decay.

If a crystal is strongly illuminated with light of suitable wavelength many electron hole-pairs are produced and the centres that capture electrons will be filled. There will also be an excess of electrons in the conduction

band and photoconductivity results.

When the illumination is suddenly removed the photocurrent decays. The decay can be divided into three sections shown in figure 7.2:-

(1) An initial fast decay which gives a measure of the free electron life time since all the traps are saturated in this region.

(2) An intermediate region associated with various trapping levels.

(3) A long tail to the curve due to the emptying centres with levels just above the electron Fermi level in the dark.

The long tail (3) has been used extensively in the present work to obtain information about the defect levels responsible for it. The region was often found to be clearly defined and due to a set of levels at a discrete energy depth E.

If there are initially n_{to} filled levels at this depth, and there is no retrapping replenishing the emptying defect levels, the rate of thermal excitation of electrons into the conduction band at constant temperature is $\frac{dn}{dt} = -\frac{dn_t}{dt} = n_{to} f e^{-ft}$. The conductivity due to electrons excited from these defects is

$$\Delta\sigma = \frac{dn}{dt} e\mu\tau = n_{to} f e^{-ft} \mu e \tau \qquad (7.19)$$

This represents an exponential decay of photoconductivity with a decay time constant $\tau_d = \frac{1}{f}$.

From equation (6.10) the decay time

$$\tau_d = \frac{1}{f} = \frac{1}{N_c v S} \exp (E/kT) \qquad (7.20)$$

since $\nu = N_c v S$.

Thus for a discrete set of defect levels emptying under monomolecular conditions the long tail of the photoconductive decay will be exponential and the decay time will vary the temperature.

If τ_d is measured over a range of temperatures, a plot of $\log_e \tau_d$ against $1/T$ should give a straight line of slope E/k, and intercept $1/N_c v S$, if $N_c v S$ is independent of temperature. The values of energy depth and cross section obtained in this way will be referred to as E_τ and S_τ.

If retrapping is appreciable the decay is not exponential (see section 6.4~~last section~~) and it is necessary to know the ratio of cross sections of the trapping and recombination centres to obtain information about the defects from the decay measurements.

CHAPTER 8.

Crystal Growth in Cadmium Sulphide.

8.1 The Difficulties Involved.

There are several difficulties in growing single crystals of cadmium sulphide. Cadmium sulphide dissociates at atmospheric pressure and has no clearly defined melting point. Under high pressures of inert gas, however, it can be made to melt. For example Addamiano has found the melting point to be 1475°C under a pressure of 2 atmospheres of argon.

In order to investigate the inherent defects in cadmium sulphide it is necessary for the crystals produced to posses not more than a few parts per million of various impurities and defects. No suitable solvent has been found to permit growth from solution.

Growth of crystals from the vapour phase in an inert atmosphere at temperatures between 900°C and 1150°C overcomes these difficulties.

8.2 Methods Based on the Frerichs Technique.

Methods used to grow the crystals on which the measurements in this thesis were made included two based on the Frerichs technique.[50]

The apparatus for one of these methods is shown in the diagram in figure 8.1. High purity argon (B.O.C. 5 9's) was dried in a drying tower and then split into two measured

flows controlled by clips. One flow entered the 2.5 cm. diameter silica tube, situated in an electric furnace, and passed over molten cadmium held in a silica boat at 600°C. In this way a stream of argon and cadmium vapour was carried to the hottest zone of the furnace.

The second stream of argon passed through a silica pipette containing sulphur. The function of the pipette was to maintain a separation of the two flows until the hottest region of the furnace was reached. The sulphur was held at a temperature of 500°C, while the hottest region of the furnace where the reaction between sulphur and cadmium took place was at 1100°C. The temperature profile of the furnace is shown in figure 8.1.

With argon flow rates over the molten cadmium and sulphur of 60 ml/min and 30ml/min respectively, crystal growth took place in about 3 hours in a region of the main silica tube at about 1000°C. After this time the sulphur and cadmium supplies were nearly exhausted. When the crystal growth was complete the furnace was cooled slowly to a temperature below 100°C before the argon supply was removed and air allowed to enter the silica tube. The whole cooling process took about 1½ hours.

The sulphur used was of high purity, and outgassed by heating to 400°C in high vacuum. The cadmium was also of high purity, and had been etched in dilute nitric acid,

washed in distilled water and dried. The elements were further outgassed by heating in situ in the growing tube before crystal growth began.

The furnace comprised a kanthal resistance wire element cemented on to an alumina tube with furnace bricks as insulation. The furnace winding had a central tapping and one half of the furnace was shunted by a rheostat to produce the lower temperature zone of the furnace. The power was supplied by a "Variac" variable tapping transformer.

The cadmium sulphide crystals grew radially inwards from the walls of the silica tube. They were mainly hexagonal rods although a few thin plates were also obtained. The largest of the rods were about 0.5 cm. long and 0.1 cm. in diameter. The crystals varied in dark resistivity from more than 10^{10} ohm cm. to 100 ohm cm. The more resistive crystals tended to be the more photosensitive. The thin plates as well as the hexagonal rods had a hexagonal (wurtzite) type lattice. Cadmium sulphide can be prepared in a cubic (zinc blende) modification.

To grow crystals doped with chlorine, the argon was bubbled through hydrochloric acid before passing into the drying tower. The doped crystals grown in this way were larger than the pure crystals. The resistance of the chlorine doped crystals was a few ohms cm. They were not measurably photoconducting.

It should be noted that the density of chlorine incorporated into the crystal is only a small fraction of one per cent. Unless another impurity (or appropriate lattice vacancy) is at the same time incorporated into the crystal with an effective charge in the crystal opposite to that of the chlorine, high densities of doping are not possible. "Charge compensation" has to be maintained. The charge compensation mechanism that allows some chlorine impurity in the crystals is "free electron compensation" in that a S^{--} ion is replaced by Cl^{-} ion and one free electron.

The other flow method, related to the Frerichs technique, which has been used to provide crystals for this work involved the sublimation from cadmium sulphide powder in a stream of argon (see figure 8.2). This technique was employed by another member of the group to produce thin plates about 100μ thick and up to 0.5 cm. diameter. Some rods were also grown using this method. The predominance of plates was attributed to a high temperature gradient in the growth region rather than the method of growth. Before entering the furnace the argon was passed over heated copper to remove oxygen and prevent the oxygen entering the crystals during growth. The cadmium sulphide used was Messrs. Light Company high purity grade outgassed in high vacuum at 800°C.

8.3 Other Methods of Growth of Single Crystals of Cadmium Sulphide.

An entirely different method of sublimation was used

by a third member of the group. The cadmium sulphide powder was sublimed from one end to the other of an evacuated silica tube (about 20 cm. long). The charge was either powder which had been outgassed at 800°C, or crystals previously prepared using one of the two flow methods. The tube was placed in a furnace with a temperature profile such that the charge end of the tube was at 1150°C and the other at 1100°C. After a day or two the powder at the hotter end of the furnace had sublimed to the colder end forming a polycrystalline aggregate containing a few large crystals. The sublimation could if necessary be repeated several times.

Several other growth methods have been described in the literature[51] but were not used in this work as they tend to produce conducting crystals which are poor photoconductors. These techniques include the transfer of cadmium sulphide along a sealed tube under a low temperature gradient, at a mean temperature of 700°C, by the reaction of the powder with small quantities of iodine.[52] Large crystals can be grown under pressure from the melt at high temperature, but these are contaminated by impurities from the material of the container, usually graphite.[53]

8.4 Nomenclature of Crystals.

Crystal rods grown by the reaction of the elements in a stream of argon will be denoted by the letter R. Crystal

rods grown by sublimation in a stream of argon will be distinguished by an S and plates grown by this method by P. When crystals grown in vacuum by sublimation are referred to they will be denoted by V. Some of the crystals were treated after growth by heating to 500 - 700°C in vacuum. Such crystals will be given a suffix v in this thesis.

8.5 Contacts.

To make satisfactory electrical measurements it is desirable to make ohmic contacts to the crystal. Pure indium melted on to the crystals using a soldering iron was found to give ohmic contacts. As was mentioned earlier indium produces ohmic contacts for two reasons. Firstly it has a lower work function than cadmium sulphide, and secondly the indium can diffuse a short distance into the crystal under the contact.[54] The first condition is necessary for electrons to enter the crystal without encountering a barrier. The diffusion of the indium produces a semi-conducting layer at the surface of the crystal under the contact allowing carriers to pass between the contact and the bulk of the crystal.

CHAPTER 9.

Experimental Arrangement.

9.1 Vacuum Cryostat.

For optical and electrical measurements the crystals were mounted in the cryostat illustrated diagrammatically in cross section in figure 9.1.

All the metal parts above f--f in the diagram were made of German-silver and those below of copper. The German-silver and the double tube were used to reduce heat losses from the copper mounting block and formed a Dewar. The walls of the cryostat below f--f were made of plates of copper soldered together. The quartz window was demountable and was held in position with the cryostat under vacuum by an 'O'-ring seal.

The vacuum in the cryostat was produced by a mercury-in-glass diffusion pump with a liquid air trap. The cryostat was evacuated to allow the crystal to be cooled to liquid air temperature. The vacuum provided good thermal insulation and thus reduced heat losses and prevented the deposition of ice and solid CO_2 on the sample. Another function of the vacuum was to maintain the crystal in an inert atmosphere and reduce the effect of adsorbed gases, particularly oxygen, on the photoconducting properties of the crystal. For this reason the crystal, when not under examination, was kept continuously under a rough vacuum provided by the backing

pump once the investigation had begun.

The crystal was mounted between indium contacts on a thin sheet of mica. Indium wets mica and can be made to adhere firmly to it. The mica was cemented to the copper block with hot setting araldite. This resulted in the crystal being in good thermal contact with the copper block but electrically insulated from it.

A thermocouple was embedded in one of the indium contacts so that the crystal temperature could be measured. All wires to the contacts were of 40 s.w.g. to reduce heat losses through them. A Siemens sintered multiple glass to metal seal was used to make vacuum tight electrical connections through the walls of the cryostat.

The crystal was cooled by pouring liquid air down the central tube of the metal Dewar of the cryostat. The temperature was raised by a heater comprising a coil of resistance wire covered by woven silica sleaving. The heater was situated in the central tube of the Dewar.

9.2. Advantages of the Cryostat.

Apart from providing vacuum facilities the cryostat has several other advantages.

(1) The good thermal contact between the crystal and the liquid air in the central tube, coupled with the insulation provided by the German-silver and the vacuum, enabled the crystal to be cooled to (about 85^{o}K) within a few degrees of the temperature of liquid air.

(2) The low thermal capacity of the copper mounting block and the close proximity of the crystal to the heater made it possible to heat the crystal quickly allowing a wide range of heating rates to be used. A fast heating rate leads to larger thermally stimulated currents.

The low thermal capacity of the crystal and its mounting block, and the proximity of the crystal to the heater and coolant, provided a fast response of actual crystal temperature to changes in the heater wattage dissipation. This made it simpler to maintain the crystal at a constant temperature over the range 90°K to 370°K. The fast thermal response was also useful in terminating a run at a predetermined temperature. This facility was essential to the technique of thermal cleaning of stimulated current peaks. (see section 10.2). This technique is somewhat similar to that used by Hoogenstraaten[42] and described by him as the method of 'decayed' glow curves.

(3) The quartz window was used so that if required illumination with a wide range of wavelengths could be employed.

(4) The voltage applied to the heater could easily be altered to ensure that the heating rate during a thermally stimulated current run was linear with time. Thevoltage on the heater was altered by a Variac transformer driven by an electric motor. The voltage programme required to keep the heater was determined experimentally. The variation

in the heating rate was less than 15% over the width of the peak ($\sim 50^{\circ}C$).

9.3 Ancillary Apparatus.

The apparatus used for thermally stimulated current and photoconductive decay experiments is shown in figure 9.2. The inside of the light tight box was blackened to avoid reflections. A hole about 3 x 2 $cm.^2$ provided the window between the two halves of the box.

Filters could be placed in a holder covering the window. The blade of the light chopper also completely covered the beam entering the window so that stray light falling on the crystal was reduced to a minimum. The illumination in most experiments was provided by a 1000 watt tungsten lamp run from a 120v D.C. supply. The intensity of the illumination could be varied by means of a graded rheostat in series with the lamp.

The electrical circuit used for thermally stimulated current measurements is shown in figure 9.3. The applied voltage, variable up to 100 volts, was provided by a dry battery. The small currents were measured with a Hatfield instrument type LE 490 D.C. amplifier, the sensitivity of which was adjusted by changing the shunt resistance across its input. Care was taken to ensure that the voltage across the input of the amplifier did not exceed 1% of the applied voltage.

The amplifier comprised a mixed valve-transistor amplifier. The valve input was designed for a maximum input resistance of 2.2 MΩ so that high resistance samples could be used. The transistor output worked into a load of 78 ohms which was ideal for use with a graphic recorder. The recorder and amplifier made measurements possible to a lower limit of 10^{-8} amps. The limit was set by leakage across the cryostat. The recorder speeds were 1"/min. and 6"/min. which were adequate for the heating rates used. Temperature calibration points were marked manually as the thermally stimulated current curve was traced automatically on the recorder.

Essentially the same apparatus was used for the photo-current decay measurements. The light chopper was used to cut off the illumination from the crystal. Either the amplifier and recorder, or a D.C. oscilloscope (Solartron AD 577), was used to display the decay curve depending on the speed of the decay being investigated.

CHAPTER 10

Measurements.

10.1 The Measurement of Thermally Stimulated Currents.

To make a measurement of the total thermally stimulated current the following procedure was adopted.

The crystal was mounted in the cryostat which was then evacuated. The crystal was cooled by pouring liquid air into the central tube of the cryostat dewar. The intense illumination was switched on for 10 minutes to fill the electron traps. With the crystal in the dark again a potential of 100 volts was applied to the crystal, and as soon as the photocurrent had decayed the cryostat heater and the recorder were switched on.

A typical thermally stimulated current curve is shown in the graph in figure 10.1. The theories introduced earlier deal with a single isolated thermally stimulated current peak. A typical experimental curve such as that shown in figure 10.1 comprises several overlapping peaks. It is possible however to obtain from such a curve the approximate temperatures of the maxima of the peaks associated with the major sets of defect levels. It is possible to separate the peaks by (1) varying the temperature at which the traps are filled, (2) changing the wavelength of the excitation filling the defects, (3) using a different heating

rate or (4) applying the method of thermal cleaning. In practice this last method provided the most efficient means of separating peaks.

10.2 The Thermal Cleaning of Peaks.

If the thermally stimulated run is stopped at the temperature T_a shown in figure 10.1, the defects responsible for the peaks appearing at temperatures lower than T_a will have been practically emptied. If the crystal is recooled, and subsequently reheated without refilling the defects, the rise of current will be determined more exactly by the traps responsible for the peak centred on T_b. However the descending side of this second curve will still be affected by the traps which empty at still higher temperatures. If the crystal is now heated uniformly until the temperature T_c is reached and then cooled and reheated an estimate can be made of the effect of the higher temperature peaks on the peak centred on T_b. Subtraction of this background, due to the unwanted peaks (together with any dark current present), from the previous curve will give the thermally stimulated current peak centred on T_b.

Several points are worth emphasizing for a peak measured in this way:-

(1) Not all the electrons trapped in the set of defects under investigation contribute to the peak. Some of the traps are emptied during the initial heating to T_a, while others are not emptied until the background current is

being measured. The shape of the peak is not affected by the loss of some of the electrons from the traps responsible for the peak at T_b but the estimate of the number of defects present will be too small.

(2) As some of the traps causing peaks at temperatures higher than T_b will be partially emptied by heating to T_c, the background current then measured will be less than that present during the measurement of the peak at T_b. As the background current increases rapidly with temperature, inaccuracies in its value will be more serious on the descending side of the peak than on the rise side (see section 11.10).

(3) If the peak situated at T_b is overlapped by another, smaller peak on the low temperature side, the defects responsible for the unwanted contributions to the total current will not have been completely emptied by heating to the temperature T_a. As a result there will be some thermally stimulated current due to the second set of traps on the rise side of the peak attributed to T_b. This can seriously affect results obtained using an analysis involving the initial rise of the thermally stimulated current (see section 11.15).

(4) The temperatures at which the maxima of the glow curves occur, vary as the heating rate is changed. The magnitude of the change in temperature of a maximum depends on the

energy depth of the defect levels involved, and the extent of overlapping of the peaks varies as a result. The cleaning of a peak involves removing more electrons from the defects being studied if the maxima are closer at the new heating rate. This results in a decrease in the number of electrons released subsequently to form the required thermally stimulated current peak. The use of methods of evaluation of defect properties, which depend on experiments made at a variety of heating rates, is invalidated due to the variations in the number of filled traps (see section 11.12).

(5) It has been assumed in all the theories of thermally stimulated currents discussed in chapter 7 that the trapping levels are in groups at specific discrete depths. That is, there is not a continuous distribution of defect levels. If there were such a continuous distribution an initial thermal cleaning would empty the shallower traps but not the deeper ones. As a result subsequent heating would produce a peak characteristic of the deeper levels only. This provides a method of determining whether the defect levels are distributed over a continuous energy range. (see section 11.5).

(6) The analysis of isolated peaks obtained by the method of thermal cleaning has been carried out in this thesis assuming that the gain (G) is independent of the degree of filling of the defects, and of the temperature cycles

necessarily involved. In other words measured currents are assumed to depend only on the rate of release of electrons into the conduction band. Because of the effect of the defects on the free electron life time the assumption may not be jusitified, but no evidence of its invalidity was found. All the theories used in the calculation of the depths of energy levels in the crystal neglect the possibility of such a variation in gain.

In one crystal it was found that heating above 50°C in the dark created new donor levels. This production of donors caused a variation in dark current at high temperatures for the different heating runs in the thermal cleaning process. The change in dark current was small, however, except for measurements made at slow heating rates.

10.3 Thermally Stimulated Current Programme.

When a new crystal had been mounted the straight forward thermally stimulated current curve was measured between -180°C and 100°C for various physical states of the crystal.

With the crystal in a particular state (see next section) the principal current peaks were picked out. Up to five peaks were found in a sample, each with a half width of 15 - 30°C.

The crystal was cooled to -180°C and the defects were filled with electrons by illumination. The crystal was then heated in the dark to a temperature just less than

that at which the maximum of the first peak occurred. The crystal was then cooled once again and reheated to record the first (lowest) peak. When the current had fallen to about half its maximum value the crystal was again cooled and reheated to the temperature required to clean the second major peak. In this way the various thermally stimulated current peaks were studied. In a few cases two peaks were too close for the thermal cleaning to be effective and they were treated as single ones.

The extent of the cleaning on the low side of the peak (i.e. how near it was necessary to approach the temperature of the maximum under investigation) depended on the magnitude of the current due to other peaks present within that temperature range. On the descending side of a peak the crystal was recooled when the current had reached about half its maximum value. This value was chosen in order that the half width of the peak could be determined with a minimum reduction in the background current. It was found in some crystals that a few peaks were so well separated that no thermal cleaning process was necessary.

Using the technique described in the previous paragraphs isolated thermally stimulated current peaks were measured for several heating rates with the crystal in the same physical state. Under some circumstances the physical state of the crystal changed during the course of the

measurements. The effects of such complications will be discussed in section 11.5 .

The measurements were then repeated for other physical states of the crystal which were of interest.

10.4 The Physical States of Crystals.

In making a series of current glow measurements on any particular crystals it is desirable that the crystal should be in the same physical state each time it is illuminated at liquid air temperature. In practice the physical condition of a crystal may be different at the start of each thermally stimulated run. The reasons for this are twofold, namely (1) the density of defects present in the crystal may have changed and (2) the extent to which the traps are filled during illumination at the low temperature may vary.

With regard to (1) it was found that with some crystals intense illumination and heat treatment produced changes in the defects present, by photochemical and thermal reactions. For example, after one crystal (R1) had been heated to 100°C in the dark a peak was found in the thermally stimulated current at 0°C (see figure 12.1 (a) and (b)). If, however, the crystal was irradiated with tungsten light of 800 ft. candles intensity at room temperature, no peak could subsequently be found at 0°C, but a new double peak was observed at about +80°C. The 0°C peak reappeared while

the 80°C peak disappeared after the crystal had been reheated to 100°C in the dark. In these measurements the defects were filled as usual by illumination at liquid air temperatures.

The variation of the initial occupancy of traps, by filling the defects at a temperature other than that of liquid air, was used as an additional method of separating overlapping thermally stimulated current peaks. The peaks then observed were only those which normally appeared at temperatures above the temperature of filling and were therefore associated with the deeper traps. In this way the unwanted effects of shallower traps could be minimised. In addition some of the peaks previously observed at the higher temperatures were not detected when trap filling was carried out at temperatures higher than 80°K. The failure of these peaks to appear was either due to a photochemical reaction which annihilated the corresponding trapping centres, or alternatively they were emptied by a quenching process.

10.5 Photoconductive Decay.

The slow photoconductive decay associated with levels near the quasi electron Fermi level was measured over the range - 180°C and 100°C. The change in illumination required was provided by the light chopper. The photocurrent decay was either displayed on the D.C. oscilloscope, or, for

the slower decays, on the graphic recorder.

Since traps empty more slowly at low temperatures the long decay due to a single set of defects becomes slower as the temperature of the crystal is reduced. At the same time the initial conductivity at the start of the decay decreases because the area under the conductivity versus time graph is a measure of the density of traps and must be largely independent of temperature. There is, therefore, a limit to the lowest temperature at which satisfactory measurements can be made which is due either to the low conductivity involved or to the inordinate length of the decay. At the high temperature end of the range, the decay due to such a level would be swamped by the decay processes associated with other recombination mechanisms. The variation in decay time measured generally lay between 200 sec. and 100 msec. for a temperature range of about $50^{\circ}K$.

The measurements were repeated for each long decay observed in the crystal. Each change of scale of the amplifier changed the sensitivity by a factor of $\sqrt{10}$ i.e. 3.16. The decay time is defined as the time required for the conductivity to decrease by a factor of 1/e (1/2.71) where e is the base of Naperian logarithms. Because of the approximate equality of e and $\sqrt{10}$, the time for the conductivity to decrease by $\sqrt{10}$ (τ_s) was often used for convenience instead of the exact decay time.

Only the ratio of decay times is needed to evaluate the trap depths. This means that using $\sqrt{10}$ values obtained from curves which were approximately exponential introduced negligible error. The determination of the values of cross section from these measurements required the absolute value of decay time, but the error involved in using $\frac{\tau_s}{1.12}$ for the decay time was far less than other experimental errors.

10.6 Other Measurements.

Measurements of steady state photoconductivity can often lead to information concerning the depth of defect levels. The curve of photoconductivity against temperature usually decreases steadily as the temperature is increased from liquid air to room temperature (see figure 10.2 (a)). Eventually it levels off or increases slowly up to 100°C. The decrease is due to thermal quenching and to the decrease in mobility with temperature.

In several crystals sudden increases in photoconductivity were superimposed on the general decrease (see figure 10.2 (b)). These discontinuous effects occur when the Fermi level falls below recombination centres which then cease to assist recombination and begin to behave as electron traps. As the position of the electron Fermi level can be calculated from equation 4.10 when the conductivity and temperature are known, the energy depth of the levels in such recombination centres

can be calculated. It must be borne in mind however that an alternative explanation is that the discontinuity might be caused by the hole Fermi level passing through recombination centres with levels.

Conventional semiconductor measurements of the dark current, I_D, as a function of temperature can also give the depth of donor levels.

CHAPTER 11.

Results.

11.1 Evaluation of Trap Depths and Cross Sections from the Experimental Curves.

On the whole the differently grown and treated crystals led to similar distributions of peaks in the thermally stimulated current curves. Some typical curves are shown in figure 11.1 (see also figures 12.1 and 12.2). With most crystals there were one or more peaks with maxima near liquid air temperatures, and a series of peaks between $0^{\circ}C$ and $100^{\circ}C$. The position, size, and shape of the higher temperature peaks were often dependent on the physical history of the sample and the conditions under which the traps were filled with electrons.

Of the higher temperature peaks the two which were observed with maxima in the vicinity of $30^{\circ}C$ (see figure 11.2) tended to overlap to such an extent that it was not possible to separate them satisfactorily by thermal cleaning. All other peaks were subjected to the experimental cleaning techniques described in Chapter 10. The curves in figures 11.3 and 11.4 illustrate the sequence of obtaining a satisfactory isolated peak on which the various analyses described in chapter 7 could be performed.

All crystals examined were subjected to the same

thermal cleaning techniques, and the resulting isolated conductivity glow curves were analysed using as many of the mathematical methods described in chapter 7 as possible. It was concluded that the evidence indicated that there were, in all, six different sets of traps with energy depths of 0.05, 0.14, 0.25, 0.41, 0.63 and 0.83 eV. The traps responsible for the overlapping peaks near 30°C, referred to above, were those with energy values of 0.41 and 0.83 eV. The rather surprising conclusion that two sets of traps with vastly different energy depths lead to approximately identical values of T^{*} can be explained by widely different values of cross section. In the case of the 30°C peak however the value of 0.83 eV is not thought to be associated with a simple trapping mechanism but the basic concept of a trap with a large cross section of interaction is still valid (see section 11.5).

The results of the detailed analyses of the individual glow peaks are recorded in tables 11.1 to 11.4. All the peaks on which calculations were made have been fitted into one or other of the six sets of traps, although there was some evidence that another set of defects may have been present, associated with a peak atabout 280°K. However this peak was so small compared with neighbouring, overlapping peaks, that it was not possible to obtain any useful information concerning the traps involved.

In the tables POOR signifies that for several thermally stimulated runs the values obtained lay well outside the stated errors. BAD means that the results were completely inconsistent, or that no values at all could be obtained because of severe overlapping. N.M. means that no measurements of the right type for evaluation by a particular method were made.

The errors quoted are not strictly Gaussian, but errors estimated by taking into consideration the variation in the accuracy due to the extent of the overlap of other peaks. With the methods based on the variation of the heating rate, and the Haering and Adams technique, the order in which the measurements were made affects the error (see section 13.5).

The symbols used in compiling the tables have been described in chapter 7 and in section 8.4. To avoid confusion however, the symbols are explained again at the foot of table 11.1.

T^{*} is the approximate temperature of the maximum current of the peak in question. The column headed "Condition" refers to either the prior illumination and/or heat treatment which led to the particular peak becoming large.

Where two values of trap depth are given it means that with some heating rates one value was obtained, while with

different rates the second value was obtained. Where values for cross sections are quoted the figures in brackets indicate the value of energy depth which was used to calculate the cross section. The majority of the values of cross-section was evaluated using the values of energy depth determined experimentally.

The values of cross section calculated from the experimental thermally stimulated current curves, which are given in the tables, were for the most part evaluated using Grossweiner's method, equation (7.6). The reason for this is that all the methods advocated for calculating cross sections make use of equation (7.8). Thus once T^{*} and β have been measured, the magnitude of the cross section depends only on E. Grossweiner's method almost always led to an estimate of E in agreement with values obtained from the majority of the methods of analysis.

For all the observed traps the order of magnitude of the cross section is determined by $\exp(E/kT^{*})$, i.e. it depends on E/T^{*}. For this reason the accuracy of the estimated cross section is limited by the accuracy in determining the trap depth E, and since a high power exponential term is involved, the calculated cross section values can easily be in error by an order of magnitude. However since various crystalline defects can have electron capture cross sections which can differ by over ten orders

of magnitude, the inaccuracy of the values quoted is not too alarming.

All energy depths are given in electron volts, temperatures in degrees Kelvin and cross sections in square centimetres.

11.2 The Traps at 0.05 eV.

Halperin and Braner's method of calculating the energy depth of the traps associated with the peak occurring at the lowest temperature was unsatisfactory because the correction term was too large. The relatively small magnitude of E/kT^* prevents high accuracy being obtained with any of the methods used. With these particular trapping centres the best estimates of energy depth are likely to be those obtained from the photoconductive decay measurements.

Garlick and Gibson's initial rise technique, and to a lesser extent the methods of Grossweiner, and Franks and Keating, were affected by variations in the linear heating rate on the low temperature side of the maximum. A linear heating rate was difficult to achieve experimentally because with some crystals the peak occurred at temperatures which were at the lowest limit of those obtainable with the cryostat employed.

The peak is almost certainly associated with the same type of trap as that studied by Franks and Keating.[55]

Their calculated value of trap depth (0.053 eV) agrees closely with the present results. However the glow peak isolated by thermal cleaning processes differs in three respects from their published curve. (1) The value of γ i.e. $\frac{T'' - T^*}{T^* - T'}$, for our curve was about 0.8, compared with a value greater than unity reported by Franks and Keating. (In fact 1.0 is outside the range of γ values for which the mathematical expression employed by Keating is valid. In addition the magnitude of E/kT^* is too small to lie within the permitted range of 10 to 30 required by Keating's analysis). (2) The temperature of the maximum was different. This leads to differences in the values of cross section 10^{-24} cm^2 compared with 10^{-21} cm^2 estimated by Franks and Keating. In the present work the temperature, T^*, was different for different crystals. The variation in the apparent value of cross section was probably due to retrapping effects.[37] (3) The variation in energy depth with heating rate as reported by Franks and Keating was not observed.

The apparently anomalous value of energy depth obtained from decay measurements in crystal S3 is probably due to the fact that the crystal contained a different set of traps. In some crystals three sets of shallow traps were detected but one of these was at too low a temperature for the corresponding thermally stimulated curve to be determined. The presence of these different shallow traps was verified

by measurements on the very slow decay of photocurrent at liquid air temperatures, which indicated that the depth of one of the sets was 0.068 eV (see also values obtained from log Ivs $\frac{1}{T}$ plots reported in the next section).

The calculated capture cross section of the traps at 0.05 eV is very small, between 10^{-24} and 10^{-25} cm.^{2} With such a small cross section retrapping is negligible, and it is therefore not surprising to find that Bube's method of calculation gives erroneous values of 0.2 eV. The good agreement with Lushchik's method suggests that his technique does not lead to great inaccuracies in evaluating peaks associated with monomolecular kinetics.

11.3 The traps at 0.14 eV.

Good agreement was again found between different crystals and various method of calculation for isolated curves associated with the set of traps at a depth of 0.14 eV. The agreement is good both for values of cross section and energy depth. This is probably due to the small cross section ($\sim 10^{-22}$ cm.^{2}), and the consequent absence of retrapping.

The presence of a value of 0.068 eV in the table, which was obtained from Garlick and Gibson plots for some of the curves may have been due to insufficient cleaning, but on the other hand this result adds weight to the evidence for the existence of a trap at that energy depth, namely

one of the three shallow traps mentioned in the last section.

The error in the value of energy depth in crystal VI as calculated by Grossweiner's method is due to non-linearity in the heating rate at such low temperatures. The difference in the calculated energy depth comparing Haering and Adams' method with the heating rate method was also observed with other trapping peaks. The heating rate method tends to be more reliable if there is a variation in occupancy or density of traps because the position of the maximum is independent of the occupancy with monomolecular kinetics.

11.4 The Traps at 0.25 eV.

The good agreement between cross section values as well as energy depths for these particular trapping centres is again a consequence of the small cross section ($\sim 10^{-24} cm^2$), which makes retrapping unlikely. The associated peak in the thermally stimulated current curve was destroyed by strong illumination at room temperature, being replaced by one at about $70^{\circ}C$. This effect is almost certainly the same as that described by Woods and Wright[56]. The implications of this will be discussed in section 12.1.

The spread of values obtained for crystal S3 is due to the facts (1) that this was one of the first crystals to be measured, and (2) that the thermal cleaning technique had not then been fully developed. The three major types of trapping

centre discussed so far all have very small capture cross-sections, and consequently recombination is a monomolecular process. As a result, it can be seen from the values quoted in the tables, that trap depth analysis using Bube's method, which is only applicable when fast retrapping occurs leads to values of energy depth which are consistently too large.

11.5 The 0.41 and 0.83 eV Traps.

As mentioned earlier the glow peaks associated with the traps at 0.41 and 0.83 eV were too close together to be easily separated by thermal treatment when both sets of traps were present in the same crystal. Neither was it practicable to separate them completely by optical means. Separation by varying the heating rate seemed a practical proposition, but the peaks coincided at an intermediate heating rate so that only limited separation was effected with the fastest and slowest heating rates obtainable.

An attempt was made to use thermal cleaning in order to clarify (1) whether the peaks were due to two distinct trapping levels which happened to empty at about the same temperature, or (2) whether there was in fact only one trapping level emptying, during which time some of the electrons were being temporarily retrapped, eventually giving rise to a second peak. After cleaning, the subsequent

glow curve exhibited the high temperature peak with only a little current from the low temperature peak superimposed. This showed that the two peaks were independent (see figure 11.5).

It was still possible that there might be a continuous distribution of trapping levels. The peaks in the glow curves for crystals S2 and S3 were studied to discover whether such a distribution of traps existed. To do this the crystal under test was heated to a temperature somewhat lower than the temperature of the first maximum and then cooled and reheated several times.[42] Garlick and Gibson plots were then made for the initial rise curves obtained. The energy depths calculated in this way for crystal S3 are shown in table 11.5 and some of the plots are shown in figure 11.6. The low energy depth indicated by the first run was due to a small peak which lay at slightly lower temperatures than the peaks being studied. The next two values obtained were intermediate between 0.41 and 0.83 eV. This was due to the fact that both trapping centres were still being emptied (the experimental points did not lie very well on a straight line). All the subsequent runs indicated the presence of the 0.41 eV traps only. There was no evidence of a distribution of traps. The scatter of values obtained from the last runs is to be expected in view of the extremely small stimulated currents

TABLE 11.5

Run	Energy Depth eV	Run	Energy Depth eV
1	0.20	10	0.45
2	0.58	11	0.44
3	0.69	12	0.46
4	0.46	13	0.45
5	0.48	14	0.47
6	0.42	15	0.47
7	0.46	16	0.40
8	0.41	17	0.47
9	0.48	18	0.40

GARLICK AND GIBSON ENERGY VALUES FROM REHEAT CURVES IN CRYSTAL S3.

being measured at that stage.

Having decided there were two distinct sets of trapping levels the following line of argument was adopted. As the temperature of the maxima were the only peak parameters that could confidently be identified initially, the use of different heating rates was concentrated on more than usual. For this reason thermal cleaning was kept to a minimum. By a coincidence the densities of traps in the crystals VI and $S5_V$ were the same. The results for both these crystals gave points on an Haering and Adams plot (see figure 11.7) that fell on two straight lines with slopes leading to energy depths quoted in the tables namely 0.41 and 0.83 eV. The accuracy with which the points lay on two lines was surprisingly good considering the extensive overlap of the peaks. The heating rate method applied to these particular crystals gave values in good agreement with those quoted above. The failure of these methods when applied to the corresponding peaks observed with other crystals was probably due to the failure to distinguish the current maxima due to the different traps.

Other methods, not surprisingly often gave values lying between 0.41 and 0.83 eV, though sometimes one value predominated. For example the slope of a Garlick and Gibson plot always lead to a value of 0.41 eV corresponding to the shallower trap depth. This is due to the fact that the

peak for the shallower trap is broader than that for the deeper trap. The contribution to the stimulated current at a temperature well removed from the maxima is therefore dominated by the shallower trap.

The method suggested by Franks and Keating which requires an individual peak so that T' and T'' can be determined on the rise and fall sides of the maximum respectively can only be used when a single peak is present, or extensive cleaning has been achieved. Thus their method was clearly unsuited to an analysis of the double peak under discussion.

The occurrence of the 0.41 and 0.83 eV peaks was strongly dependent on the physical condition of the crystals. Thus this double peak was that which replaced the peak at $\sim 0^{\circ}C$ (0.25 eV) after strong illumination at room temperature. The details are discussed in section 12.1.

Agreement between the values of cross section ($\sim 10^{-20} cm^2$) obtained for the 0.41 eV traps for several crystals was quite good, but was very poor for the 0.83 eV traps. This result might have been expected because the larger cross section, associated with the latter, increased the extent of retrapping, which leads to greater inaccuracies in estimating cross sections. The situation is not quite as simple as this in fact and a more complete explanation is given in section 12.2.

Even with the 0.83 eV traps, however, the recombination

mechanism could not be described as a fast retrapping process. This conclusion was reached from the disagreement between the value of energy depth calculated according to Bube, and the occurrence of a long photoconductive decay which was approximately exponential and was associated with traps at a depth of 0.83 eV. That fast retrapping did not occur was confirmed by measurements on the crystals R1 and S3 which showed that the temperature of the current maximum was independent of the density of filled traps.

The traps may be of the same kind as those described by Wright[56]. This possibility will be discussed in section 14.5.

11.6 The Traps at a Depth of 0.63 eV.

These traps gave rise to the only peak observed which was thought to be produced under fast retrapping conditions. The reasons which led initially to this conclusion were (1) The agreement of values of energy depth, calculated using Bube's Fermi level analysis, with values obtained from all the remaining methods (see table 11.4). (2) The almost complete failure to observe an exponential decay in photoconductivity associated with a trapping level at 0.63 eV. Additional support for the idea that the cross section of these traps is large, was the discovery by another member of the group that traps at a depth of 0.61 eV were the most important in space charge limited current

measurements.[57]

One apparent inconsistency with this interpretation is that the traps at 0.83 eV might have been expected to have an even larger cross section, but it would appear that these had not emptied under fast retrapping conditions.

It is not possible to measure cross sections of traps when fast retrapping occurs, but the cross section of the recombination centres involved can be estimated (see section 7.5(i)) if a single set is assumed. The cross section for recombination was calculated from the experimental information on the 0.63 eV traps, using Boer et al's theory. The values obtained are compared in table 11.6 with those for the "capture cross section" of the 0.83 eV traps calculated on the basis that these deeper traps are associated with monomolecular processes. This comparison emphasizes the apparent inconsistency. According to the calculations the cross section of the traps at 0.83 eV is much larger than that of the recombination centres so that fast retrapping should occur.

The peaks in crystals $S5_V$ and $S6_V$ at 270°K were probably due to an entirely different set of traps. They are examples of the peaks from which accurate values could not be obtained because of the considerable overlapping and the small maximum currents.

The standard deviation in the values of energy depth

TABLE 11.6

Crystal	(1) (cm^2)	(2) (cm^2)
S4	3×10^{-18}	10^{-12}
S5	5×10^{-18}	10^{-12}
$S5_v$	10^{-19}	10^{-13}
VI	10^{-19}	
P2	5×10^{-19}	10^{-13}
S3	5×10^{-19}	
R1		10^{-16}
R2		10^{-14}
$S4_v$		10^{-16}
Ave	$10^{-18} \times 10^{\pm 1}$	$10^{-14} \times 10^{\pm 2}$

COMPARISON OF THE CROSS SECTIONS BETWEEN

(1) RECOMBINATION CENTRES ASSOCIATED WITH THE EMPTYING OF THE 0.63 eV DEEP TRAP AND

(2) THE TRAPS AT A DEPTH OF 0.83 eV ASSUMING MONO-MOLECULAR KINETICS.

of the 0.63 eV traps as measured by Bube's formula was only 0.01 eV for any one crystal. The values for different crystals however did not agree with one another to the same extent. The reason was that the dimensions of the irregularly shaped crystals could not be measured accurately which led to errors in the Bube value of between 5 and 10%.

The few values differing greatly from 0.63 eV in table 11.4 are the result of insufficient thermal cleaning of peaks (E_{GG} in crystals S3 and S5), and a variation in the number of filled traps (E_{HA} and E_{HR}) at the beginning of the heating schedule.

The agreement between the results obtained using Bube's method with other methods, which are also valid under fast retrapping conditions and which are independent of crystal dimensions, substantiates the assumption that the bulk properties of the crystals were being measured.

11.7 Summary.

The trap parameters found by the thermally stimulated current and photoconductive decay measurements are summarised in table 11.7. The errors quoted are the observed experimental errors. Allowing for theoretical inaccuracies, the probable errors vary from 5 - 10% for the deeper traps to 10 - 15% for the shallower traps.

TABLE 11.7

Energy Depth eV	cross section cm^2
0.051 ± 0.002	$5 \times 10^{-24} \times 10^{\pm 1}$
0.14 ± 0.01	$10^{-22} \times 10^{\pm 1}$
0.25 ± 0.01	$5 \times 10^{-24} \times 10^{\pm 1}$
0.42 ± 0.02	$10^{-20} \times 10^{\pm 1.5}$
0.63 ± 0.02	
0.83 ± 0.02	$10^{-14} \times 10^{\pm 2.5}$

SUMMARY OF PARAMETERS OF TRAPPING DEFECTS.

CHAPTER 12

Photochemical and Other Effects.

12.1 The Photochemical Reaction and the Filling of Traps.

It is not always possible to decide if the disappearance of a thermally stimulated current peak on remeasurement after some particular treatment is due to: (1) the corresponding traps being destroyed, (2) failure of the traps to fill with electrons at the lowest temperature employed or (3) a decrease of the photoconductive gain, which would result in loss of overall sensitivity, and the possible failure to detect a peak when the number of traps had not changed.

In connection with (3) above, the gain (as determined from measurements of the photoconductivity) changed by about an order of magnitude as a result of treatments such as heating to 100^{o}C in vacuum or subjecting the crystal to intense illumination. This effect was not large enough to explain the observed variations in the size of thermally stimulated current peaks.

With regard to (2), in view of the high intensity illumination used to fill the traps, it is unlikely that the traps would not be filled on this account, but it is possible that optical quenching processes could empty them.

It is unlikely that all traps would be completely empty even if quenching processes did occur, since all the illumination is switched off at the same time.

The appearance of one peak as another disappears suggests they are related in some way, which depends on the treatment given. Thus it is quite clear from the experimental results that the effects of type (1) above do occur, and in particular photochemical effects can be presumed to be responsible. Whether there is a one to one relationship between traps which are created and those which are destroyed cannot be confirmed until measurements of the densities of the traps associated with the stimulated current have been made.

Variations in the thermally stimulated currents observed after heat and optical treatments of two typical crystals will now be described in detail. It was concluded that two effects occurred. The first (i) was thought to involve a well defined chemical reaction, but the second (ii) might be due at least in part to variations in photo-conductive gain, or to quenching phenomena.

(i) Changes in the Thermally Stimulated Current of Crystal R1.

Figure 12.1 shows the peaks observed in the various thermally stimulated current measurements made on the crystal. In every case the crystal was heated to 370^{o}K in the dark before the treatment stated, and illuminated at

90°K before the thermally stimulated current was determined. Figure 12.1 shows the thermally stimulated current:-

(a) After cooling from 350°K to 90°K in the dark, (the peak due to traps at 0.25 eV is very much in evidence).

(b) After irradiating with intense illumination (1000 watt tungsten lamp at 1 ft.). (The peaks with energy values of 0.83 and 0.41 eV are present in the thermally stimulated current curve and the peak corresponding to the 0.25 eV traps is greatly reduced).

(c) After illuminating with red light (7100 Å), obtained using an interference filter.

(d) After illumination with green light (5460 Å), also obtained using an interference filter.

The inference from these results is that the traps at 0.25 eV were created by heating the crystal in vacuum in the dark. However, they disappeared and were replaced by traps at 0.83 eV and/or 0.41 eV after illumination at room temperature. Whether one or other, or both of the deeper traps were formed depended on the wavelength of the illumination used. Unfortunately, because of their small size it was not possible to determine which of the peaks in curves (c) and (d) of figure 12.1 was equivalent to which of the sets of deeper traps. From the measurements

on the double peak it does, however, seem likely that the 0.41 eV traps were formed by the red illumination. This is in agreement with photon energy indications (i.e. the high photon energy causes greater change in energy depth).

The absence of traps at 0.25 eV in some crystals, and the significance of this fact in attempting to establish the possible physical nature of the defect is discussed in section 14.4.

(ii) Changes in the Thermally Stimulated Current of Crystal $S6_V$.

Crystal $S6_V$ was also heated to 370°K before any particular treatment was given. The treatment and trap filling now however, consisted of illumination at a series of temperatures over the range of temperature attainable. After illumination the crystal was cooled to 90°K in the dark, and then heated at a linear heating rate to obtain a glow curve without any further illumination at the lowest temperature. The subsequent stimulated current curves for three different temperatures of illumination are shown in figure 12.2. Illumination at 90°K did not produce any peaks above 200°K. The temperatures at which the crystal was illuminated before the curves shown in figure 12.2 were obtained were (a) 370°K to 90°K (b) 220°K (c) 350°K.

It is to be expected that peaks, which normally

appear at temperatures below that at which the illumination filled the corresponding traps, would be absent in a subsequent thermally stimulated current run. This was in fact confirmed. In addition, however, some peaks which normally appear at much higher temperatures, were not observed if the temperature of illumination was less than a certain value, e.g. after illumination at 220°K, the peak at 350°K (due to traps at 0.63 eV) was missing, but illumination at higher temperatures (e.g. 270°K) produced the peak at 350°K. It was not always clear whether this was due to some quenching process, or more probably to a photochemical reaction, which either destroyed the traps responsible for the peaks or reduced the photoconductive gain by affecting the recombination centres.

Most of the traps discussed in the previous chapter appeared only after certain treatments. A summary of the conditions under which a particular peak was observed is given below in terms of the energy depth of the traps responsible for the peaks.

Trap Depth.	Prior treatment necessary in order to observe the associated peak.
0.05 eV	Treatment independent.
0.14 eV	After heating to 370°K in the dark and cooling in the dark.
0.25 eV	After heating to 370°K in the dark and cooling in the dark.
0.41 eV	After illumination (with red light particularly)
0.83 eV	After illumination (with green light particularly)
0.63 eV	After illumination (above 250°K).

12.2 The Photochemical Reaction and Retrapping.

There are several possible explanations of the apparently anomalous situation concerning the discrepancy between the suggested recombination kinetics and the magnitude of the cross sections for the 0.83 eV and 0.63 eV traps (see section 11.6). Only the fourth possibility discussed below is thought to fit the facts reasonably well.

(1) A set of recombination centres with very large cross sections may exist and may be responsible for the 0.83 eV traps emptying under monomolecular conditions. However, in order that such large cross section centres should have little effect on the recombination process when the traps at 0.63 eV are being emptied, they must become trapping levels by the time the 0.63 eV traps have started to release electrons into the conduction band. To do this they must cease to become recombination centres when the hole demarcation level has passed through them (not the electron demarcation level). If this happens it is surprising that the defects always changed from recombination to hole trapping centres in the small temperature range between the appearance of the 0.83 eV peak and the 0.63 eV peak. There is no other evidence for the existence of such levels.

(2) The magnitude of the cross section of the recombination centres may change rapidly with temperature. However it is very unlikely that the cross section of a set

of recombination centres could change by a factor of 10^3 for a temperature change of less than 20%.

(3) It may be that the conclusions concerning the types of kinetics are incorrect, due to the fact that surface rather than bulk properties were being measured. The evidence which contradicts this view is as follows:-

(i) The 0.83 eV peak could not have been produced under fast retrapping conditions. If it were then the trap depths yielded by calculations following Bube should be valid and should agree from crystal to crystal and with other methods. This was not in fact observed. To explain the discrepancy in terms of surface effects the crystal would have had to be inhomogeneous to such an extent that the 100 volts applied were dropped across a barrier less than 10^{-4}cm. thick. This would be impossible as the crystal would break down under such a high field of 10^6v/cm.

(ii) The evidence that the 0.63 eV peak was formed under fast retrapping kinetics was very strong. The agreement between values calculated according to Bube and other values was within the limits of experimental error. The fact that space charge limited current measurements have shown traps at this depth to be important in limiting the current found in very thin plates suggests that these traps must have a large cross section. The value of ~~the~~ cross section ~~for~~ these traps would have had, if it were correct

to assume monomolecular kinetics, has been calculated. This value is of such a magnitude ($\sim 10^{-18} cm^2$) that at least some retrapping would have been expected. The extent of retrapping would vary from crystal to crystal and thus cause a much wider range of temperatures at which the peak maximum would occur than was observed. The almost complete absence of a long approximately exponential decay of photoconductivity would be surprising if the kinetics were monomolecular.

All these arguments support the suggestion that the traps at 0.63 eV are emptied under fast retrapping conditions while those at 0.83 eV are associated with monomolecular processes.

(4) It is suggested that the best explanation of these facts is as follows. The 0.83 eV peak was destroyed by heating the crystal in the dark (as was shown in the crystals R1 and R2 for instance). It seems possible that the provision of thermal energy destroys the 0.83 eV trap, which is a complex defect, and either releases an electron into the conduction band simultaneously, or an electron is excited from one of the resultant new defects almost immediately. The concept of electron capture cross section then ceases to have any meaning. A limited amount of retrapping would be possible if only a small fraction of the traps were initially full, but in general the results indicate that the freed electrons take part in a monomolecular

recombination process.

One objection to this suggestion is that in crystal $S6_v$ two peaks at different temperatures, T^* are both attributed to traps at an energy depth of 0.83 eV. This is explained by the experimental fact that the higher temperature peak appeared only after the crystal had been illuminated at 350°K, and the two peaks were never present simultaneously. The lower temperature peak is that solely due to the trap complex ascribed to an energy depth of 0.83 eV.

If the further assumption is made that the trap complex is stable at temperatures even higher than 300°K, T^*, provided it has not captured an electron, the higher temperature peak can be explained. Illumination at 350°K would tend to produce the trap complex and fill it, but the complex would be destroyed as soon as it were filled. As a result the immediate cooling on cessation of the irradiation would lead to a number of unfilled trap complexes. When the crystal was subsequently heated, nothing would happen until the traps at a depth of 0.63 eV started to empty. The freed electrons would be captured by 0.83 eV trap complex and held there before excited into the conduction band. In this way a peak characteristic of the 0.83 eV traps would be obtained in crystals containing traps at 0.63 eV. The peak produced in this way has a maximum about 10°K higher

than the 0.63 eV peak. This would suggest the life time in the 0.83 eV trap complex is of the order of several seconds, which seems surprisingly long in view of the elevated temperature, but is otherwise in agreement with this theory.

A phenomenon which supports the above explanation is the absence of any long decay that could be connected with the 0.63 eV trap, in crystal $S6_V$. Such a decay would have been expected to be present, although not exponential in shape. Using the ideas developed here, the 0.63 eV traps would on emptying be expected to produce an exponential decay characteristic of the 0.83 eV traps. Such decays were found.

Another aspect of the complicated behaviour of the traps at 0.83 eV is that wide differences are observed in the temperatures at which the peak maximum appears in different crystals. Such variations are not characteristic of the monomolecular recombination. This could be due to differences in initial occupancy of the traps, differences in the defect density, or delays in the emission of the electron after the complex had been destroyed.

Some evidence that a reaction of some sort took place when the crystal VI was heated in the dark is discussed in section 12.3 (iv). The activation energy for the reaction was 0.88 ± 0.05 eV.

12.3 Other Methods of Evaluating Defect Parameters.

(i) Slow Rise of Photocurrent under Weak Illumination.

This phenomenon was discussed in section 5.1 (2). By measuring the height and time length of the plateau, the density of traps and cross section can be obtained. The value of trap density is not critical to the present investigation and the cross section is only of interest in conjunction with values of energy depth. Because of this only an exploratory investigation of the method was made. Some of the results are shown in the curve in figure 5.1.

Well defined plateaux were observed, though sometimes at current values which were too small to be measured accurately with the equipment available. Correlation with specific traps may be possible by comparing the values of cross section, and noting the temperature above which the various plateaux were not observed. The fact that two curves obtained with the same crystal at the same temperature, but with different light intensities, were found to possess plateaux with lengths in time inversely proportional to the final value of conductivity, was in good agreement with theory. The method would appear to be most promising for evaluating trap densities.

(ii) Photoconductivity as a function of Temperature.

In most crystals the usual trend is for the steady state photocurrent to decrease as the temperature is

increased. Superimposed on the general decreasing trend there is often a steep temporary rise as the temperature passes through certain values see figure 10.2.

The position of the electron quasi-Fermi level was calculated for all the steep increases in photocurrent which were observed. The results are shown in table 12.1. The crystals R3 .....R7 were ones which showed comparatively low photosensitivity and no appreciable thermally stimulated currents.

In crystals on which detailed measurements were made the quasi-Fermi energy depths obtained from the photoconductivity v temperature measurements were different from trap depths found by thermally stimulated current measurements. Thus it is unlikely that the sudden steep increases in photocurrent are due to the electron Fermi level passing through a set of levels which then cease to act as recombination centres and start to act as traps. There would appear to be two possible explanations of the sudden increases in photocurrent.

(1) Defects may cease to act as recombination centres because the hole demarcation level has passed through them.

(2) The recombination centres may have been destroyed in a photochemical reaction (see section 14.8). The second suggestion is favoured by the fact that the higher temperature increases ($\sim$ E = 0.3 eV) in photocurrent only

occurred when the crystal had been placed in the dark and heated to 370°K, and then cooled prior to measuring the photocurrent as a function of temperature. In this connection it should be noted that the measurements were made while the temperature was increasing slowly (~ 0.1°/sec.).

There was often an increase in photocurrent near the lowest temperature limit of measurement (~ 100°K). This was quite separate from the rise of photoconductivity when the illumination was switched on. The energy depth of the electron quasi Fermi level at these temperatures was about 0.14 eV. The fact that the steep rise in photocurrent when the Fermi level reached a distance of 0.14 eV from the conduction band, even when traps at this depth were not detected by thermally stimulated current measurements, suggests that traps at this energy depth might have been present in more crystals than was apparent from the glow measurements. This was a distinct possibility since the traps at 0.14 eV might sometimes be already empty at liquid air temperatures in the dark. To resolve this problem glow measurements starting at temperatures much lower than those of liquid nitrogen would be necessary.

(iii) Spectral Response.

In general spectral response measurements showed no well defined maxima of photoconductivity on the long wavelength side of the absorption edge, though the crystal was

sensitive for some way into this region (see figure 12.3).

In crystal R1 however there was some indication of a peak at 6100 Å when the measurement was made at about 100°K. The separation from the wavelength of maximum photosensitivity represented 0.45 ± 0.05 eV. This is in good agreement with the trap depth at 0.41 eV. If this observation represents a genuine correlation it would imply that the photocurrent excited by irradiation at 6100 Å is due to the motion of holes. This speculation could be checked by measuring the photo-thermo-electric or photo-Hall effect.

(iv) Dark Current.

It was mentioned earlier that donors were produced in the crystal VI after heating the crystal in the dark at temperatures above 200°K. A plot of $\log_e I_D$ against 1/T gave a straight line between 180°K and 400°K. I_D is the measured dark current. Neglecting the change in N_c and μ with temperature, the calculated slope (E_D/k) gave E_D = 0.53 ± 0.03 eV, where E_D is the donor depth. It is possible though unlikely in this case, that the slope should be $E_D/2k$ which would lead to an energy depth of 1.06 eV.[58]

The activation energy for the process leading to the production of the donors was found from measurements of the variation of dark current at constant temperature over the range 350°K to 400°K. The curves were analysed in terms of

a time constant t_d where the current after a time t is given by $I = I_\infty (1 - \exp(-t/t_d))$. I_∞ was the final current at this temperature. A plot of $\log_e t_d$ against $1/T$ gave a straight line of slope E_d/k with $E_d = 0.88 \pm 0.05$ eV (see figure 12.4). This activation energy is the energy required to create the donors in question.

This could be regarded as added evidence for the suggestion that the apparent trap depth energy 0.83 eV is the energy required to destroy a complex defect. The fact that the process produced a significant density of donors at 0.5 eV in one crystal only was surprising.

CHAPTER 13.

Comparison of the Methods of Evaluating the Thermal Glow Curves.

13.1 Introduction.

The chief reason for the work done during the present investigation was to decide on the most suitable method of evaluating conductivity glow curves, and to determine whether the results obtained were meaningful. It is difficult to give a universal rule as to which method of analysis is most suited to a particular peak in the glow curve, since this depends not only on the recombination kinetics but also on the extent of overlap with other peaks. The various methods of analysing individual peaks are discussed below.

13.2 Bube's method.

This method, which involves determining the position of the electron quasi Fermi level, gave accurate results for fast retrapping only. Similar remarks apply to the technique for Boer et al (see section 7.5(i)). This is a great disadvantage, particularly if the method is applied indiscriminantly. This is liable to happen since the method offers no means of determining whether fast retrapping does in fact occur. The method cannot give any information about trapping cross sections as is sometimes claimed. Even

if Bube's method of determining energy depths is valid (fast retrapping conditions) no information can be obtained about the trap cross section because the cross section does not affect the peak parameters under fast retrapping conditions. Under these circumstances the electrons in the traps and the electrons in the conduction band are in thermal equilibrium with one another, and the recombination is dominated solely by the nature of the recombination centres. If fast retrapping does occur, it is however possible to calculate the cross section for electron capture of these centres. This can be most useful as demonstrated by the discussion of the 0.63 eV and 0.83 eV traps in chapters 11 and 12.

13.3 Franks and Keating's method.

Keating's theory is based on the assumption of monomolecular recombination, but the authors claim that the technique gives satisfactory results for energy depths even if retrapping is present. This was confirmed by the present measurements. It is almost the only theory of those considered which allows for some degree of temperature variation of trapping cross sections.

The disadvantages of the method are mainly of a practical nature. For calculations of energy depths the method requires measurements at, and on both sides of the

maximum of the peak being studied. This means that a very clean peak is essential. Usually a peak can be cleaned on the low temperature side by thermal cleaning methods, but beyond the maximum measurements are very difficult and inaccurate if there happens to be a peak at a slightly higher temperature than the one under investigation. The failure to satisfy the requirements of a clean peak resulted in a wide spread of experimental values of energy depth in the present work.

It was found in practice that for clean peaks the experimental values fell within the limits of validity of Keating's mathematical approximations which he used to derive equation (7.4). Energy depth values from peak parameters which lay within these limits of validity tended to agree with values obtained using other methods of calculation.

Theoretically this method allows for temperature variations in trapping cross sections and it might have been expected that the resultant, calculated energy depths would be more accurate than energy depths determined by other measurements. In fact our results gave no indication that this was borne out in practice. Theoretically the failure to allow for temperature variations was found to lead to an accuracy in values of energy depth (except for very shallow traps) of not greater than 15%. The practical

results of the present work produced no evidence of inaccuracy as large as this (see section 13.8).

13.4 Lushchik's Method.

This method is for fast retrapping kinetics but the results were found to differ only slightly from those based on monomolecular theories.

The method suffers from the practical disadvantage that it requires the determination of the half height on the high temperature side of the maximum. As mentioned in the preceding section this was often difficult to obtain. Occasionally, for example at very low temperatures, where the rise side of the peak was inaccurate due to an unavoidable non-linear heating rate, this method had some advantages.

13.5 Methods Utilising Variable Heating Rates.

These methods have the advantage of applying for any kinetics (except for Schon's treatment under certain circumstances). They suffer from the disadvantage of requiring the same initial density of filled traps, and unchanged values of photoconductive gain for each curve obtained at a different heating rate.

In the discussion of the results in chapter 11 any apparent inaccuracies in the magnitude of a trap depth obtained by these methods was attributed to the process of thermal cleaning which necessarily alters the initial density of filled traps. This was only one of the causes of error.

As described in detail in chapter 12 the density of filled trapping levels depended strongly on the thermal and optical treatments given to the crystal. Also there was often a gradual variation in the properties of the crystal over a period of time. The period of time involved for an appreciable change in properties varied from hours to days. For these reasons it was difficult to reproduce the same density of filled levels for measurements at different heating rates.

Making all the measurements within as short a time as possible ($\sim$ 10 hrs.), and taking care to illuminate the crystal for the same length of time, at the same temperature, with the same intensity and spectrum of illumination, often led to satisfactory results for uncleaned peaks.

The lack of thermal cleaning threw some doubt on the validity of results where extensive overlapping occurred. As mentioned earlier methods based on the variation of the heating rate require measurements of the maxima of the peaks (T^* and I^*) only which is a considerable advantage. The results obtained were fairly satisfactory, though the accuracy obtained was not high.

Another slight disadvantage, compared with other methods, was that variable heating rate methods require several runs before a value for an energy depth can be

obtained.

In general the most important feature of these methods is that they form a useful guide where values obtained by methods which assume monomolecular or fast retrapping kinetics do not agree.

13.6 Halperin and Braner's Approximation.

This theory had the advantage of providing formulae applicable to both monomolecular and bimolecular kinetics, and rules for deciding which of the formulae to use. In practice all the observed peaks, according to Halperin and Braner's rules of distinguishing the nature of the recombination processes, were associated with bimolecular kinetics. This was a surprising conclusion especially for traps with very small cross sections, so that considerable doubt is cast upon this method of determining whether the kinetics are first or second order.

The method is not applicable when $E/kT^{*} < 10$, because the correction factor involved is then too large. A value of E/kT^{*} as small as this was only occasionally found, and most other methods were also inaccurate under these conditions.

The theory is based on a geometrical approximation which involves representing an isolated glow curve as a triangle. The validity of this procedure is questionable, and may explain why the resulting trap depths were often

higher than the values given by other methods employing the same parameters (e.g. Grossweiner).

The fact that Halperin and Braner's technique requires a measurement of the half width on the rise side of the peak only is an experimental advantage, but the Grossweiner method appears to be at least as accurate, simpler in use, and in addition provides more information.

13.7 Grossweiner.

Mention of some of the advantages of Grossweiner's method is made in the previous section. The theory deals solely with monomolecular kinetics and is limited by the assumption that $N_c Sv$ is independent of temperature. No evidence of inaccuracies due to failure to limit its use to situations where these conditions obtained was found. This agrees with Keating's[37] theoretical conclusions. He predicted that estimate of energy depths using the Grossweiner technique should be insensitive to variations in cross section with temperature.

Apart from a few exceptions (e.g. peaks near the lowest temperature of the thermally stimulated current curve) the method gave good results for all the peaks present. The magnitude of the capture cross section, and the photoconductive decay time at the temperature of maximum current can also be determined easily by this method of analysis.

13.8 Garlick and Gibson's initial rise method.

This is the only method which theoretically is valid for any kinetics, and at the same time allows for the variation of the cross section as a power of temperature. To allow for the temperature variations of cross section it is necessary to use equation 7.1 which contains the extra term b $\log_e T$ where the cross section $S = S_o T^{b-2}$, S_o and b are constants. In practice it was found that the extra term had only a small effect for reasonable values of b($b < 3$) except for the very shallow traps. The agreement between values of energy depth obtained by this method, and those obtained by other methods which do not allow for variations in the value of S or of $N_c Sv$ leads to the conclusion that the temperature variation of cross section could usually be neglected in evaluating trap depths.

The method has the advantage over other techniques that in many cases the stimulated current is measured over a wide range of temperature ($\sim 100^{\circ}K$), so that accuracy in temperature measurement is not so critical. As long as the temperature variations in $N_c v S \mu \tau$ are negligible this method in turn leads to accurate values.

Thermal cleaning is particularly useful, when studying the initial rise of the glow curve, and makes measurement possible over such a wide range of temperatures that the criticisms of Haake are overcome. Haake states that equation

7.1 is valid on the rise side of a peak to a certain temperature, which is usually about 20°K below T^{*}.

The main disadvantages associated with measuring the initial rise are:-

(1) The method is insensitive for deep trapping levels in the presence of shallow trapping levels. For example it was pointed out in section 11.5 that Garlick and Gibson plots on the double peak due to traps at 0.41 and 0.83 eV almost always had a slope characteristic of the 0.41 eV traps. The explanation of this was given in that section.

On the other hand there is the equivalent advantage that it is possible to obtain energy values for shallow traps whose peaks are almost completely hidden by a set of deep traps (e.g. 0.25 eV traps in the presence of 0.41 eV peak in crystal P2).

(2) It is necessary to assume that $N_c v S \mu \tau$ does not vary over a wide range of temperature unless the accuracy of the measurements allows its variation to be calculated assuming it varies as a power of temperature.

(3) It is difficult to apply the technique to peaks near the lower limit of temperature, but this is balanced by its effectiveness on peaks with a current maximum just beyond the high temperature limit of measure.

(4) A more extensive set of measurements on the curves rather than the usual determination of the three points at T', T^{*} and T'' is necessary, although this is balanced by

the fact that only one thermally stimulated current curve may be needed to obtain an accurate value of energy depth. In addition when automatic curve tracing is used this is not a serious handicap.

The adaptation of this method to investigate whether peaks were due to a set of traps at a discrete energy depth, or to a continuous distribution of traps is extremely useful (see section 11.5 and reference 42).

The inaccuracies of this method arise from temperature variations in S and τ. In principle the extension due to Keating is useful in this respect, but in practice the slow variation with temperature of the extra term usually makes it impossible to estimate the temperature variation of these parameters from the curvature of the peak (assuming $S\tau$ proportional to a power of T). The magnitude of the errors involved can be obtained from Table 7.1 assuming reasonable values of S and b. The low values of E, even in the range of applicability mentioned by Haake, are at least in part probably due to the temperature variation of cross section.

13.9 Photoconductivity Decay Measurements.

The measurements of the long tail in the photoconductive decay are useful in confirming whether monomolecular kinetics are applicable for a particular set of traps. Monomolecular recombination is associated with a long exponential decay

as mentioned in section 6.4.

The value of energy depth obtained from the slope of these lines agreed well with values obtained from the thermally stimulated current measurements. The cross section values also showed good agreement (see the tables of results).

The method was limited to situations where monomolecular kinetics apply and assumed that $N_c v S \tau \mu$ was independent of temperature. The values obtained from decay measurements were usually employed to confirm the values obtained from the thermally stimulated current measurements.

CHAPTER 14.

Comparison of Results with those of Other Workers.

14.1 Introduction.

Table 14.1 shows the comparison of the results of the present work with those reported by other workers in respect of energy depths and the temperatures of current maxima. The latter are included in the table as this acts as a good guide towards identifying equivalent peaks in different crystals, particularly if the conductivities of the crystals are the same, or the energy depth values for the traps causing the peaks are the same.

Comparisons with values based on Bube's method of calculation are only reliable for fast retrapping or where the behaviour of a peak under different physical conditions can lead to a reasonable correlation. Agreement between maximum temperatures and the energy depths obtained following Bube can be taken to indicate a high probability that two peaks in different crystals are equivalent.

Agreement with trap depths measured by other workers which are enumerated in table 14.1 is clearly good. In contrast with other reported results the crystals used in this work gave no indication of the existence of traps at depths of about 0.33 eV and of 0.5 eV, though donors were found at 0.5 eV in crystal VI. With respect to the

values of Woods and Wright,[63] and Bube and Barton[64] quite good correlation with other results is possible. For example in the work of Woods and Wright maxima were found under different conditions at 270°K and 320°K. Similar peaks appeared under the same conditions and at the same temperatures in the present work, and almost certainly the peaks in the different crystals are due to traps of the same two types emptying their electrons into the conduction band.

14.2 Nature of Defects.

For an accurate determination of the nature of the defects important in the trapping and recombination processes in cadmium sulphide, detailed investigations of the variation of trap densities under controlled treatments and addition of impurities is necessary.

At present, however, several suggestions can be made on the basis of the limited treatments given to crystals studied in the current work, and comparisons with other results published in the literature.

14.3 The Traps at Energy Depths of 0.05 eV and 0.14 eV.

Care must be taken in determining which crystals show the presence of traps at 0.05 eV and 0.14 eV from the evidence provided by thermally stimulated currents. This is because some peaks are too near the low temperature limit of the thermally stimulated current curves for a linear heating rate to be guaranteed, so that no reliable calculations

could be made on them. Several of these peaks were probably due to the emptying of traps at 0.05 and 0.14 eV. The shallower of these two sets of traps has previously been observed by Franks and Keating[55], and Trofimenko[59], but in neither paper was the nature of the defects discussed. Franks and Keating analysed the thermally stimulated current peak they obtained by their own method (see section 7.2 (i)), and a comparison of the results of the present work and their's was made in section 11.2. Trofimenko detected the presence of the traps by photoconductive decay measurements.

Niekisch,[60] using an alternating light measuring technique found a set of traps at about 0.12 eV; as did Sokol'skarya,[61] but only by assuming the "usual thermally stimulated current formula were applicable under space charge limited current conditions." Clayton[62] using Grossweiner's method of calculation found traps at this depth, together with other associated traps with an energy depth of 1.0 eV at certain heating rates. No evidence was found for this second peak in the present work even though the same values of heating rate were used.

On the basis of a possible connection between the green edge luminescence and the 0.12 eV traps, Niekisch suggests these traps are sulphur vacancies (or interstitials). The present work shows, in agreement with Niekisch, that there

is a tendency for the traps to disappear after illumination at room temperature. In our work, however, they were found to reappear after heating the crystal to 350°K in the dark.

Comparison with the measurements of Woods and Wright[63] and Bube and Barton[64] is more difficult. Bube and Barton found peaks due to traps with energy depths calculated by Bube's method at 0.20 and 0.25 eV. The peaks were at similar temperatures to those of the 0.05 eV and 0.14 eV traps in the present work. The traps observed by Bube and Barton were probably of the same form as these. See table 11.1 for the depths of the 0.14 and 0.05 eV traps calculated using Bube's method.

Bube and Barton suggested they were sulphur vacancies. Woods and Wright however attributed a peak at about 120°K to chlorine. The present work showed little indication as to the nature of the defects though the 0.14 eV traps were apparently produced in one crystal after heating in vacuo. This is in agreement with the sulphur vacancy theory. 0.14 eV does however seem rather deep for the V_S^{--} configuration. The traps at 0.05 eV seem more likely to be of this form, although even these are rather deep for a doubly charged sulphur vacancy. It is for instance on the limit of Kroger[65] et al's estimate of $\leq$ 0.05 eV. Applying the formula based on the simple hydrogen-like model (see section 1.10), using the crystal dielectric

constant (11.6) and effective mass (0.25m) the calculated value of energy depth for the V_S^{--} is 0.025 eV. This is a rather low value even allowing for inaccuracies in assuming such a simple model.

It is clear however that since both the defects have a very small cross section they must have a strong negative charge.

14.4 Traps at 0.25 eV.

Niekisch (alternating light measurements), Trofimenko (activation energy plot), Unger[66] (photo/glow measurements), Broser[67] (glow curves) and Sokol'skarya (conductivity glow under space charge limited current conditions) all found traps at about 0.25 eV. The photochemical reaction described by Woods and Wright is similar to one observed in the present work (see section 12.2). This confirmed that the traps at 0.25 eV were due to the same type of defect as those causing the 270°K peak in Woods and Wright's investigations and probably also the Bube and Barton measurements.

Niekisch, however, observed traps at this depth only after illumination, contrary to the photochemical effects described in the present work. Taking the photochemical reaction as a safe guide, the traps estimated to be at 0.3 eV by Neikisch would appear to be identical with the 0.25 eV traps found in the present work.

In any event Niekisch, Woods and Wright, and Bube and

Barton all attribute traps at this depth to sulphur vacancies, or a complex including sulphur vacancies. This is because they were found in cadmium rich crystals. The small cross section is consistent with the possibility of the defects being V_S^- vacancies. Trofimenko found the same traps in sulphur rich crystals but also concluded that the defect had a negative charge.

In one crystal $S5_V$ a continuum of thermally stimulated current was found after heating in the dark. It appeared over a range of temperatures from 170°K to 270°K and reheat measurements as described in section 11.5 gave Garlick and Gibson energies in the region of 0.25 - 0.3 eV.

14.5 The Traps at 0.41 eV.

Traps at a depth of about 0.41 eV have been reported regularly in the literature. Niekisch (alternating light measurements), Unger (photo/glow measurements), Broser and Broser-Warminsky[68] (thermally stimulated current and decay measurements), Brophy and Robinson[69] (noise measurements), Bube and Macdonald (photo-Hall measurements), G. T. Wright[56] (primary thermally stimulated currents), and Lappe[70] and Tamaka[71] have all observed traps at about this depth. Some of the methods of observation and calculation are open to criticism (e.g. G. T. Wright's arbitrary assumption of a value for cross section) but there is good evidence for a trap at this depth apart from the present work.

From the nature of the photochemical reactions observed, either these traps or those ascribed to 0.83 eV must be equivalent to those causing the 320°K peak in the Woods and Wright measurements. Surprisingly Niekisch found the traps at this depth took no part in photochemical reactions.

14.6 Electron Excitation by 0.83 eV Phonons.

The only reliable reports of electron traps as deep as 0.83 eV are by Smith[72] (space charge limited currents) and Niekisch (in a few crystals 0.75 - 0.8 eV by his own unique method). It is also worth noting that quenching centres at a height of 1.65 eV from the valence band[73] would be in the same region in the energy band scheme.

Niekisch attributes the defects to sulphur vacancies or interstitials but admits some doubts about these deep traps because of uncertainties due to the onset of photochemical reactions. This is in agreement with the present work and the presence of a photochemical reaction led to the conclusion in section 12.2 that the 0.83 eV probably represented the dissociation energy for a trap complex rather than the depth of a trapping level below the conduction band.

The 320°K peak of Woods and Wright (mentioned in the last section) was suggested by them to be due to a complex of Cu^{+} or V_c^{+} with Cl^{--} or V_A^{--}. This could be a possible

configuration for the defect disrupted by a 0.83 eV phonon.

14.7 The Traps at a Depth of 0.63 eV.

The peak associated with these traps was the only one in the present work thought to have been produced under conditions of fast retrapping. The comparatively large cross section of these traps implies that they would be the most important in space charge limited current measurements. Marlor and Woods[57] and Sokol'skarya observed these traps in this way (the measurements of Marlor and Woods were made on crystals grown in the same batches as crystals P1, P2, S1, S2, S3, S4 and S5 used in this work). Niekisch (alternating light measurements), Unger (photo-glow measurements), Brophy and Robinson (noise measurements), and Bube and Barton (Bube analysis of thermally stimulated current runs), all found traps at about this depth. The good agreement with Bube and Barton adds weight to the argument that these traps empty under fast retrapping conditions.

Niekisch found these traps only rarely. Bube and Barton suggest the traps are due to anion vacancies, probably V^{+}_{Cd}, on the basis of the way in which chemical and heat treatment of the crystals affected the peak due to these traps. This is in agreement with our observations in as much as the traps at this depth only appeared in crystals

in which the peak due to 0.25 eV traps (ascribed to sulphur vacancies) was absent. There was however no evidence that heating the crystals in vacuo destroyed these traps. The fact that the traps had a large cross section means they must have a neutral or positive charge. This is in agreement with the suggested interpretation in terms of cadmium vacancies.

14.8 The Absent Traps.

The two depths at which traps have been widely reported, but not observed in our crystals are at 0.33 eV and possibly 0.51 eV. The occurrence of traps at 0.33 eV has been described by Brophy and Robinson (noise measurements), Bube and Macdonald[17] (photo-Hall measurements), Unger (photo/glow measurements) and Broser and Broser and Broser-Warminsky. The only evidence to suggest that such traps might be present in our crystals was a sudden rise in photoconductivity with temperature under strong illumination. This was only observed after the crystal had been cooled in the dark from 370°K immediately prior to making the measurements of photoconductivity as the temperature was slowly increased. In other words it is probable that the passage of the electron Fermi level through an energy depth of 0.33 eV forms an integral part of the photochemical reaction caused by the illumination. The fact that no evidence of traps at this depth was found in thermally stimulated current

measurements could be explained.

(i) by the set of traps involved having a ratio of electron to hole cross section differing greatly from unity so that the electron demarcation level is well removed from the Fermi level

(ii) the effect not being due to electron traps but hole traps near the valence band.

These suggestions could explain the photo-Hall measurements and possibly the noise measurements, but not those of Unger and Broser et al. The other more likely explanation is that the particular defect causing this peak was not present in the crystals investigated here.

The set of traps at 0.51 eV have not been widely reported and only Trofimenko (activation energy plot) and Bube and Macdonald (photo-Hall measurements) can be regarded as having definitely observed such traps. In the present work they were only observed in the crystal grown in vacuo and then as donor levels affecting the dark current. The nature of the defect is not clear, but the crystal was notable for its dark colouration caused by excess cadmium, so that the defect may be connected with a sulphur vacancy, or more likely a complex including an interstitial cadmium ion.

CHAPTER 15.

Conclusions.

The aim of the investigations described in this thesis was to provide a contribution towards the understanding of electron trapping phenomena in cadmium sulphide. The main objective was to evaluate the usefulness of thermally stimulated current method of measurement as applied to cadmium sulphide. The present work has shown that the assumption of discrete sets of trapping levels is justified. It is often maintained that traps are distributed in energy. There was some evidence from a few crystals that there was a distribution of trapping levels in the range 0.25 eV to 0.3 eV, but the predominant peaks were due to traps with the following characteristics:-

The shallowest was at a depth of 0.052 $\pm$ 0.08 eV and had an electron capture cross section of $10^{-24} \times 10^{\pm 1}$ cm^2. The nature of the trap was probably a sulphur vacancy with an effective double negative charge.

The next shallowest trap was at a depth of 0.14 $\pm$ 0.02 eV and had a cross section of $10^{-21} \times 10^{\pm 1.7}$ cm^2. The presence of the defect was only observed after heating in the dark to 370^{o}K. Its nature is unknown, though it may be connected with sulphur vacancies.

The only other defect found after heating in the dark

was at a depth of 0.25 $\pm$ 0.02 eV, and had a cross section of $5 \times 10^{-24} \times 10^{\pm 1}$ cm.^{2} There was strong evidence that the defect was connected with sulphur vacancies possibly V_S^-. In a few crystals the trap distribution from 0.25 to 0.3 eV was found in place of the 0.25 eV traps.

After illumination traps were found at depths of 0.41 $\pm$ 0.04 eV and 0.63 $\pm$ 0.04 eV. The 0.41 eV traps had a cross section of $10^{-20} \times 10^{\pm 1}$ cm^2. The trapping centre at a depth of 0.63 eV had a large cross section, so that the corresponding glow peak was produced under fast retrapping conditions, which means that the actual value of electron capture cross section cannot be calculated. The cross section of the recombination centres could however be calculated from glow data associated with these traps and was found to be $5 \times 10^{-18} \times 10^{\pm 1.7}$ cm.^{2} In view of the large cross section of these traps the defects may be charged cadmium vacancies.

The apparent energy depth of 0.83 $\pm$ 0.06 eV was thought to be the activation energy for the destruction of a trap complex and simultaneous (or almost immediately subsequent) ejection of an electron into the conduction band. A trap complex producing a peak at this temperature has previously been ascribed to the association of Cu^+ or V_{Cd}^+ with Cl^{--} or V_S^{--} .[63]

The suggestions as to the nature of the defects are only tentative, and measurements of the densities of the traps after different physical and chemical treatments would be necessary for more confident suggestions to be offered.

The chief impetus during the present investigation was the need to decide the best way to determine trap depths and cross sections.

Bube's argument was found to give incorrect values except under fast retrapping conditions. The methods of Franks and Keating and Lushchik, and all the methods using a variable heating rate had disadvantages from a practical point of view, Grossweiner's method had certain advantages over that of Halperin and Braner.

To obtain satisfactory results the following procedure should be adopted. The peak should be thermally cleaned as described in the text, and in the first instance Garlick and Gibson's plots and Grossweiner evaluations of energy depth should be made on the clean, isolated peak obtained.

Several qualifications should now be added:-

(1) For traps near the low temperature limit it may be necessary to ignore the Garlick and Gibson method and possibly the Grossweiner method if a linear heating rate is difficult to obtain in this temperature region. In this event either Lushchik's method or the variable heating rate

techniques are used.

(2) The variable heating rate methods are particularly useful if overlapping is too severe for thermal cleaning to be effective. No cleaning of the peaks should be used and consistency in the illumination and heat treatments before measuring the thermally stimulated currents is essential.

(3) If a clean peak is obtained Franks and Keating formula should be employed to determine the variation of cross section with temperature.

(4) If the peak appears to be misshapen the values of energy depth using Garlick and Gibson's, Grossweiner's, and Lushchik's methods should be compared. If they disagree the reheat method of Hoogenstraaten should be used to resolve whether there is a distribution of traps. Comparison between energy values obtained from photoconductive decay measurements and heating rate methods are also useful.

(5) If it is required to determine the nature of the recombination kinetics, agreement of the Bube evaluation with other methods forms a strong indication that the kinetics are fast retrapping. In addition exponential photoconductive decays indicate that the appropriate traps are emptying under monomolecular conditions.

(6) If the kinetics are monomolecular, once E/T^{*} has been determined, equation (7.8) or Grossweiner's formula

can be used to obtain the electron capture cross section.

(7) With fast retrapping kinetics and assuming one set of recombination centres, their cross section can be obtained using Haering and Adams method (equivalent to Boer et al's).

Two other conclusions can be drawn from the present work.

(1) The agreement between values of trap depths calculated using methods which require a knowledge of the crystal dimensions and methods which are independent of the crystal dimensions confirms that measurements of bulk properties were being made.

(2) The agreement between values of energy depths calculated from measurements made parallel and perpendicular to the c-axis shows that any anisotropy of the crystal does not seriously affect the measurement of trap parameters.

REFERENCES.

1. W. Smith, Nature 7, p.303, (1873).
2. H. Lenz, Anm. Physik 77, p.449, (1925).
3. J. C. Slater, Phys. Rev. 103, p.1631 (1956).
4. B. Gudden and R. Pohl, Z. Physik 5, p.176, (1921).
5. B. Gudden and R. Pohl, Z. Physik 3, p.98, (1920).

   B. Gudden and R. Pohl, Z. Physik 4, p.206 (1921).
6. L. Bergmann and J. Hansler, Z. Physik 100, p.50 (1936).
7. A. H. Compton and S. K. Allison, X-rays in Theory and Experiment (D. Van Nostrand 1950).
8. B. D. Saksena, Phys. Rev. 81, p.1012 (1951).
9. D. F. Browne, J. Electronics, 2, p.154 (1956).
10. F. Bloch, Z. Phys., 52, p.555 (1928).
11. R. deL. Kronig and W. G. Penney, Proc. Roy. Soc. A.130, p.499 (1931).
12. J. R. Haynes and W. Shockley, Phys. Rev. 82, p.935,(1951).
13. H. Dember,Phys. Z. 32, p.61 (1931).
14. I. K. Kikoin and M.M. Noskov,Phys. Z. Sowjet. 5, p.63, (1934).
15. T. S. Moss, L. Pincherle and A. M. Woodward, Proc. Phys. Soc. Lond. B 66, p.63 (1953).
16. P. Aigrain and H. Bulliard, C. R. Acad. Sci. Paris 241, p.46 (1953).
17. R. H. Bube and H. E. Macdonald, Phys. Rev. 121, p.473 (1961).
18. R. H. Bube, Photoconductivity of Solids (J. Wiley 1960) p.233.
19. D. C. Reynolds, R. C. Allen and C. C. Reynolds, J. Opt. Soc. Amer. 45, p.214 (1955).

20. R. H. Bube, Phys. Rev. 99, p.1105 (1955).

21. F. A. Kroger, H. J. Vink and J. Volger, Physica 20, p.1095 (1954).

22. do. do.

23. S. Z. Czyzak et al. J. Opt. Soc. America 47, p.209 (1957).

24. F. A. Kroger et al. Physica 20, p.217.

25. R. N. Dexter, J. Phys. Chem. Solids 8, p.39 and p.216 (1959).

26. J. Woods, J. Electronics and Control 7, p.243 (1959).

27. A. Rose, Proc. I.R.E., 43, p.1850 (1955) R.C.A. Review 12, p.362 (1951).

28. R. H. Bube, Phys. Rev. 99, p.1105 (1955).

29. F. Urbach, Akad. Wiss. Wien Berlim 139.2.A. p.35 (1930).

30. J. T. Randall and M. H. F. Wilkins, Proc. Roy. Soc. A 185, p.347, 365 and 390 (1945).

31. K. W. Boer and H. Vogel, Ann. Physik 17, p.10 (1955).

32. R. H. Bube, J. Chem. Phys. 23, p.18, (1955).

33. R. H. Bube, Photoconductivity of Solids (J. Wiley 1960), p.61.

34. R. H. Bube, J. Chem. Phys. 23 p.18 (1955).

35. G. F. J. Garlick and A. F. Gibson, Proc. Phys. Soc. A 60 p.574 (1948).

36. Haake, J. Opt. Soc. Amer. 47, p.649 (1957).

37. P. N. Keating, Proc. Phys. Soc., 78, p.1408 (1961).

38. D. J. Sandiford, Proc. Phys. Soc. 71, p.1002 (1958).

G. Bemski, Phys. Rev. 111, p.1515 (1958).

39. L. I. Grossweiner, J. App. Phys. 24, p.1306 (1953).

40. R. R. Haering and E. N. Adams, Phys. Rev. 117, p.451 (1960).

41. A. H. Booth, Canad. J. Chem. 32, p.214 (1954).

42. W. Hoogenstraaten, Philips Res. Rep. 13, p.515 (1958).

43. R. H. Bube, J. Chem. Phys. 23, p.18 (1955).

44. M. Schon, Physica 20, p.930 (1954).

45. H. A. Klasens and W. Hoogenstraaten, J. Electrochem. Soc. 100, p.366 (1953).

46. A. Halperin and A. A. Braner, Phys. Rev. 117, p.408 (1960).

47. K. W. Boer, S. Oberlander and J. Voigt, Z. Naturf 13a, p.544 (1958).

K. W. Boer, S. Oberlander and J. Voigt, Ann. Phys. 2, p.136 (1958).

48. Ch. B. Lushchik, Doklady. Akad. Nauk. S.S.S.R. 101, p.641 (1955).

49. A. Addamiano, J. Phys. Chem. 61, p.1253 (1957).

50. R. Frerichs, Naturwiess 33, p.281 (1946) Phys. Rev. 72, p.594 (1947).

51. D. C. Reynolds, Czyzack, Allen, Reynolds, J. Chem. Phys. 29, p.1375 (1958).

D. C. Reynolds, L. C. Greene, J.A.P. 29, p.559 (1958).

W. W. Piper and S. J. Polich, J.A.P. 32, p.1278 (1961).

P. D. Fochs, J.A.P. 31, p.1733, (1960).

J. M. Stanley, J. Chem. Phys. 24, p.1279 (1956).

52. R. Nitsche et al. J. Phys. Chem. Solids 17, p.163 (1960), J. Phys. Chem. Solids 21, p.199 (1961).

53. W. E. Medcalf and B. H. Fahrig, J. Electrochem. Soc. 105 p.719 (1958).

54. F. A. Kroger et al., Phys. Rev. 103 p.279 (1956).

55. J. Franks and P. N. Keating, J. Phys. Chem. Solids 22, p.25 (1961).

56. M. C. Driver and G. T. Wright, Proc. Phys. Soc. 81, p.141 (1963).

57. G. A. Marlor and J. Woods, Proc. Phys. Soc., 81, p.524 (1963).

58. B.R.A. Nijboer, Proc. Phys. Soc 51, p.575 (1939).

59. A. P. Trofimenko et al. Soviet Physics Solid State 2 p.1033 (1961).

60. E. A. Niekisch Z.f. Phys. Chem. 217 p.110 (1961).

61. I. L. Sokol'skarya, Soviet Physics Solid State 4, p.2439 (1963).

62. C. G. Clayton et al. Nature 192, p.349 (1961).

63. J. Woods and D. A. Wright, Solid State Phys. Brussels Conf. p.880 (1958).

64. R. H. Bube and L. A. Barton, J. Chem. Phys. 29, p.128 (1958).

65. F. A. Kroger, H. J. Vink and J. van den Boomgaard, Z. Physik. Chem. 203, p.1 (1954).

66. K. Unger, Reaktronskinetck von Elektronenprozessen in Festkorpern, Berlin (1960) p.170.

67. I. Broser, Reaktronskinetck von Elektronenprozessen in Festkorpern, Berlin (1960) p.45.

68. I. Broser and R. Broser-Warminsky, B. J. App. Phys. Supp. 4 p.90 (1954).

69. J. J. Brophy and R. J. Robinson, Phys. Rev. 118, p.959 (1960).

70. F. Lappe, Z. Phys. 154, p.267 (1959).

71. S. Tanaka and T. Tanaka, J. Phys. Soc. Japan 14, p.113 (1959).

72. R. W. Smith, R.C.A. Review 20, p.69 (1959).

73. D. A. Wright, J. App. Phys. 9 , p.205 (1958).

TABLE 12.1

Crystal	E_F eV	E_F eV
S2	0.20 ± 0.03	
S4	0.26 ± 0.03	
R1	0.14 ± 0.02	0.34 ± 0.02
R2	0.14 ± 0.03	
R3	0.21 ± 0.03	0.34 ± 0.02
R4	0.22 ± 0.02	0.30 ± 0.02
R5		0.30 ± 0.03
R6	0.16 ± 0.06	0.27 ± 0.07
R7		0.32 ± 0.04

ELECTRON FERMI LEVEL DEPTH AT WHICH PHOTOCONDUCTIVITY INCREASES SHARPLY WITH TEMPERATURE.

TABLE 11.4 (0·63 eV)

Crystal	$S6_V$	$S5_V$	S5	S4	$S5_V$	P2	P1		$S3_V$	V1	Ave.
Conds.	a.l.	a.l.	a.l.	a.l.	a.l.	a.l.	a.l.			a.l.	a.l.
T*	270	270	300	330	350	360	400		330	340	330
E_B	0·45 ±0·02	0·41 ±0·01	0·59 ±0·01	0·67 ±0·03	0·57 ±0·01	N.M.	N.M.		N.M.	N.M.	0·61 ±0·04
E_G	0·74 ±0·06	0·74 ±0·05	0·62 ±0·03	0·68 ±0·06	0·62 ±0·02	0·65 ±0·07	N.M.		0·50 ±0·05	N.M.	0·64 ±0·02
E_L	≈0·61	0·64 ±0·05	0·65 ±0·04	0·66 ±0·04	0·47 ±0·08	0·64 ±0·04	N.M.		N.M.	N.M.	0·64 ±0·04
E_{FK}	≈0·58	0·6 ±0·1	0·58 ±0·08	0·71 ±0·06	0·55 ±0·2 POOR	0·72 ±0·07	N.M.		N.M.	N.M.	0·66 ±0·05
E_{HB}	0·79 ±0·08	0·87 ±0·08	0·66 ±0·04	0·66 ±0·05	0·65 ±0·03	0·65 ±0·10	N.M.		N.M.	N.M.	0·66 ±0·04
E_{GG}	≈0·65 POOR	0·54 ±0·08 POOR	0·36 ±0·03	0·60 ±0·02	0·66 ±0·02	BAD	0·67 ±0·03		N.M.	0·62 ±0·05	0·63 ±0·03
E_{HR}	0·84 ±0·03	0·63 ±0·05	0·65 ±0·2 POOR	1·25 ±0·2	0·54 ±0·09	0·6 ±0·2	N.M.		0·72 ±0·1	N.M.	0·63 ±0·05
E_{HA}	0·64 ±0·02	0·6 ±0·1	0·4 ±0·1	2·4 ±0·5	0·46 ±0·15	0·6 ±0·1	N.M.		BAD	≈0·65	0·64 ±0·02
E_T	BAD	BAD	N. M.	0·62 ±0·04	BAD	BAD	N.M.		N.M.	N.M.	0·62 ±0·04
S_G	N.M.	5×10^{-15}	8×10^{-17}	2×10^{-18}	5×10^{-19}	5×10^{-19}	N.M.		N.M.	N.M.	10^{-18}
S_T	BAD	BAD	N.M.	5×10^{-17}	BAD	BAD	N.M.		N.M.	N.M.	5×10^{-17}

TABLE 11.3 (0·83 eV)

Crystal	S2	S3	$S3_V$	$S5_V$	$S6_V$	S1		P2	R2	R1	$S4_V$	$S6_V$	S5	S4	V1	Ave.
Conds.		a.l.	a.l.	a.l.	a.l.	a.l.		a.l.	a.l.	a.l.	a.l.	a.l.	a.l.	a.l.	a.l.	a.l.
T*	270	270	280	290	300	300		330	330	340	370	370	270	260	320	290
E_B	0·41 ±0·01	0·53 ±0·01	0·45 ±0·02	0·50 ±0·01	0·52 ±0·01	N.M.		N.M.	0·56 ±0·02	0·65 ±0·05	0·61 ±0·01	0·67 ±0·03	0·47 ±0·01	0·49 ±0·01	N.M.	0·55 ±0·10
E_G	≈0·86	0·83 ±0·06 0·42 ±0·08	N.M.	0·82 ±0·03	0·93 ±0·03	N.M.		0·70 ±0·20	0·82 ±0·06	0·72 ±0·04	0·81 ±0·02	0·86 ±0·04	0·95 ±0·10	0·78 ±0·02	≈0·42	0·82 ±0·03
E_L	≈0·74	0·26 ±0·06 0·40 ±0·08 POOR	N.M.	0·75 ±0·10	0·84 ±0·04	N.M.		N.M.	0·82 ±0·10	0·80 ±0·07	0·79 ±0·04	0·83 ±0·02	0·75 ±0·02	0·64 ±0·04	≈0·76 ≈0·44	0·83 ±0·03
E_{FK}	≈0·68	0·25 ±0·01 0·40 ±0·09 POOR	N.M.	0·76 ±0·12 POOR	0·80 ±0·09	N.M.		BAD	0·79 ±0·03	0·78 ±0·07	0·82 ±0·05	0·84 ±0·08	0·70 ±0·15	0·57 ±0·04	BAD	0·80 ±0·04
E_{HB}	N.M.	≈ 0·85 ≈ 0·45	N.M.	0·84 ±0·03	0·94 ±0·04	N.M.		0·8 ±0·2	0·88 ±0·06	N.M.	0·86 ±0·03	0·92 ±0·08	1·1 ±0·15	0·87 ±0·06	≈0·37	0·86 ±0·03
E_{GG}	0·45 ±0·04	0·42 ±0·02	≈0·42	0·75 ±0·10 POOR	0·83 ±0·04 0·40 ±0·01	N.M.		N.M.	0·88 ±0·07	0·45 ±0·04	1·06 ±0·08	~0·9 POOR	0·39 ±0·03	0·41 ±0·01	≈0·40	0·85 ±0·04
E_{HR}	N.M.	0·49 ±0·05	0·8 ±0·1	0·56 ±0·10	0·77 ±0·02	N.M.		0·43 ±0·10	N.M.	N.M.	1·2 ±0·2 POOR	0·9 ±0·3	0·76 ±0·15	0·7 ±0·1	≈ 0·47	0·78 ±0·03
E_{HA}	N.M.	BAD	0·78 ±0·10	0·44 ±0·02 0·82 ±0·03 SEE V1	0·32 ±0·20 POOR	N.M.		0·53 ±0·15	N.M.	N.M.	1·05 ±0·15	0·64 ±0·03	0·50 ±0·25 POOR	1·0 ±0·2	JOINT GRAPH WITH $S5_V$	0·80 ±0·08
E_T	≈0·8	0·45 ±0·04	N.M.	0·79 ±0·03	0·83 ±0·04	0·81 ±0·03		0·78 ±0·03	N.M.	N.M.	1·03 ±0·08	0·9 ±0·1 POOR	N.M.	0·40 ±0·04	N.M.	0·81 ±0·03
S_G	3×10^{-11}	10^{-10}	N.M.	10^{-13}	10^{-13}	N.M.		10^{-13}	10^{-14}	10^{-16}	10^{-16}	10^{-16}	2×10^{-12}	10^{-12}	N.M.	10^{-14}
S_T	N.M.	3×10^{-21} (0·45)	N.M.	2×10^{-17}	5×10^{-15}	2×10^{-12}		10^{-17}	N.M.	N.M.	N.M.	N.M.	N.M.	N.M.	N.M.	10^{-15}

TABLE 11.1

Crystal		(0.05 eV) S3	P2	S1	Ave.	(0.14eV) V1	$S4_V$	S3	Ave.		(0.25 eV) R1	S3	R2	S2	P3	S1	P1	Ave.
Conditions						a.d.	a.d.	a.d.	a.d.		a.d.	a.d.	a.d.		a.d.		a.d.	a.d.
Methods of Calculation	T*	120	160	175	150	150	190	230	190		250	270	300	300	310	310	290	295
Bube	E_B	0.21 ±0.02	N.M.	0.20 ± 0.01	0.20 ± 0.01	0.25 ±0.01	0.37 ±0.01	0.35 ±0.02	0.32 ±0.05		0.49 ±0.01	0.53 ±0.01	0.50 ±0.01	N.M.	N.M.	0.54 ±0.01	N.M.	0.52 ±0.02
Grossweiner	E_G	∿0.1 POOR	0.048 ±0.002	N.M.	0.048 ±0.002	0.28 ±0.04	0.15 ±0.01	0.13 POOR	0.15 ±0.01		0.27 ±0.02	0.83 0.42 ±0.06 ±0.08	0.25 ±0.25	N.M.	∿0.29 ∿0.43	N.M.	N.M.	0.26 ±0.01
Lushchik	E_L	0.048 ±0.009	0.055 ±0.005	N.M.	0.052 ±0.003	0.16 ±0.02	0.13 ± 0.01	BAD	0.14 ±0.01		0.25 ±0.01	0.26 0.40 ±0.06 ±0.08 POOR	0.27 ±0.06	N.M.	∿0.28	N.M.	N.M.	0.25 ±0.01
Franks & Keating	E_{FK}	BAD	0.054 ±0.006	N.M.	0.054 ±0.006	BAD	0.13 ±0.07 POOR	BAD	0.13 ±0.07		0.23 ± 0.04	0.25 0.40 ±0.01 ±0.09 POOR	0.25 ±0.01	N.M.	∿0.29	N.M.	N.M.	0.25 ±0.01
Halperin & Braner	E_{HB}	BAD	BAD	N.M.	BAD	BAD	BAD	BAD	BAD		BAD	0.85 0.45 ±0.10 ±0.10	BAD	N.M.	N.M.	N.M.	N.M.	BAD
Garlick & Gibson	E_{GG}	BAD	BAD	N.M.	BAD	0.18 ±0.02	0.14 0.068 ±0.01 ±0.001	BAD	0.15 ±0.02		0.20 ±0.05	0.42 ±0.02	0.24 ±0.02	N.M.	0.24 ±0.02	N.M.	0.22 ± 0.02	0.23 ±0.01
Heating Rate Method	E_{HR}	N.M.	0.054 ±0.006	N.M.	0.054 ±0.006	0.13 ± 0.02	0.13 ±0.02	N.M.	0.13 ±0.01		N.M.	0.49 ±0.05	N.M.	N.M.	N.M	N.M.	N.M.	N.M.
Haering & Adams	E_{HA}	N.M.	0.054 0.006	N.M.	0.054 0.006	0.13 0.04	0.25 0.03	N.M.	0.13 0.04		N.M.	BAD	N.M.	N.M.	N.M.	N.M.	N.M.	N.M.
Decay Measurements	E_τ	0.070 ±0.003	N.M.	0.052 ±0.003	0.052 ±0.003	N.M.	N.M.	N.M.	N.M.		N.M.	0.24 ±0.04	N.M.	0.22 ±0.04	N.M.	0.25 ±0.05	N.M.	0.24 ±0.03
Grossweiner	S_G	N.M.	10^{-25}	N.M.	10^{-25}	10^{-22}	3×10^{-22}	N.M.	10^{-22}		$2\ 10^{-24}$	N.M.	10^{-24}	N.M.	10^{-23}	N.M.	N.M.	10^{-24}
Decay Measurements	S_τ	5×10^{-22} (0.07)	N.M.	10^{-24}	10^{-24}	N.M.	N.M.	N.M.	N.M.		N.M.	10^{-23}	N.M.	2×10^{-24}	N.M.	4×10^{-24}	N.M.	10^{-24}

Crystal Notation	
S	Rods grown by sublimation in a stream of argon.
P	Plates grown by sublimation in a stream of argon.
R	Rods grown by reaction of the elements in a stream of argon.
V	Grown in a low temperature gradient in a vacuum.
v	Crystals treated by heating to ~600°C in a vacuum.

Crystal Conditions	
a.l.	After strong illumination at room temperature.
a.d.	After heating in the dark to about 370° C.

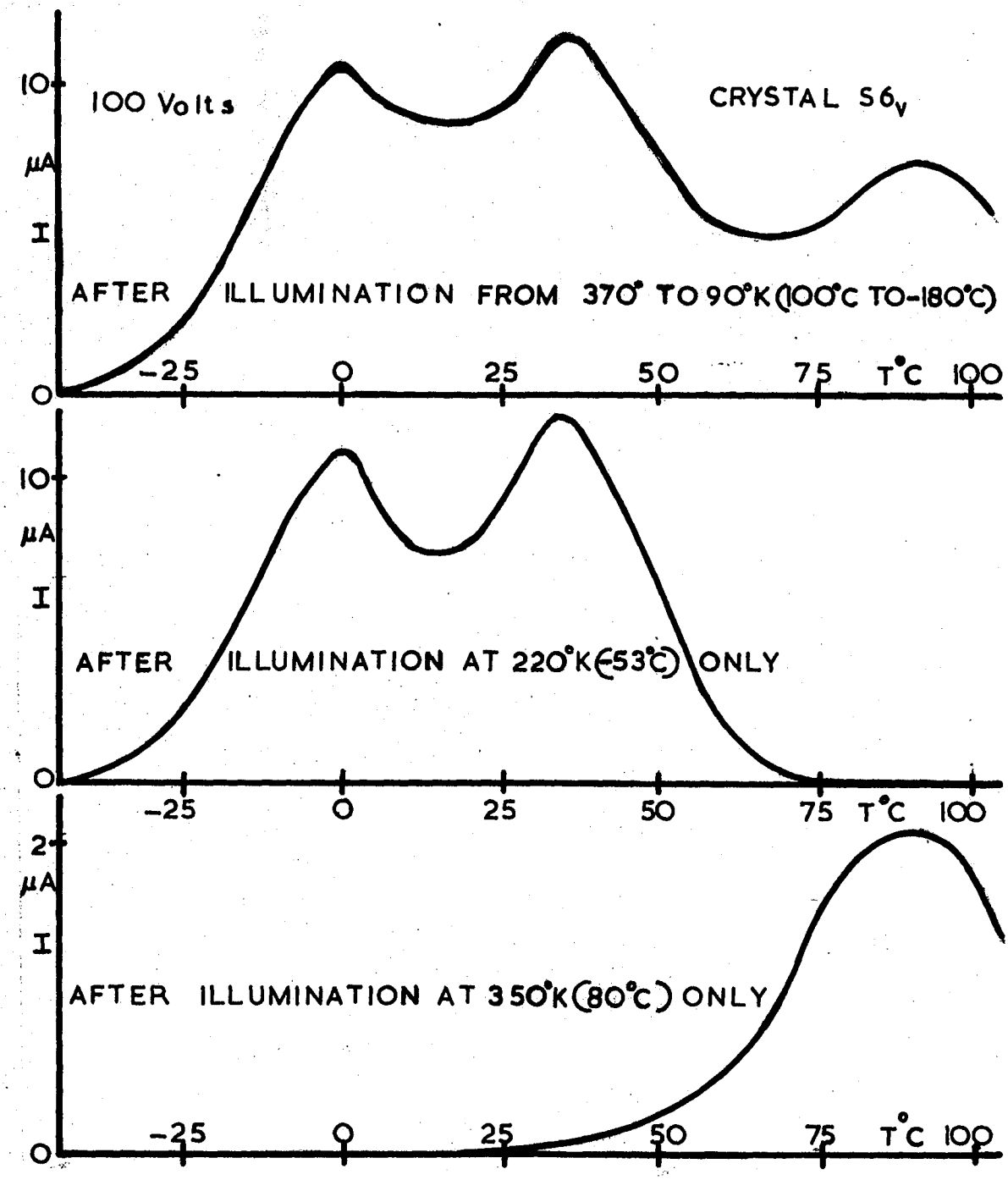

FIGURE 12.2

THERMALLY STIMULATED CURRENTS FOR DIFFERENT ILLUMINATIONS

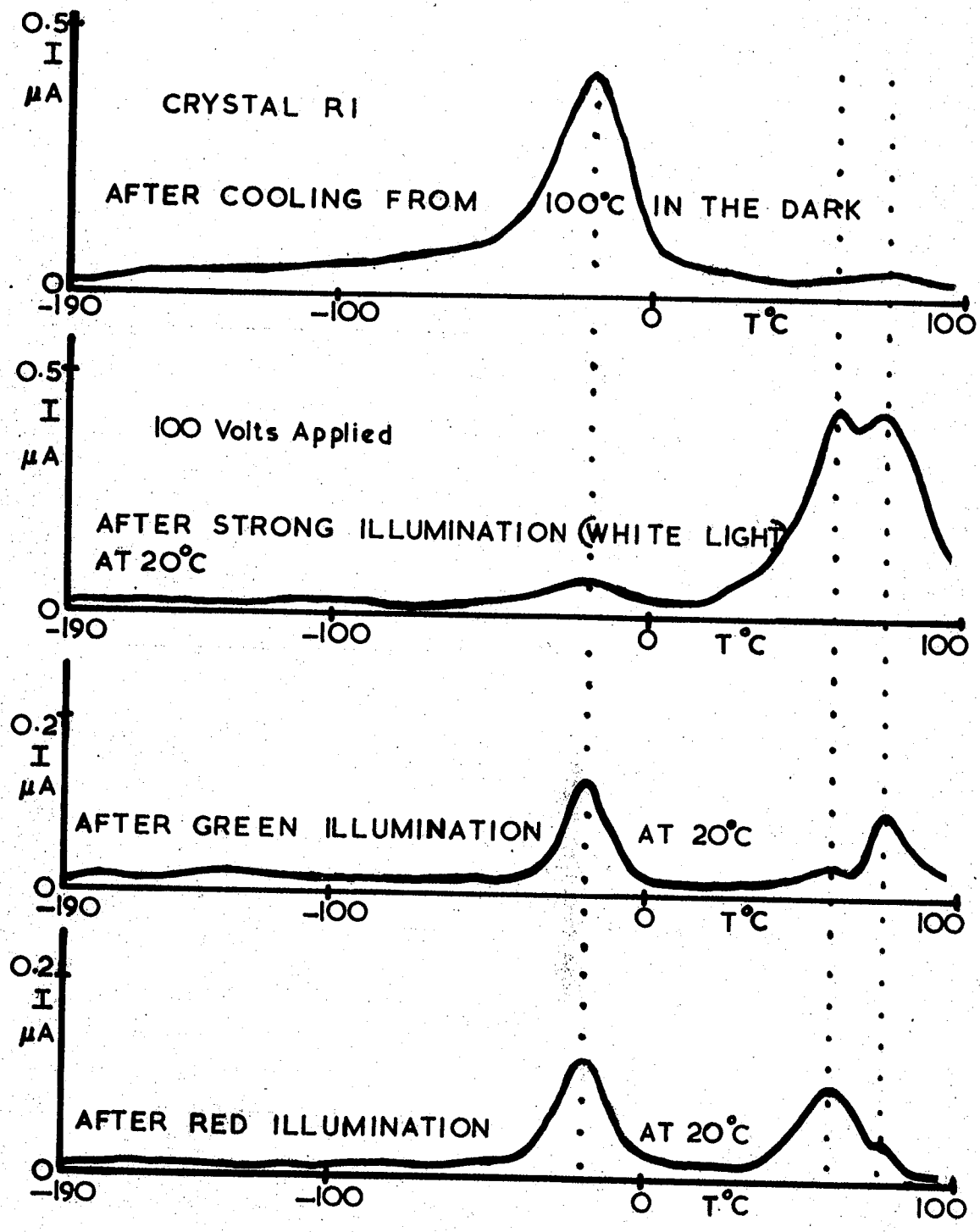

FIGURE 12.1

THERMALLY STIMULATED CURRENTS AND PHOTOCHEMICAL EFFECTS

TABLE 14.1

REPORTED BY	METHOD OF MEASUREMENT	E eV	COMPARISON OF VALUES OF TRAP ENERGY DEPTHS							
PRESENT WORK	TH. STIMLD. I PHOTO.DECAY	E	0·051	0·14	0·25		0·41		0·63	0·83
		T^X	150°K	190°K	295°K		300K		330°K	290°K
WOODS & WRIGHT	BUBE	E	0·24		0·32	0·38	0·50		0·59	
		T^X	120°K		170°K	220°K	270°K		320°K	
BUBE & BARTON	BUBE	E	0·20	0·25	0·41	0·44	0·51	0·58	0·63	
		T^X	100°K	135°K	180°K	220°K	270°K	305°K	350°K	
NIEKISCH	ALTERNATING LIGHT	E		0·12	0·22	0·31	0·4–0·45		0·55–0·65	0·7–0·8
BROPHY & ROBINSON	NOISE	E				0·36	0·43		0·6	
SOKOL'-SKARYA	SPACE CHARGE LIMITED I	E	0·09	0·12	0·22				0·66	
BROSER ET AL	TH. STIMLTD. I PHOTO.DECAY	E				0·34	0·43–0·48			
BROSER	TH. STMLD. I	E			0·22	0·31				
BUBE & MACDONALD	PHOTOHALL	E				0·35	0·46	0·54		
FRANKS & KEATING	FRANKS & KEATING	E	0·053							
DRIVER & WRIGHT	PRIMARY TH. STIMLTD. I	E					0·41			
MARLOR & WOODS	SPACE CHARGE LIMITED I	E							0·61	
TANAKA & TANAKA		E					0·4			
CLAYTON ET AL.	GROSSWEINER	E	0·09	0·13						
SMITH	SPACE CHARGE LIMITED I	E								0·8
TROFIMENKO ET AL.	PHOTO. DECAY ACTIVATION E	E	0·045		0·23–0·3			0·5		
UNGER	PHOTO/GLOW	E			0·26,	0·32	0·41		0·58	
LAPPE		E					0·4			

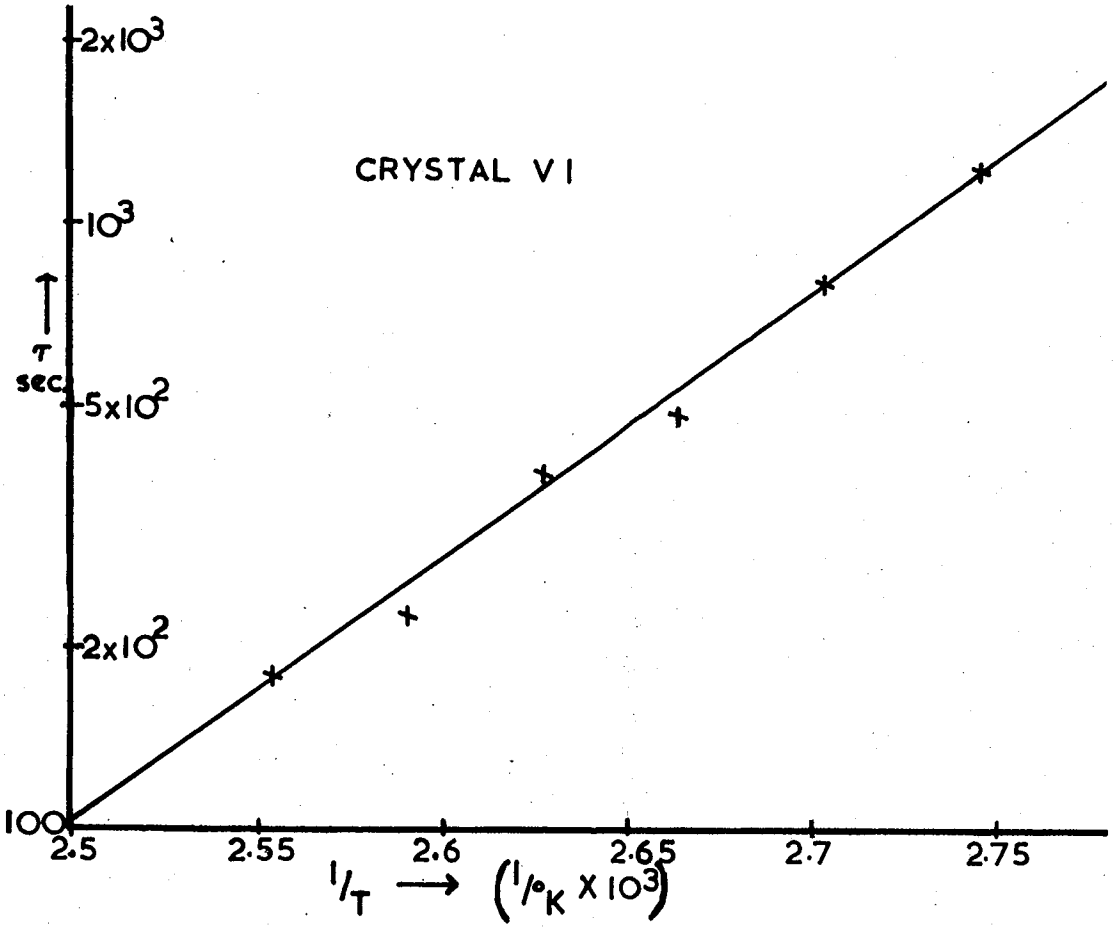

FIGURE 12.4

ACTIVATION ENERGY PLOT FOR

THE PRODUCTION OF DONORS

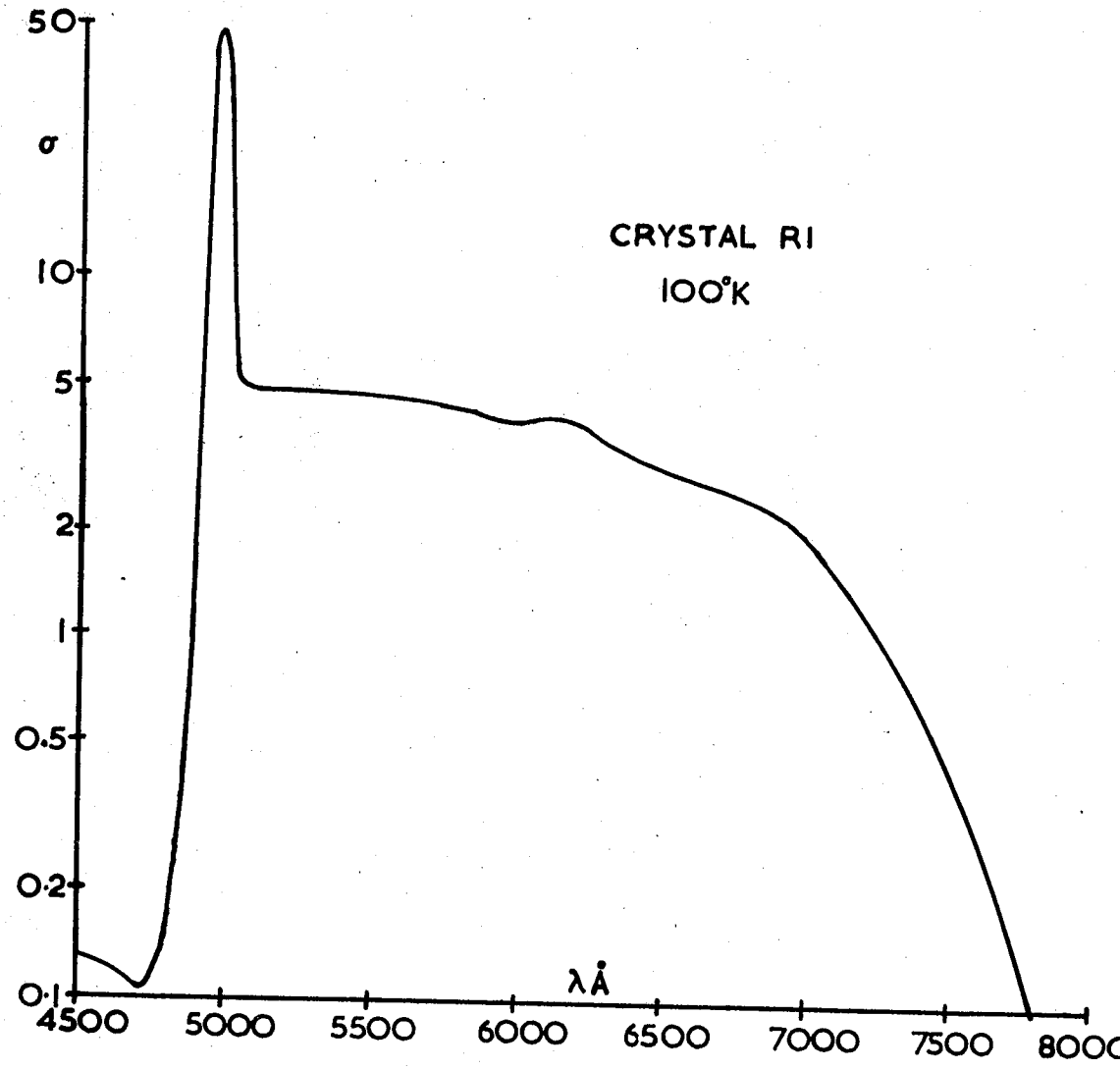

FIGURE 12·3

SPECTRAL RESPONSE OF THE PHOTOCONDUCTIVE CRYSTAL R1

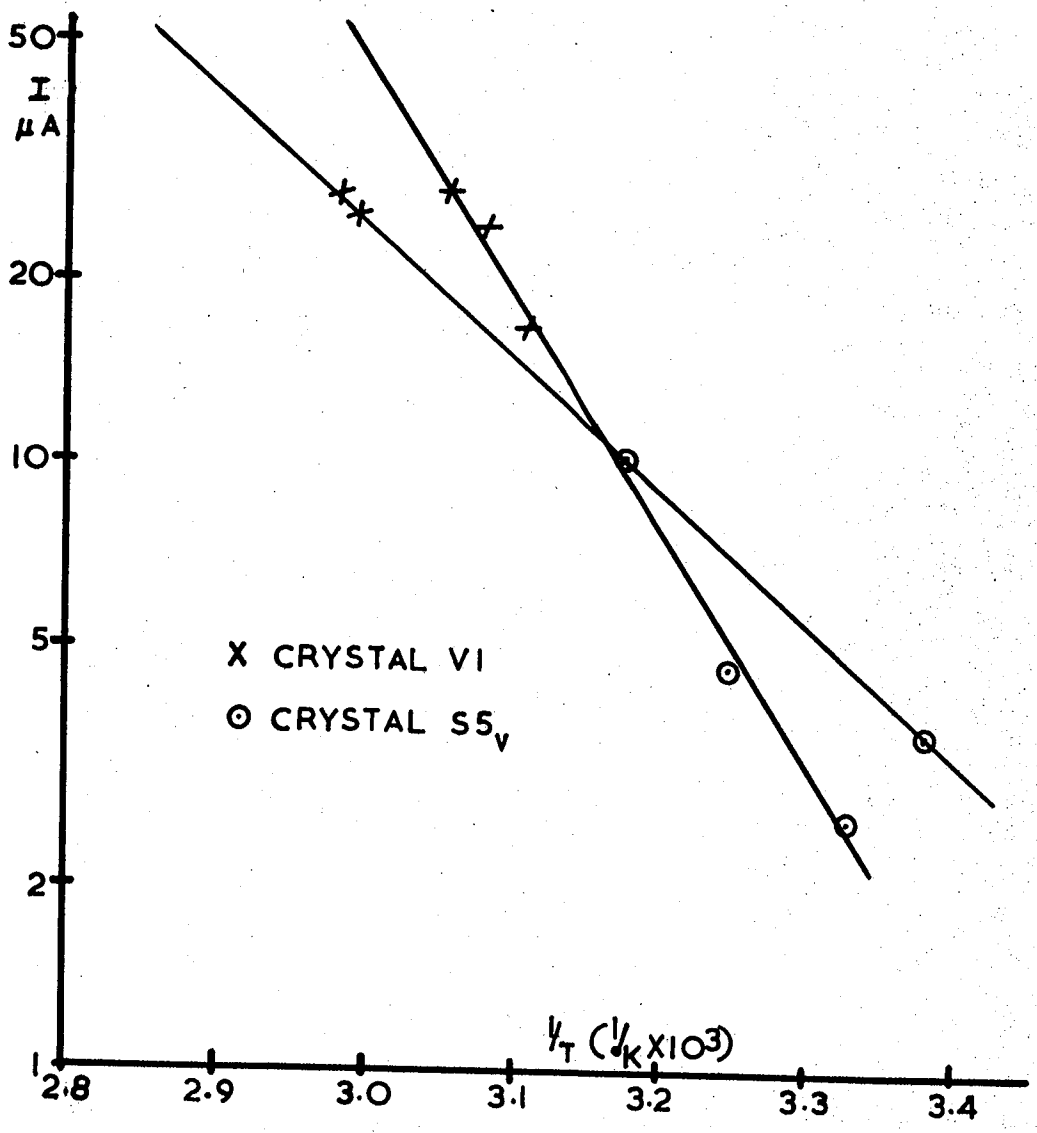

FIGURE 11.7

HAERING AND ADAMS PLOT ON THE DOUBLE PEAK AT ABOUT 300°K

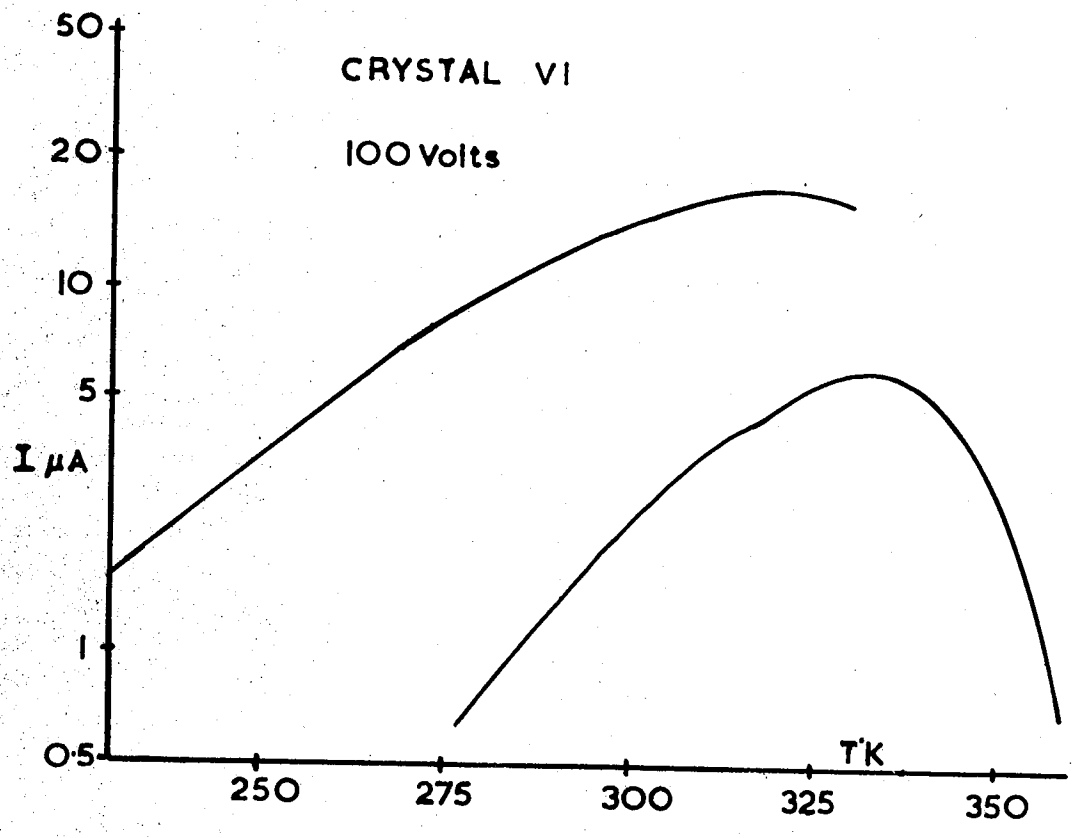

FIGURE 11·5

THE PARTIAL SEPARATION OF THE 0·41eV AND 0·83eV PEAKS

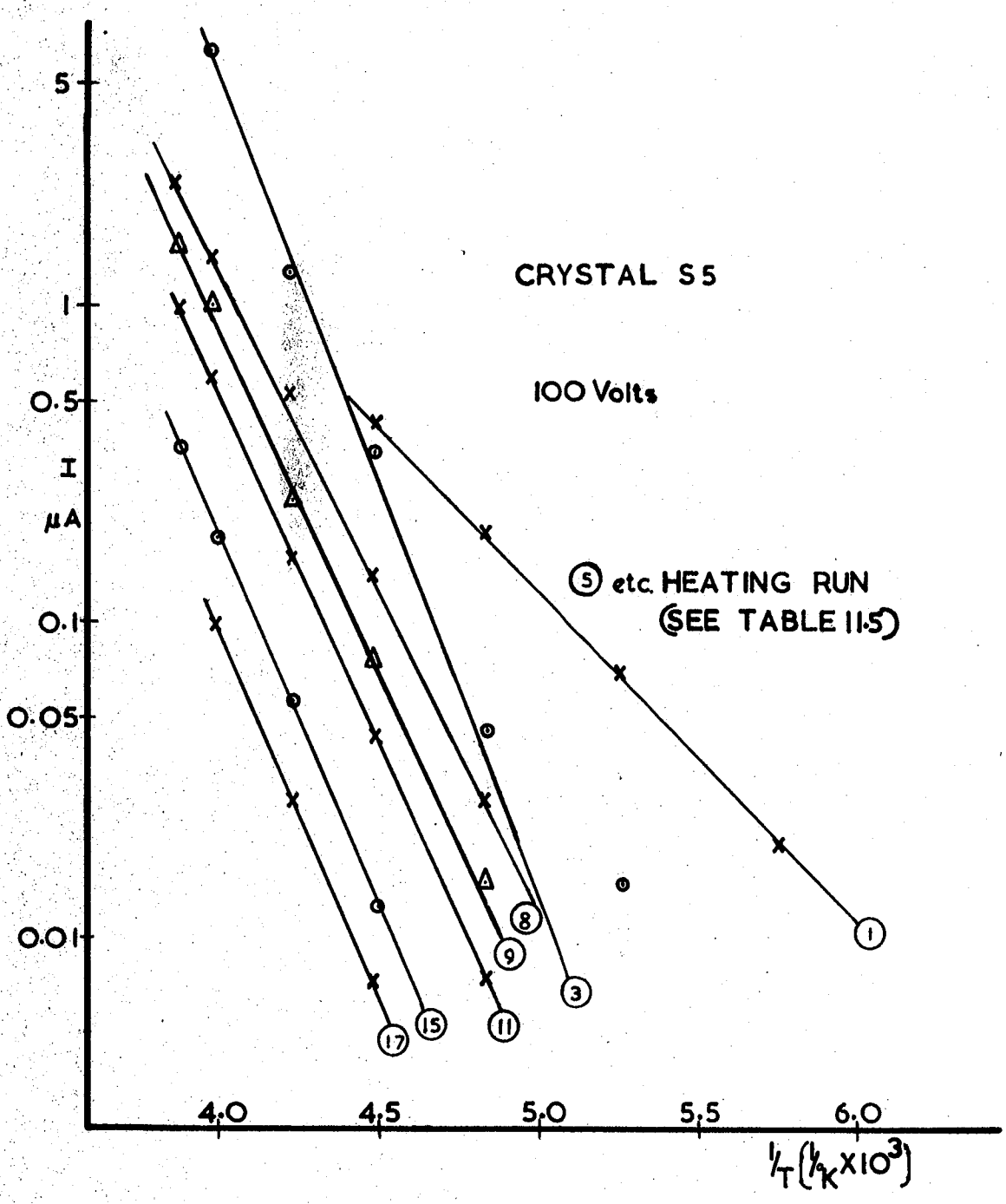

FIGURE 11.6

GARLICK AND GIBSON PLOTS

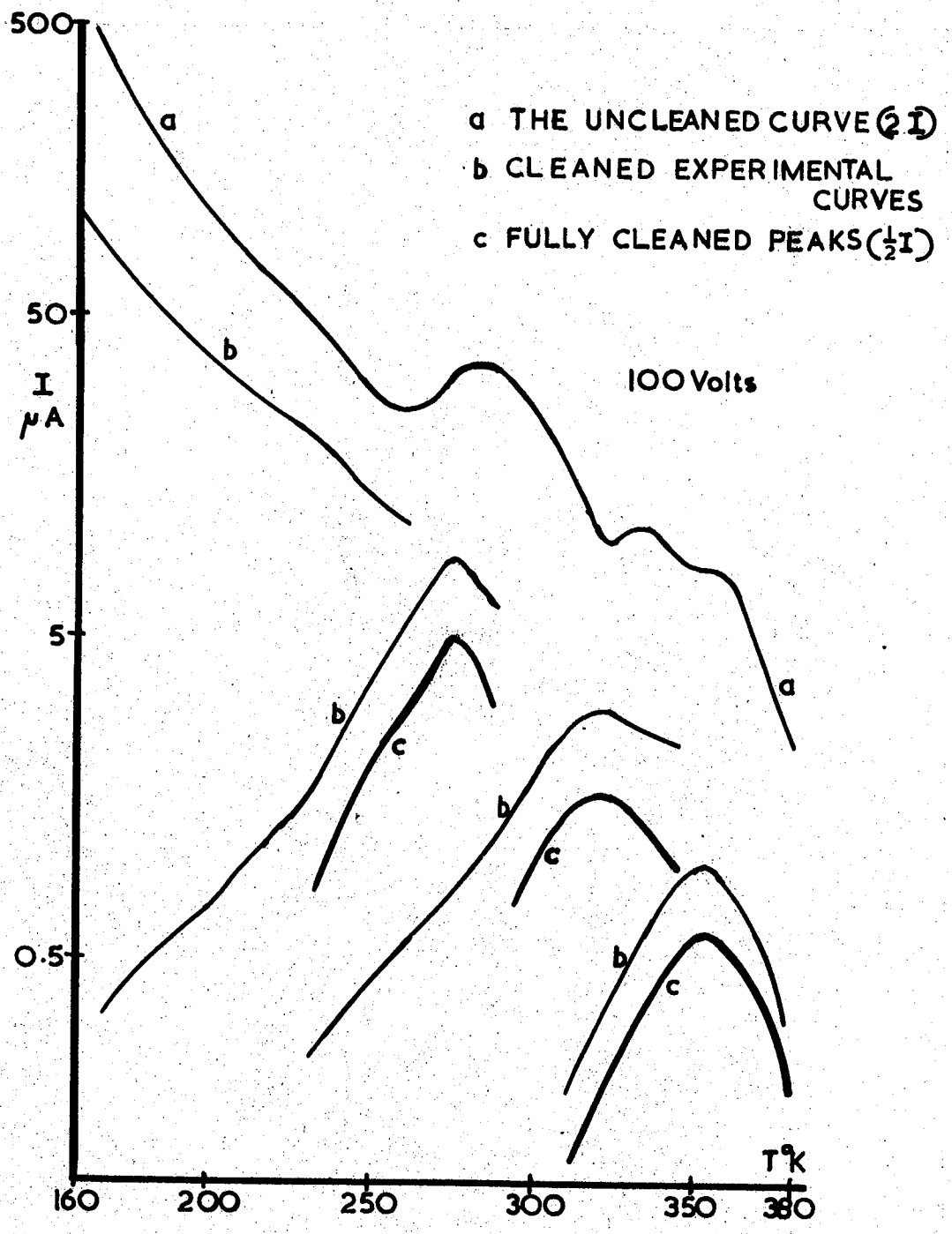

FIGURE 11.4

THE THERMAL CLEANING OF PEAKS

CRYSTAL P2

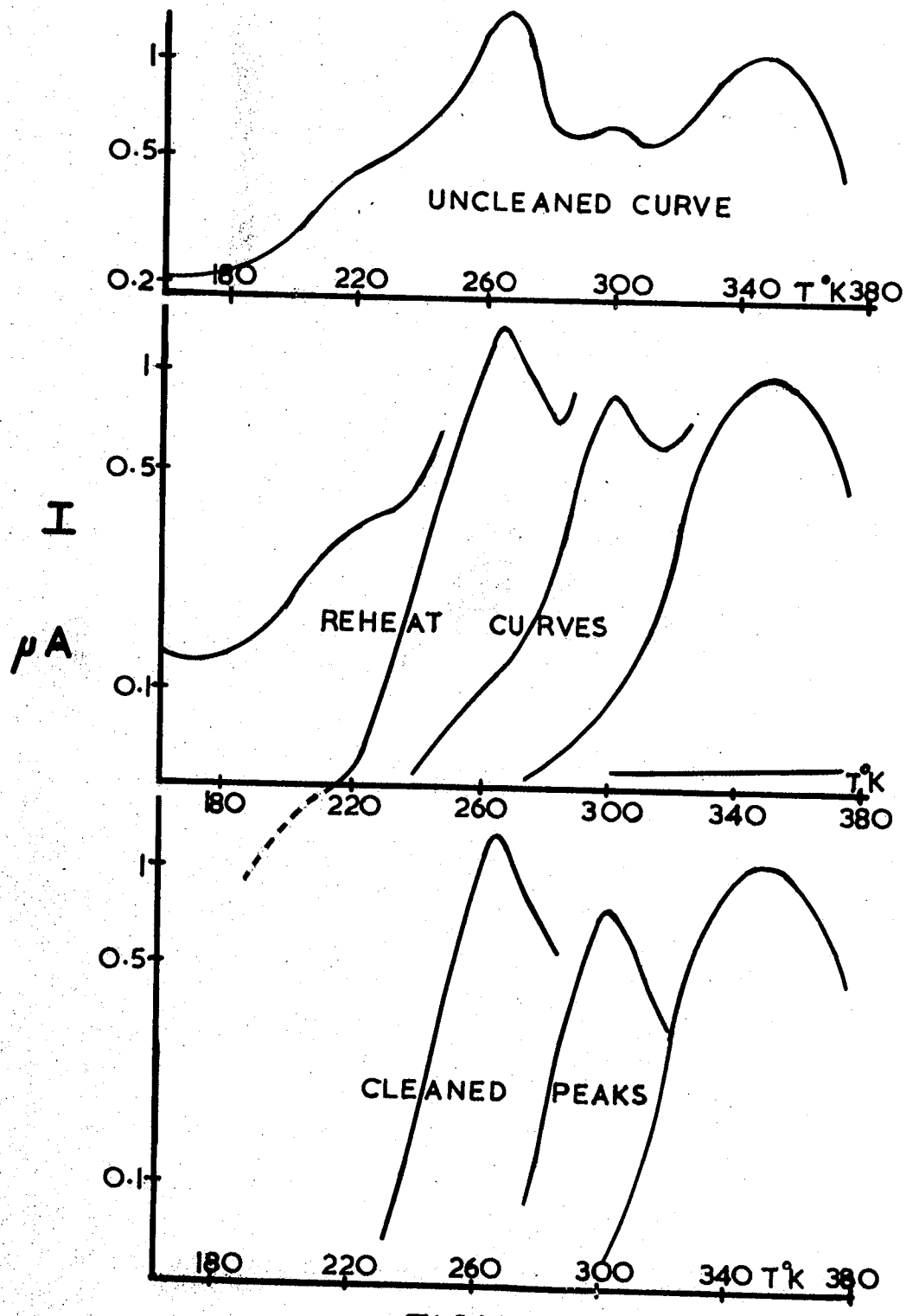

FIGURE 11.3

THE THERMAL CLEANING OF PEAKS
CRYSTAL S5.

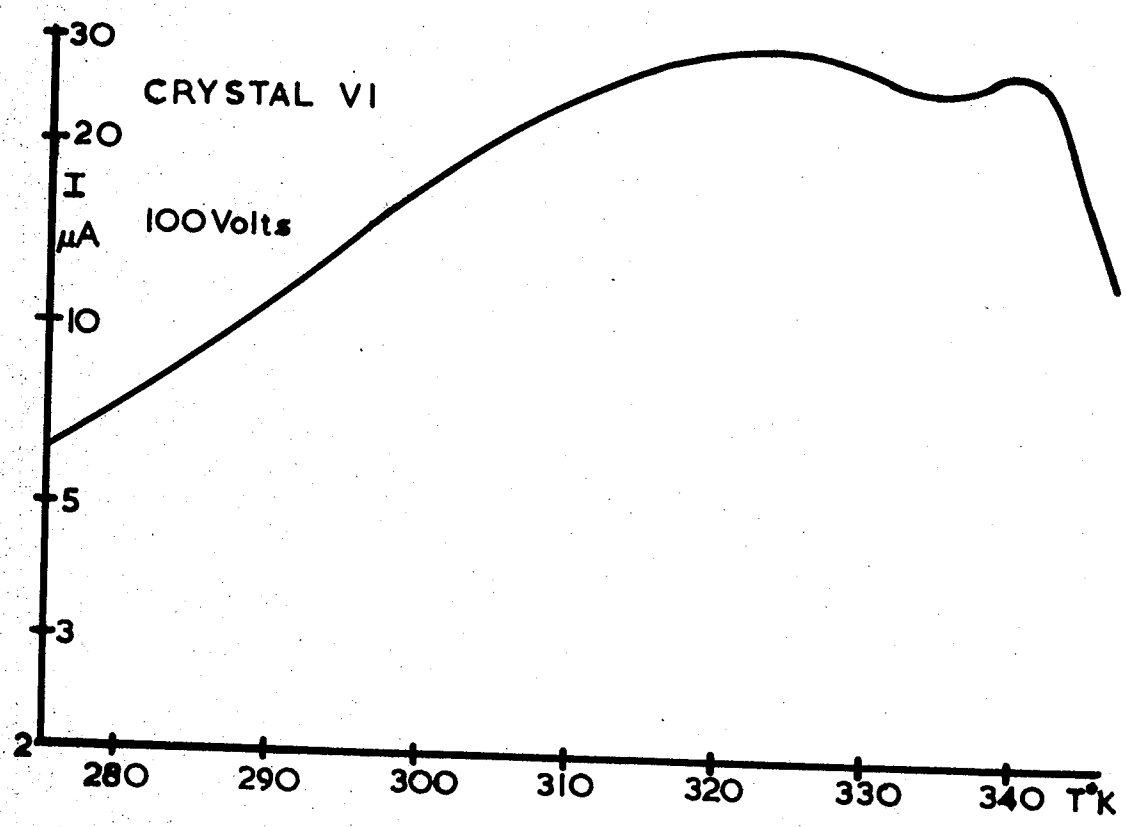

FIGURE 11.2

THE DOUBLE PEAK AT ABOUT 300°K
(~ MAXIMUM SEPARATION)

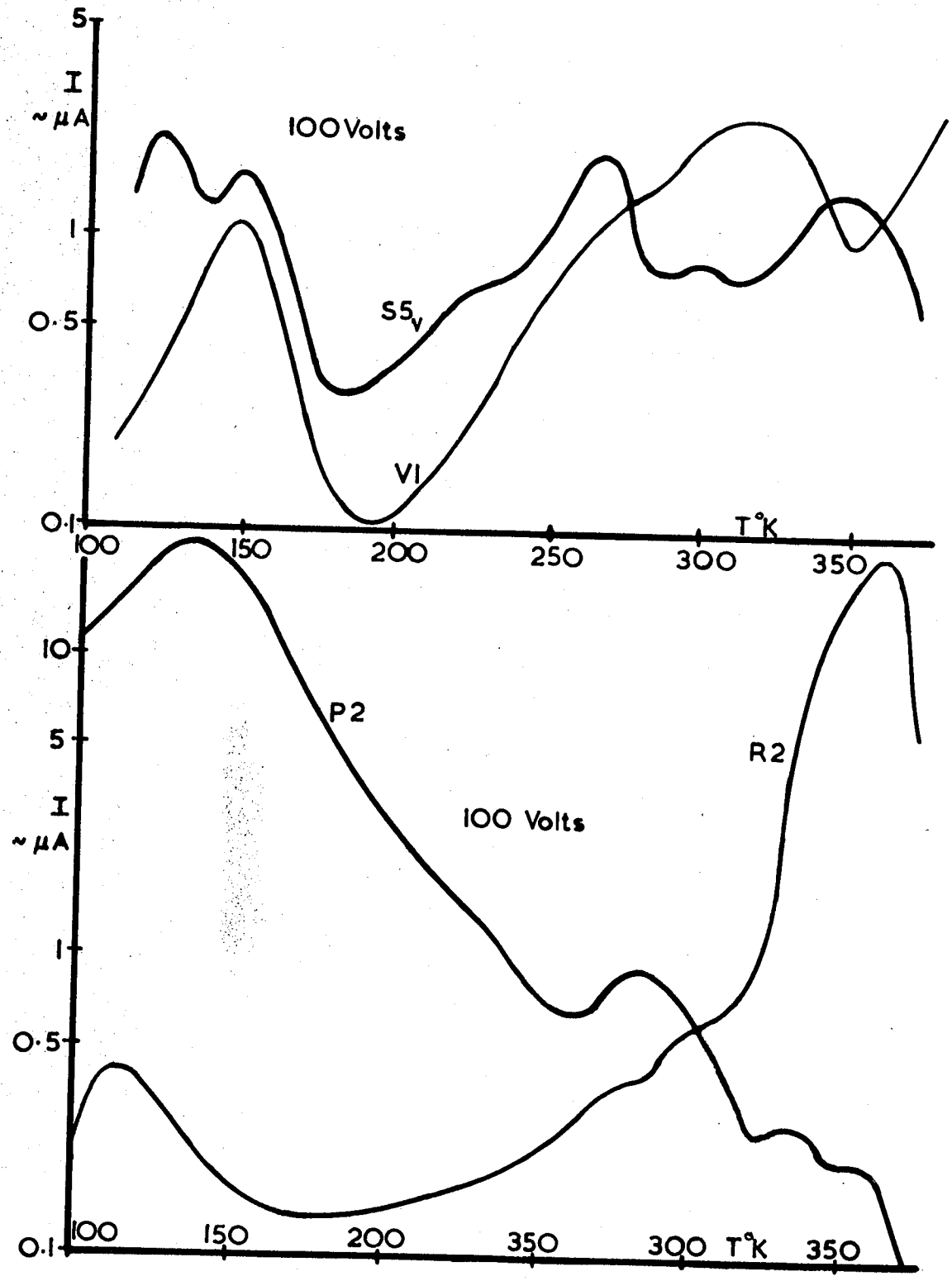

FIGURE 11.1

TYPICAL THERMALLY STIMULATED CURRENT CURVES

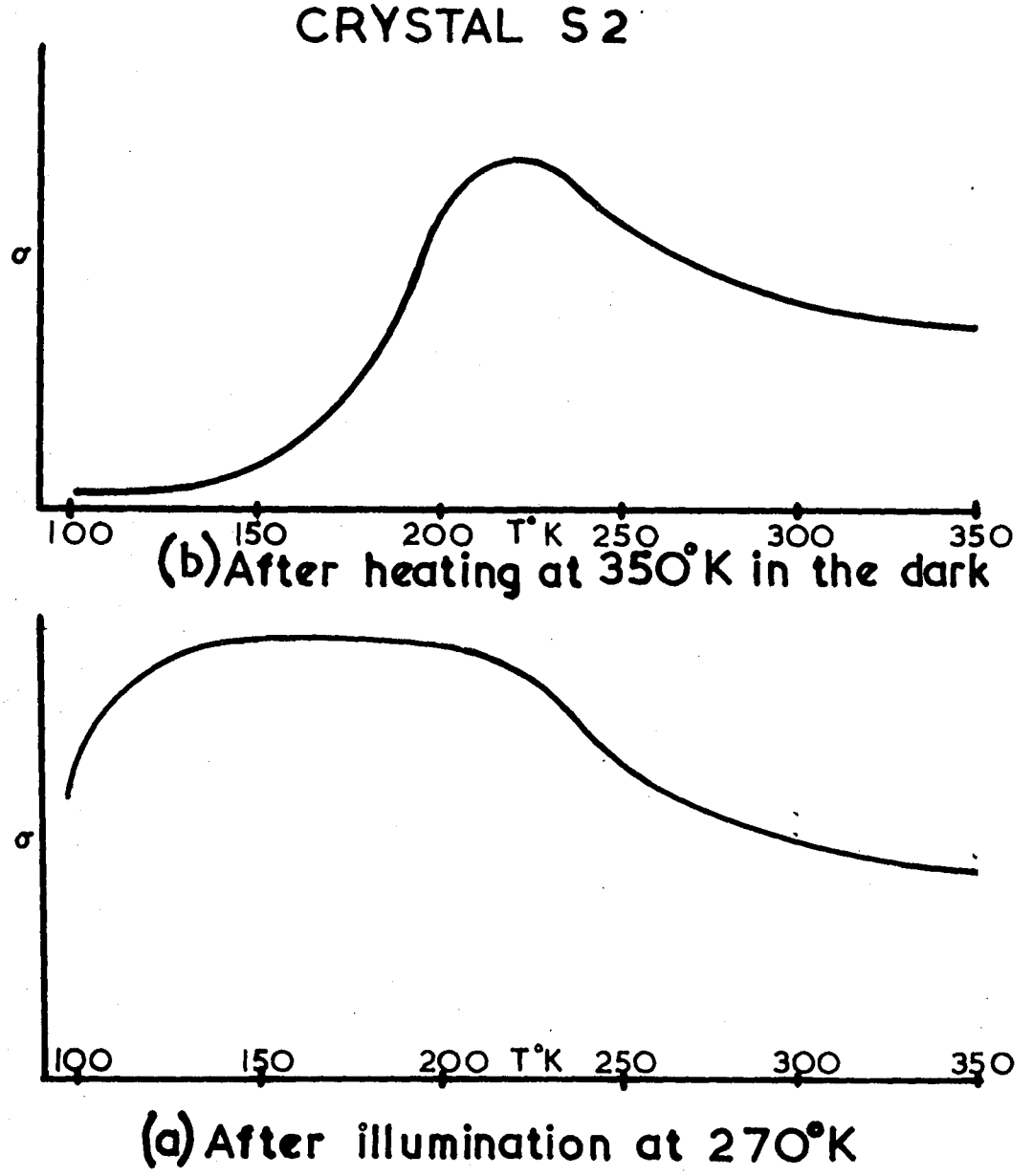

FIGURE 10.2

PHOTOCONDUCTIVITY versus TEMPERATURE

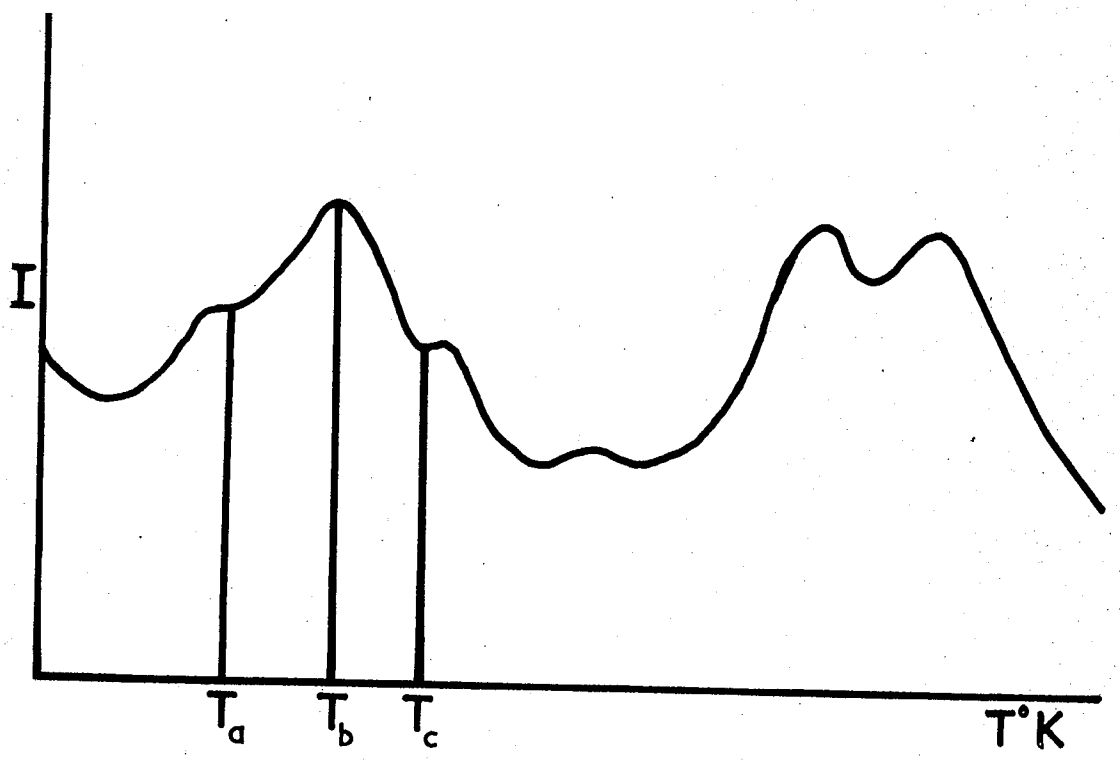

FIGURE 10.1

THERMALLY STIMULATED CURRENT CURVE

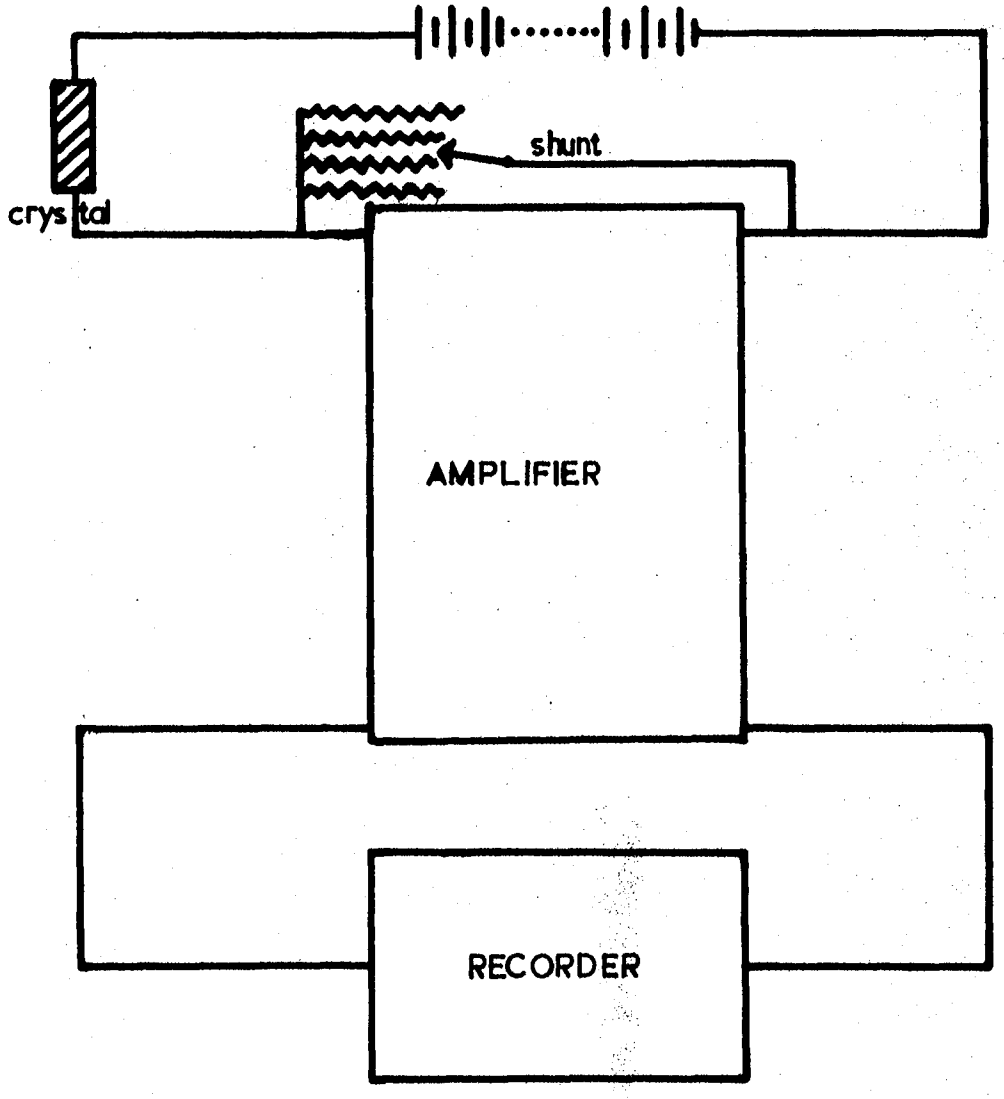

FIGURE 9.3

CIRCUIT FOR CONDUCTIVITY MEASUREMENTS

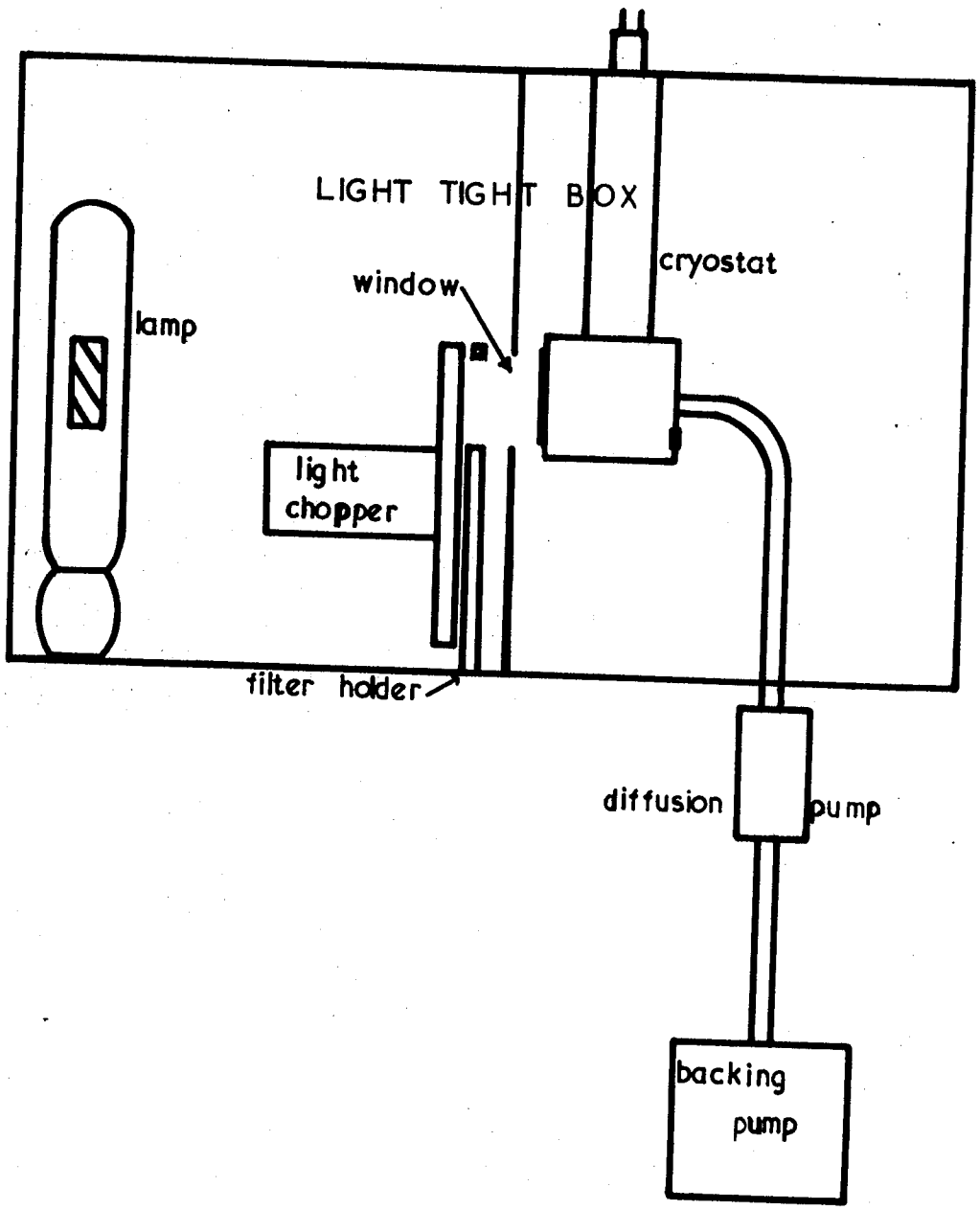

FIGURE 9.2

THE APPARATUS FOR OPTICAL AND ELECTRICAL MEASUREMENTS

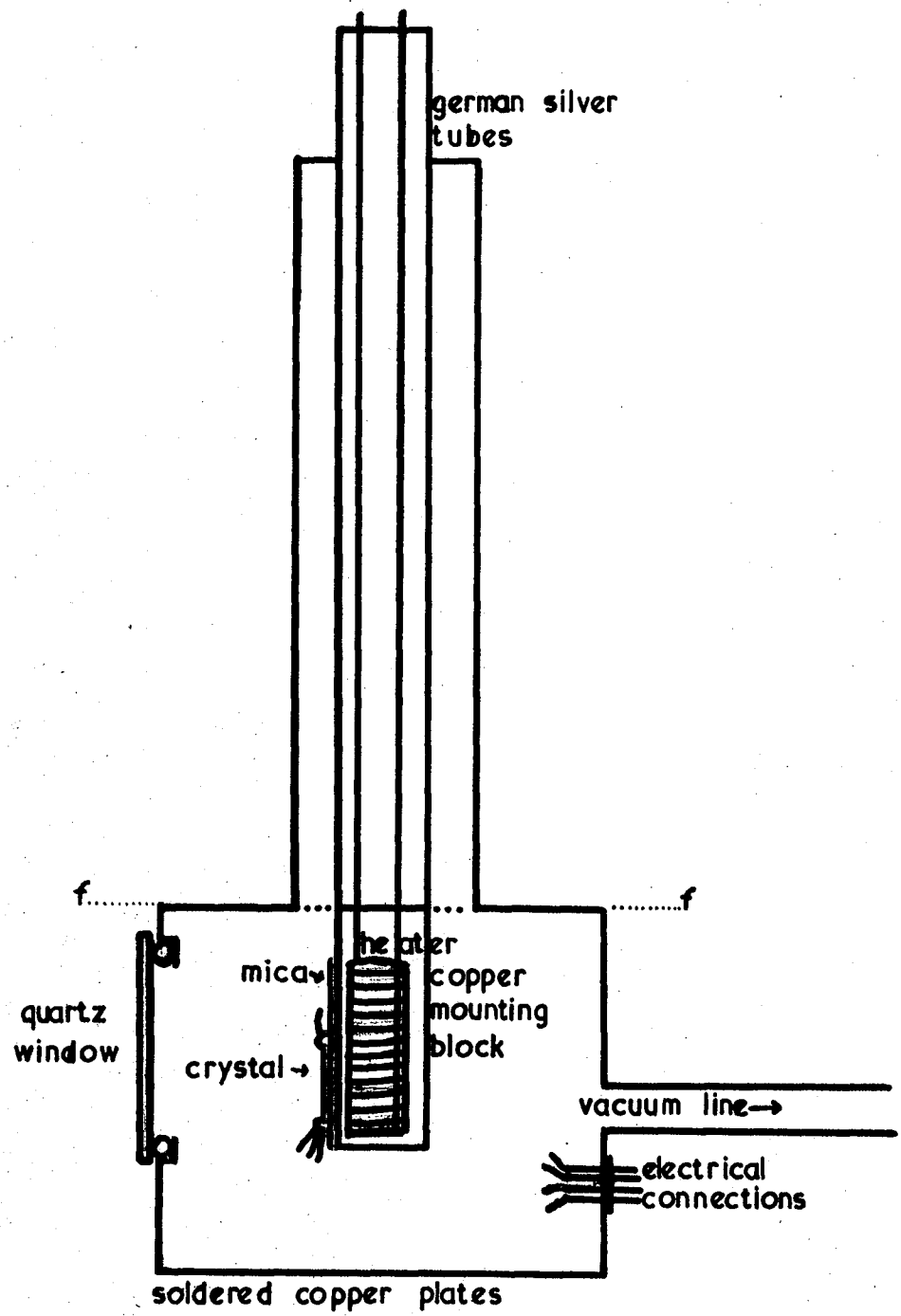

FIGURE 9·1

THE CRYOSTAT

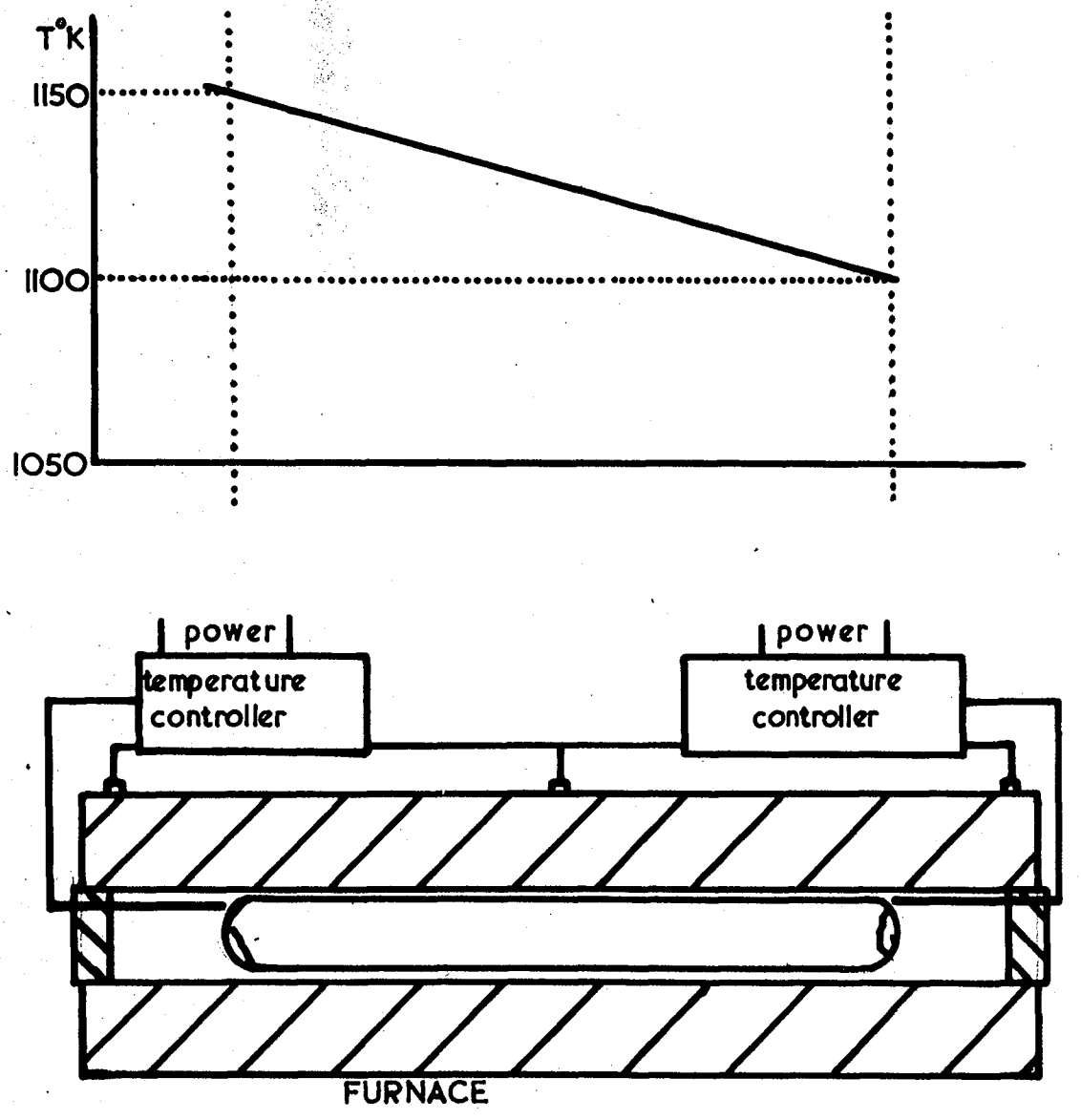

FIGURE 8·3

CRYSTAL GROWTH IN VACUO

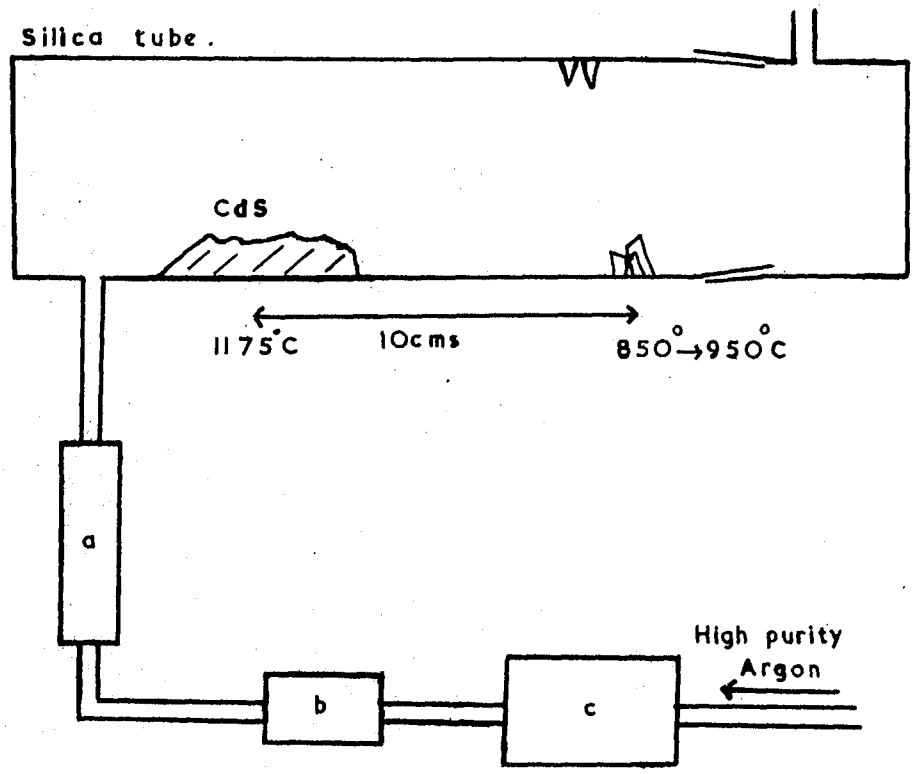

a Flowmeter

b Drying tower (Aluminium Calcium Silicate.)

c Copper at 400°C

Not to scale.

FIGURE 8.2

CRYSTAL GROWTH IN ARGON

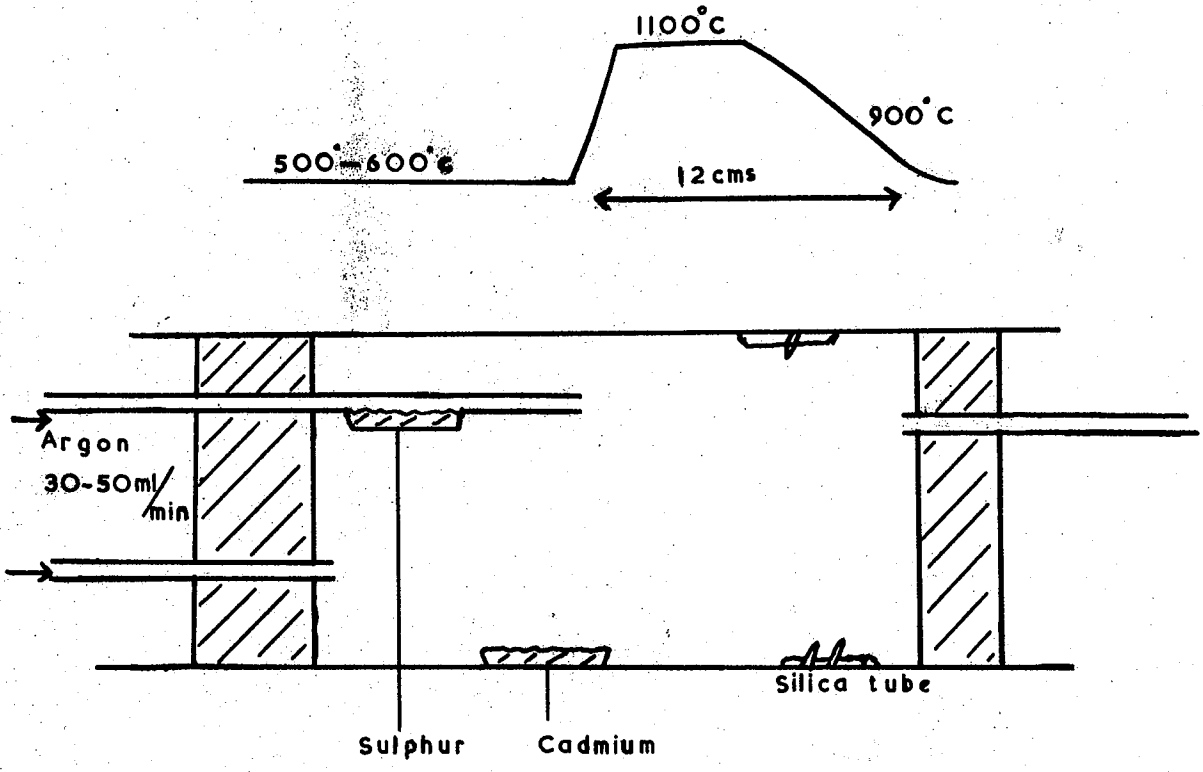

Not to scale.

FIGURE 8.1

CRYSTAL GROWTH BY REACTION IN ARGON

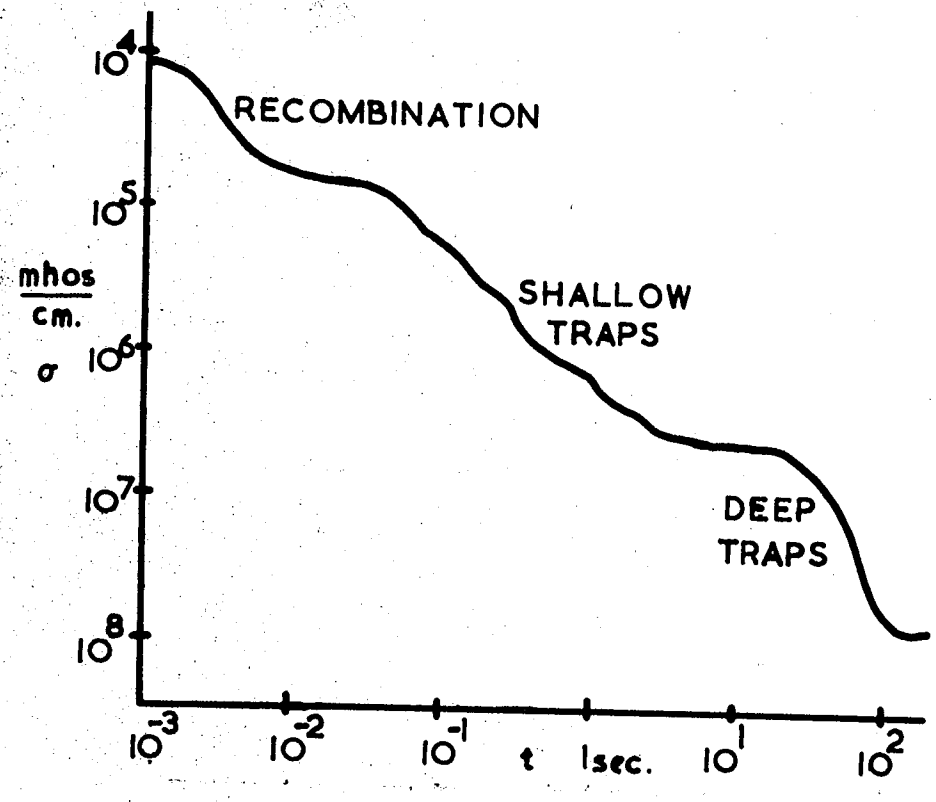

FIGURE 7.2

PHOTOCONDUCTIVE DECAY CURVE

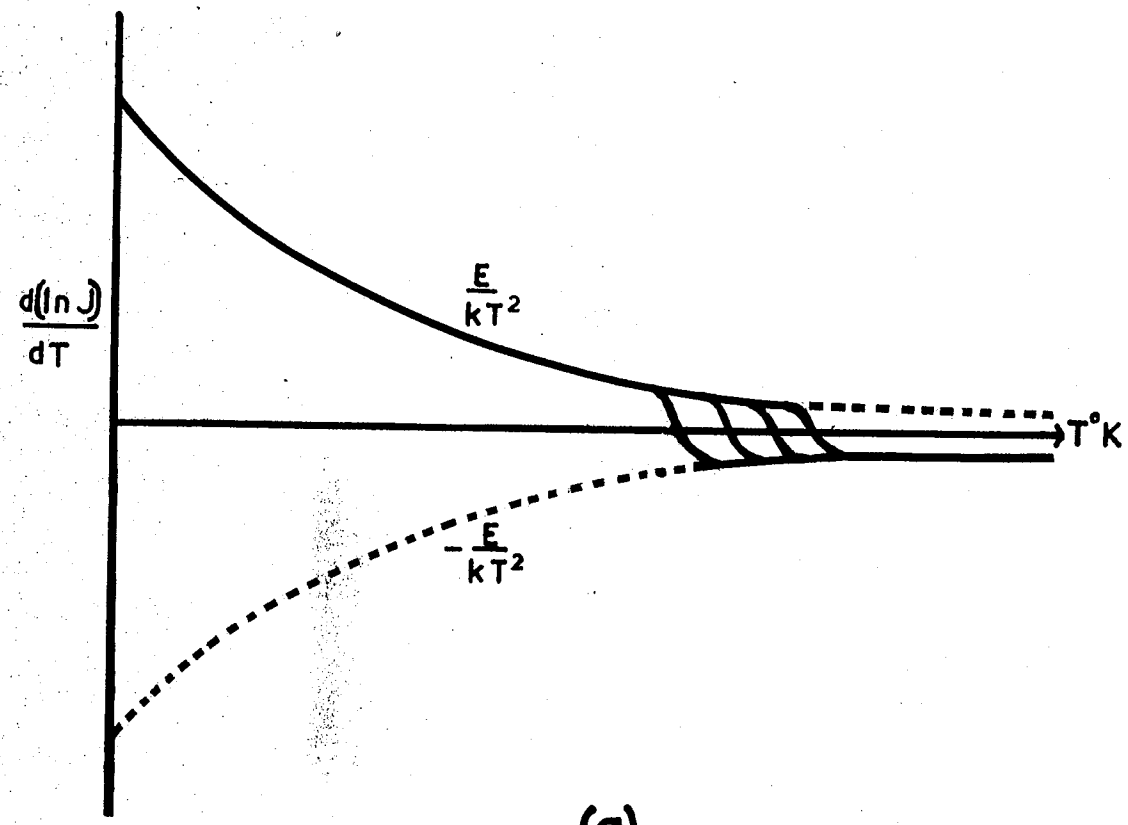

(a)

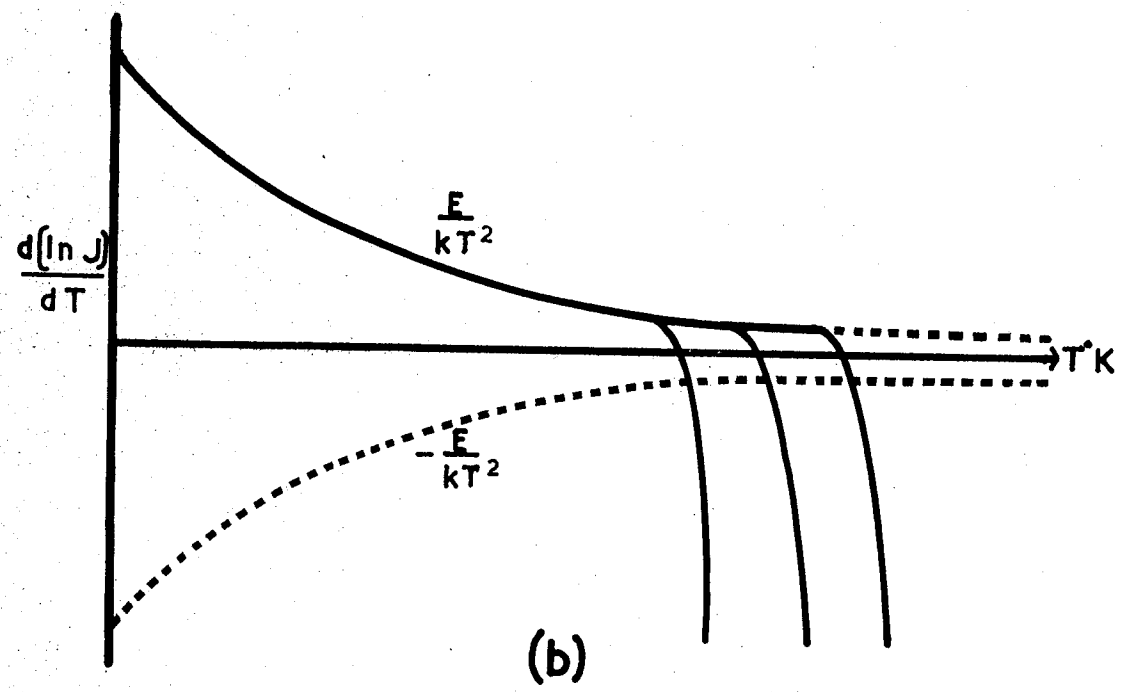

(b)

FIGURE 7.1

SCHON PLOTS

a MONOMOLECULAR KINETICS

b BIMOLECULAR KINETICS

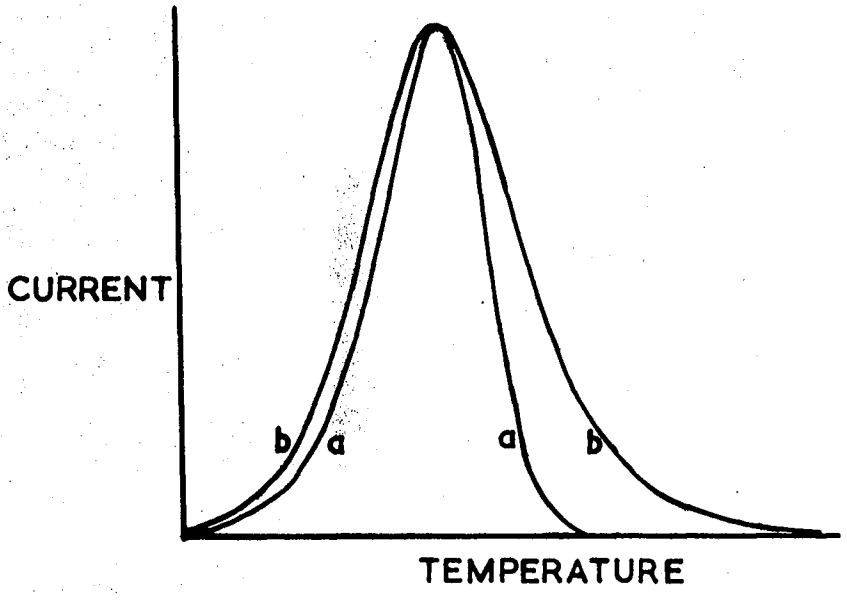

FIGURE 6·2

A COMPARISON OF THERMALLY STIMULATED CURRENT PEAKS PRODUCED UNDER MONOMOLECULAR AND BIMOLECULAR KINETICS (same E, S and β)

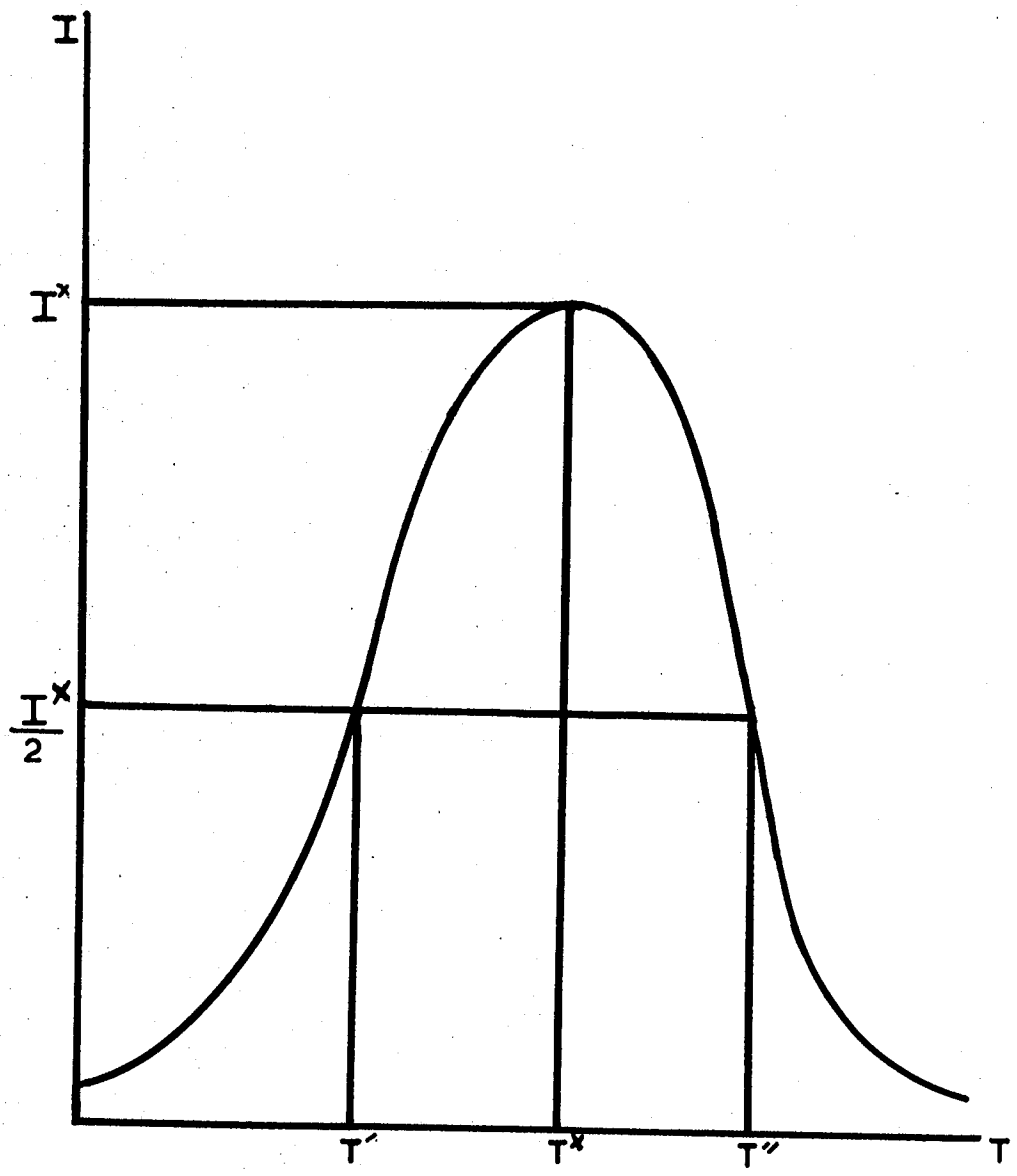

FIGURE 6.1

PARAMETERS OF A THERMALLY STIMULATED CURRENT PEAK

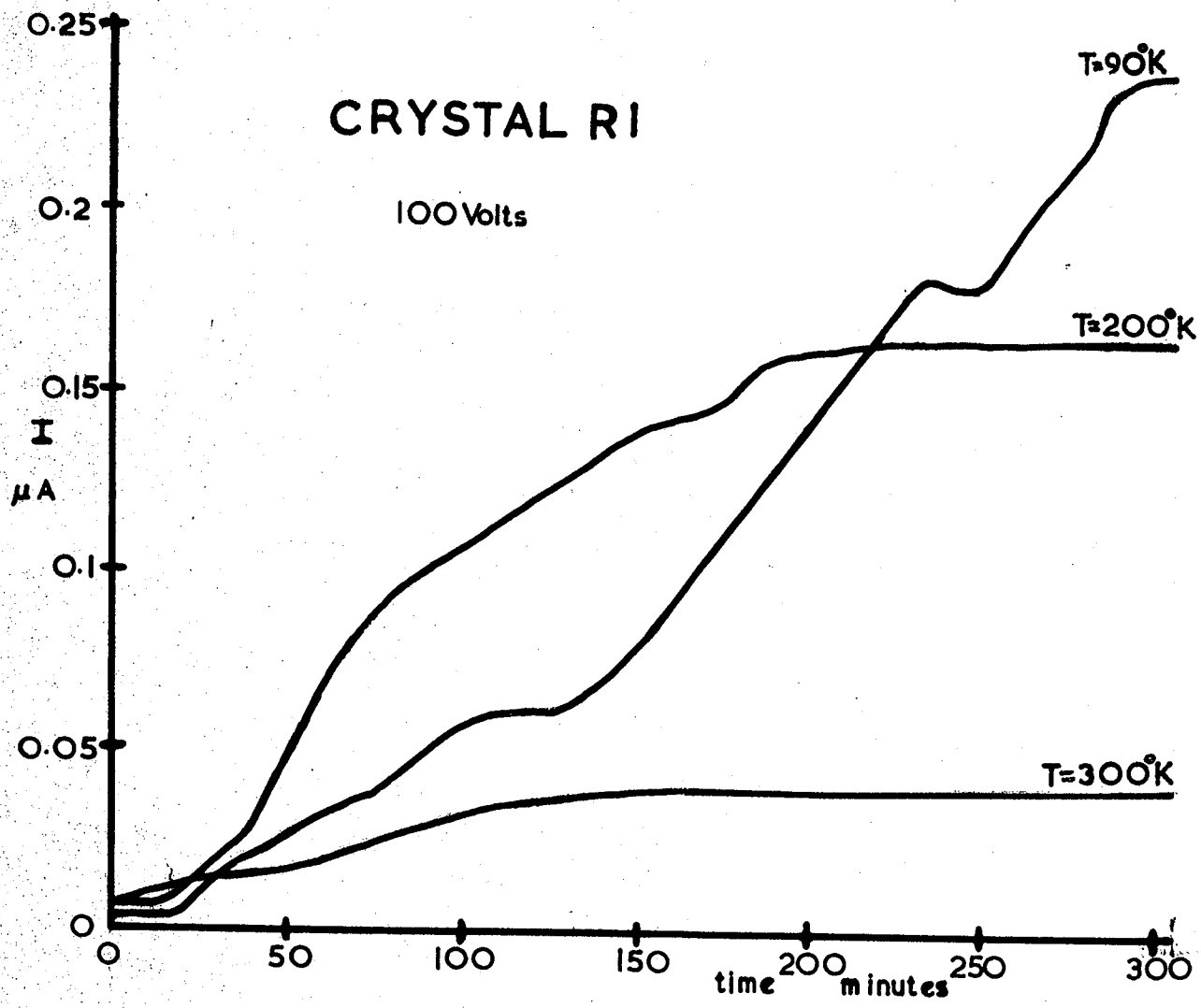

FIGURE 5.1

THE SLOW RISE OF PHOTOCURRENT

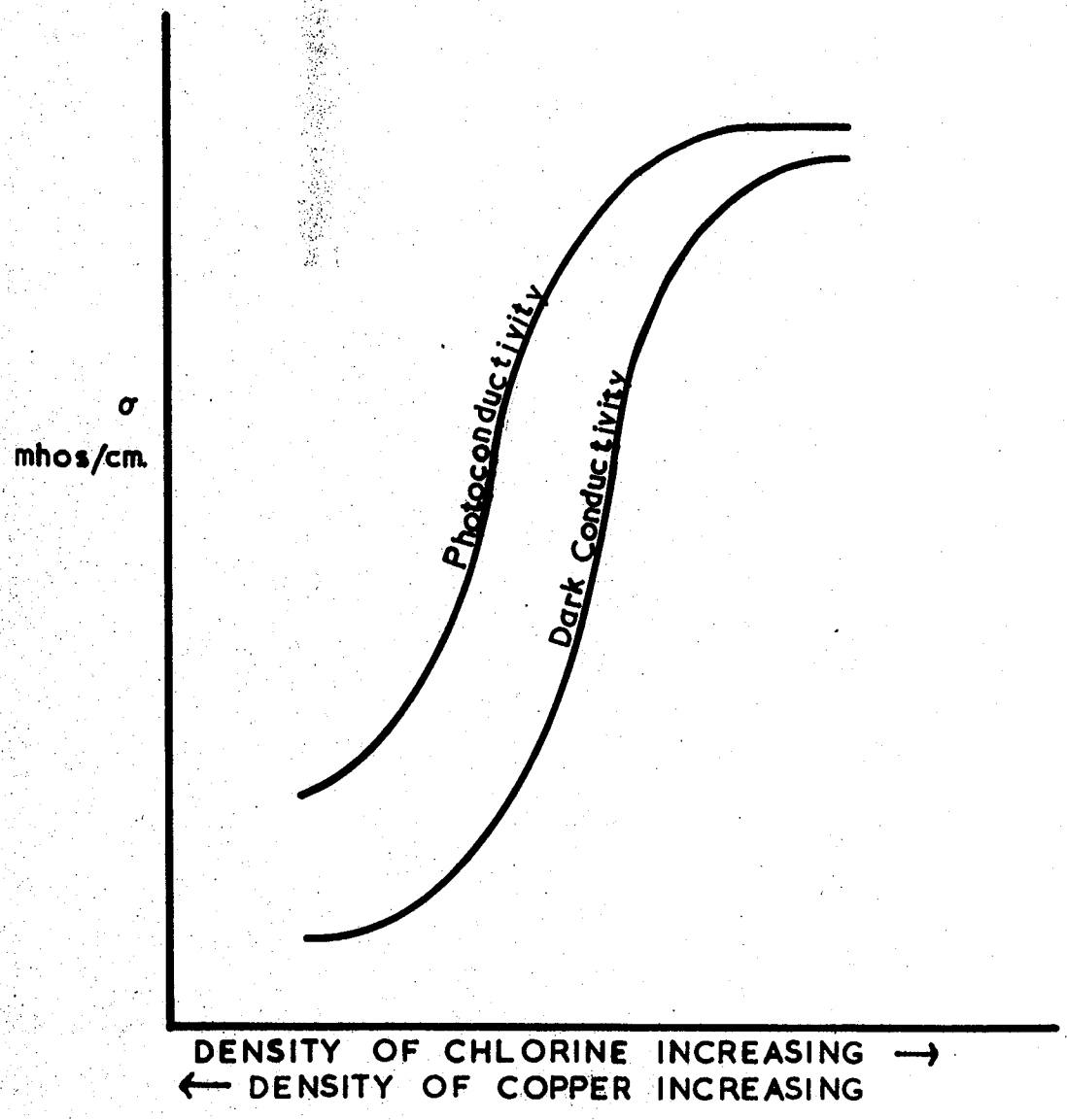

FIGURE 4.3

THE EFFECT OF IMPURITIES ON THE CONDUCTIVITIES OF CADMIUM SULPHIDE

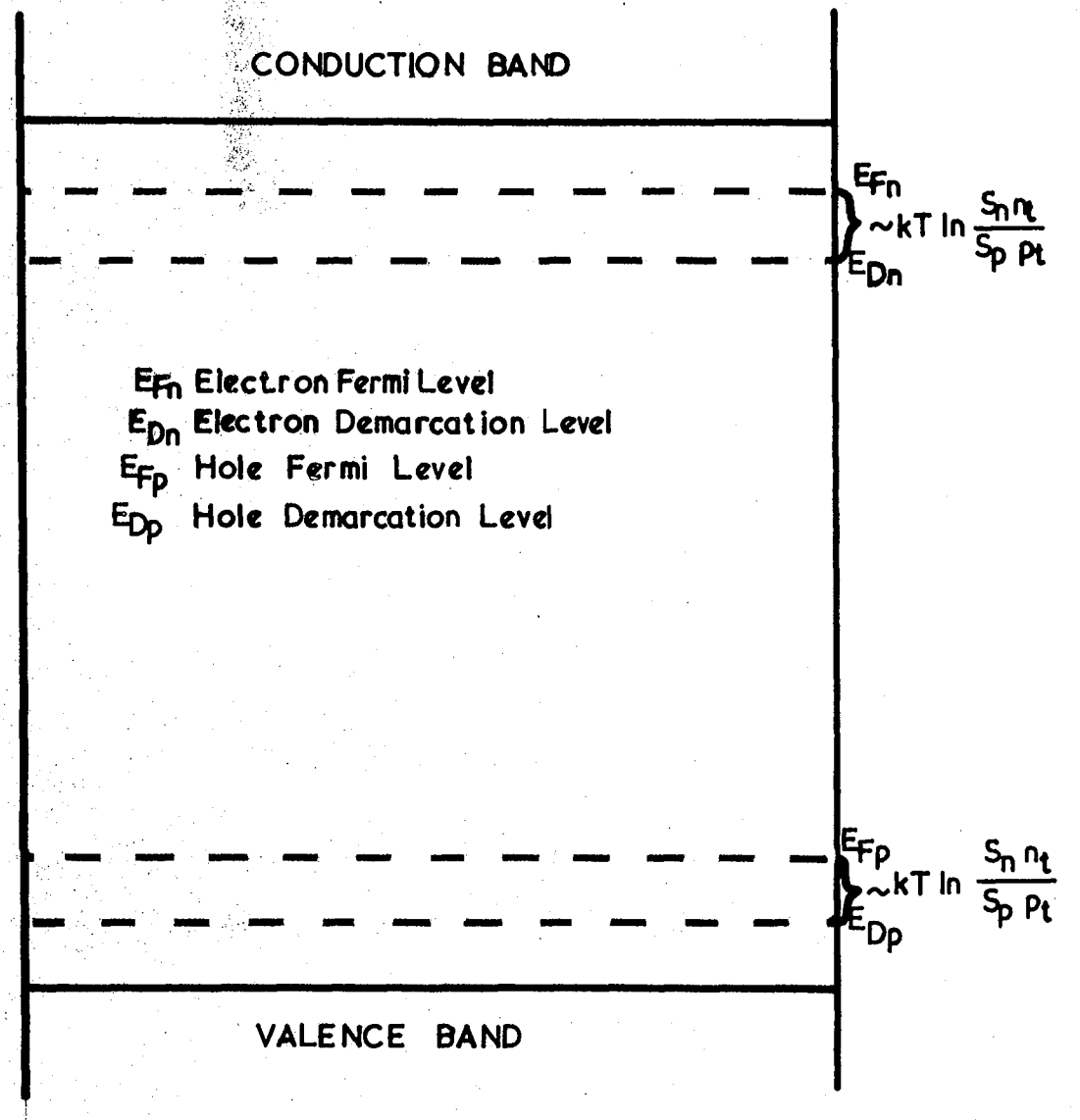

FIGURE 4.1

THE FERMI AND DEMARCATION LEVELS OF A SEMI-INSULATOR

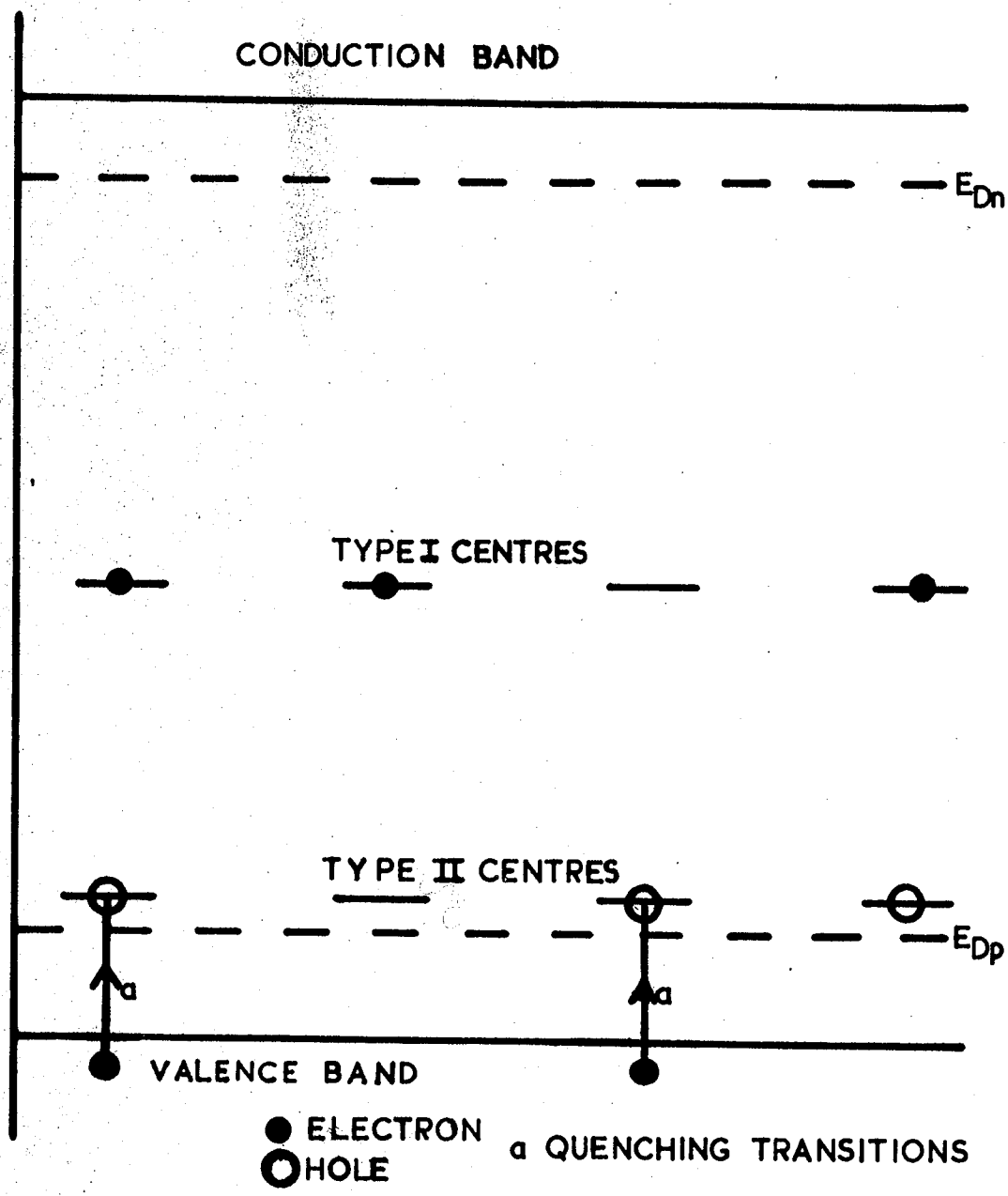

FIGURE 4.2

SENSITISING CENTRES IN CADMIUM SULPHIDE

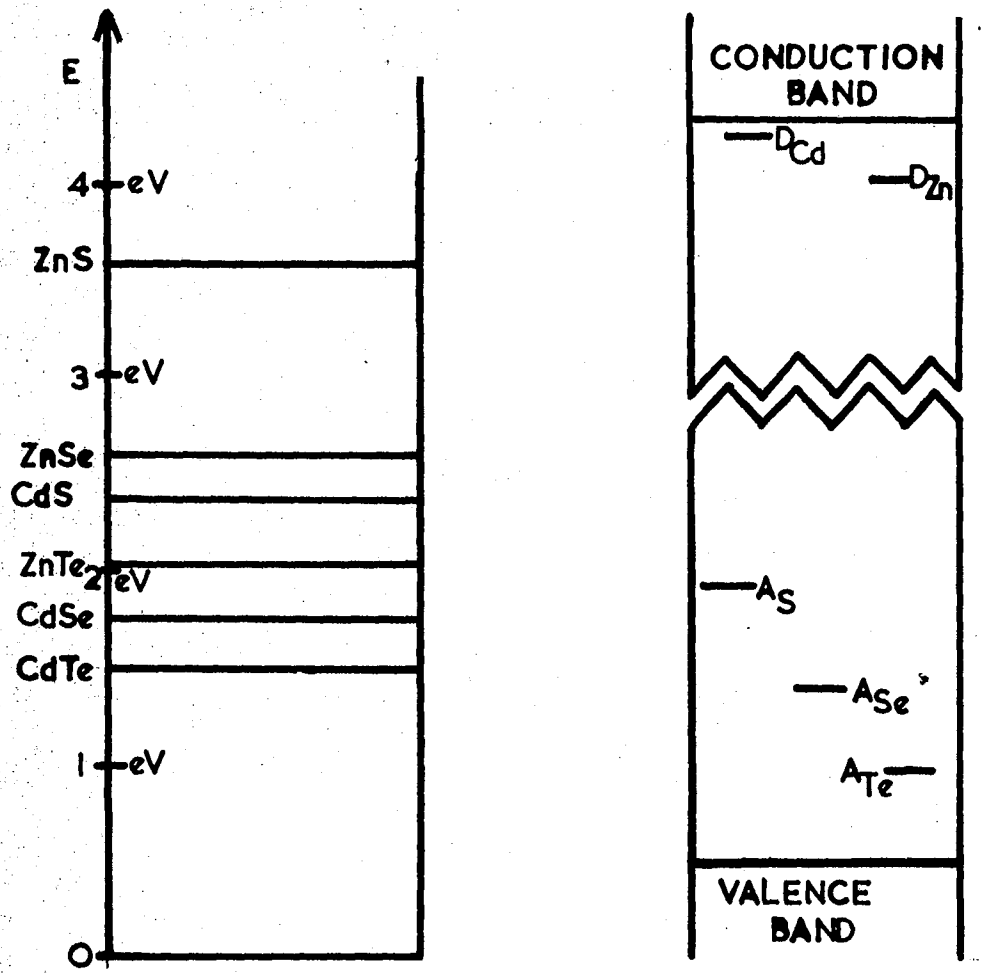

FIGURE 3.1

BAND GAPS AND DEFECT ENERGIES IN SOME WIDE BAND GAP II-VI COMPOUNDS

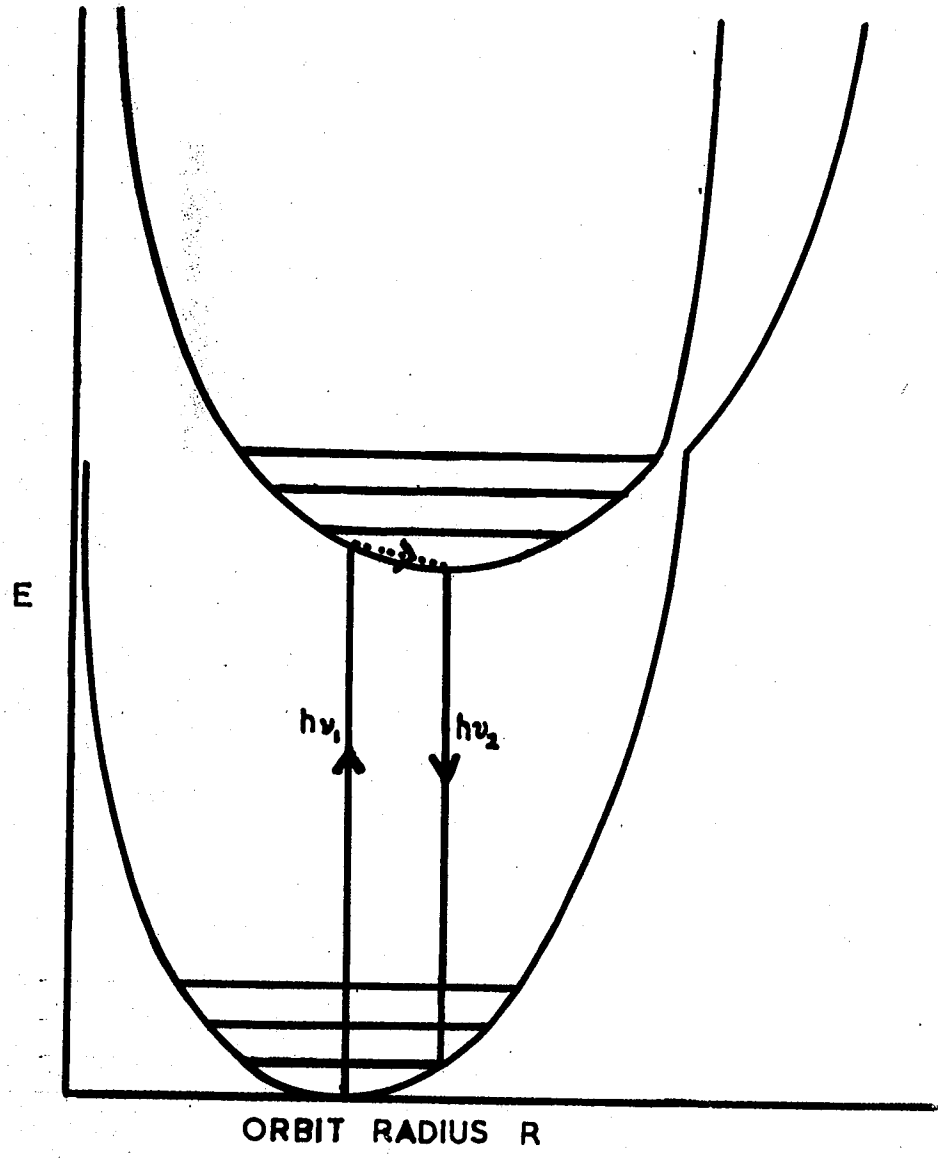

FIGURE 2.8

THE FRANCK–CONDON PRINCIPLE

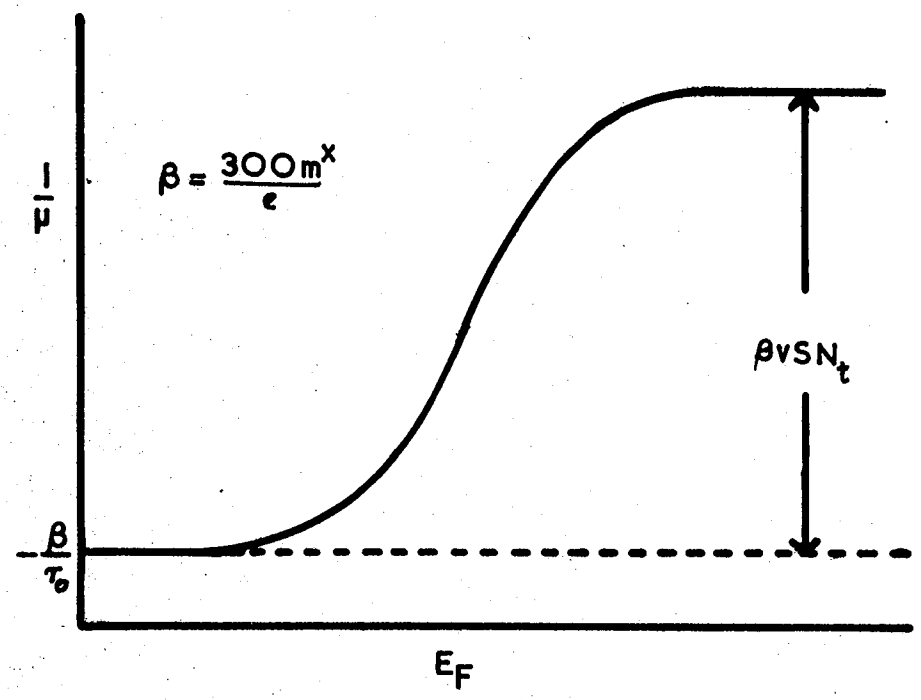

FIGURE 2.7

THE INTERPRETATION OF THE PHOTOHALL EFFECT

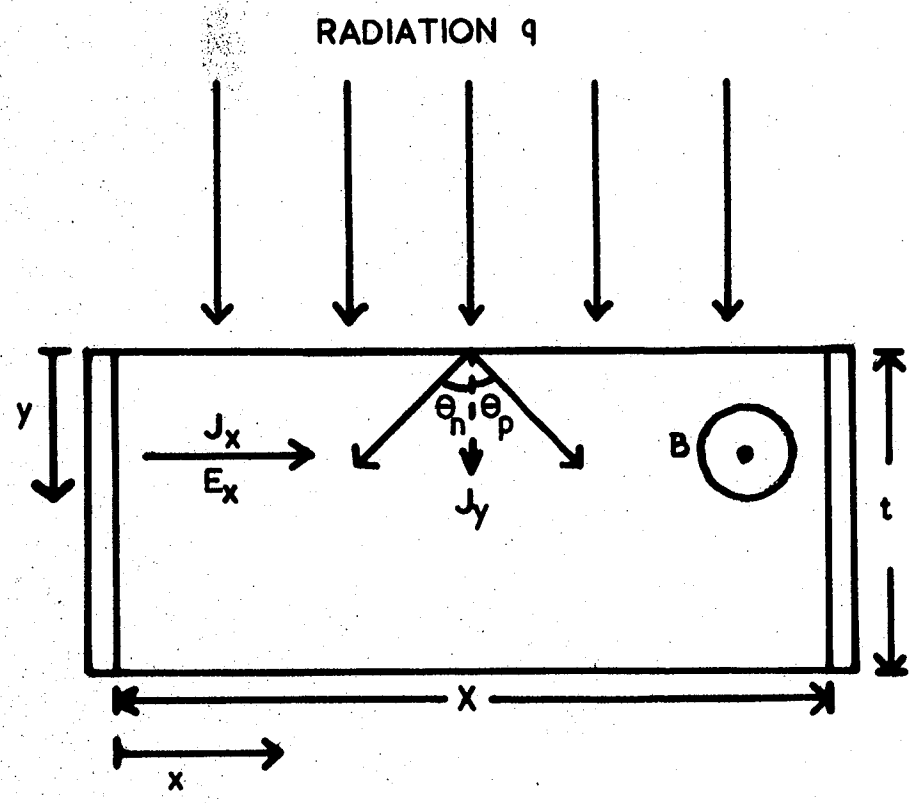

FIGURE 2·6

PHOTOELECTROMAGNETIC EFFECT

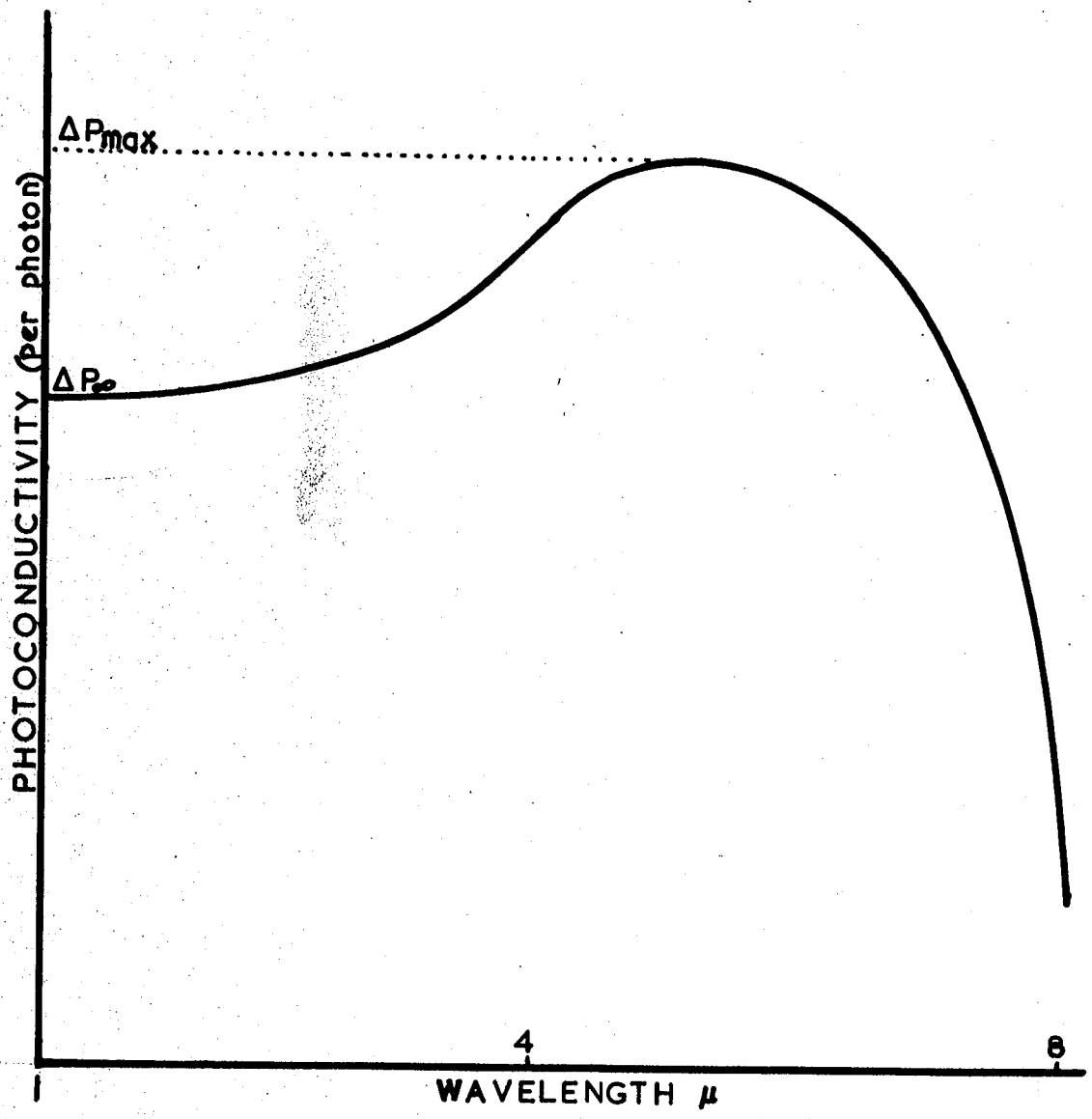

FIGURE 2.4

THE SPECTRAL SENSITIVITY OF A SEMICONDUCTOR (In Sb)

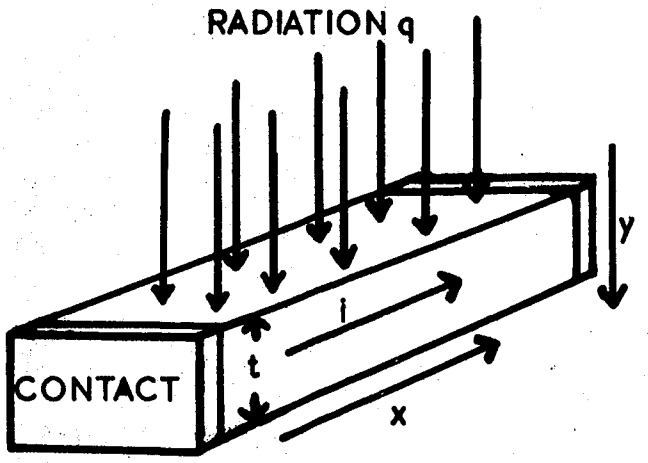

PHOTOCONDUCTIVITY

FIGURE 2.3

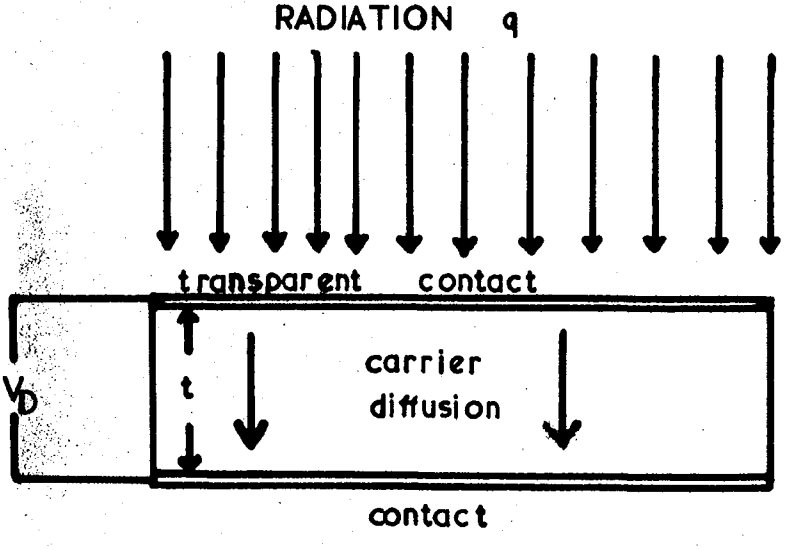

DEMBER EFFECT

FIGURE 2.5

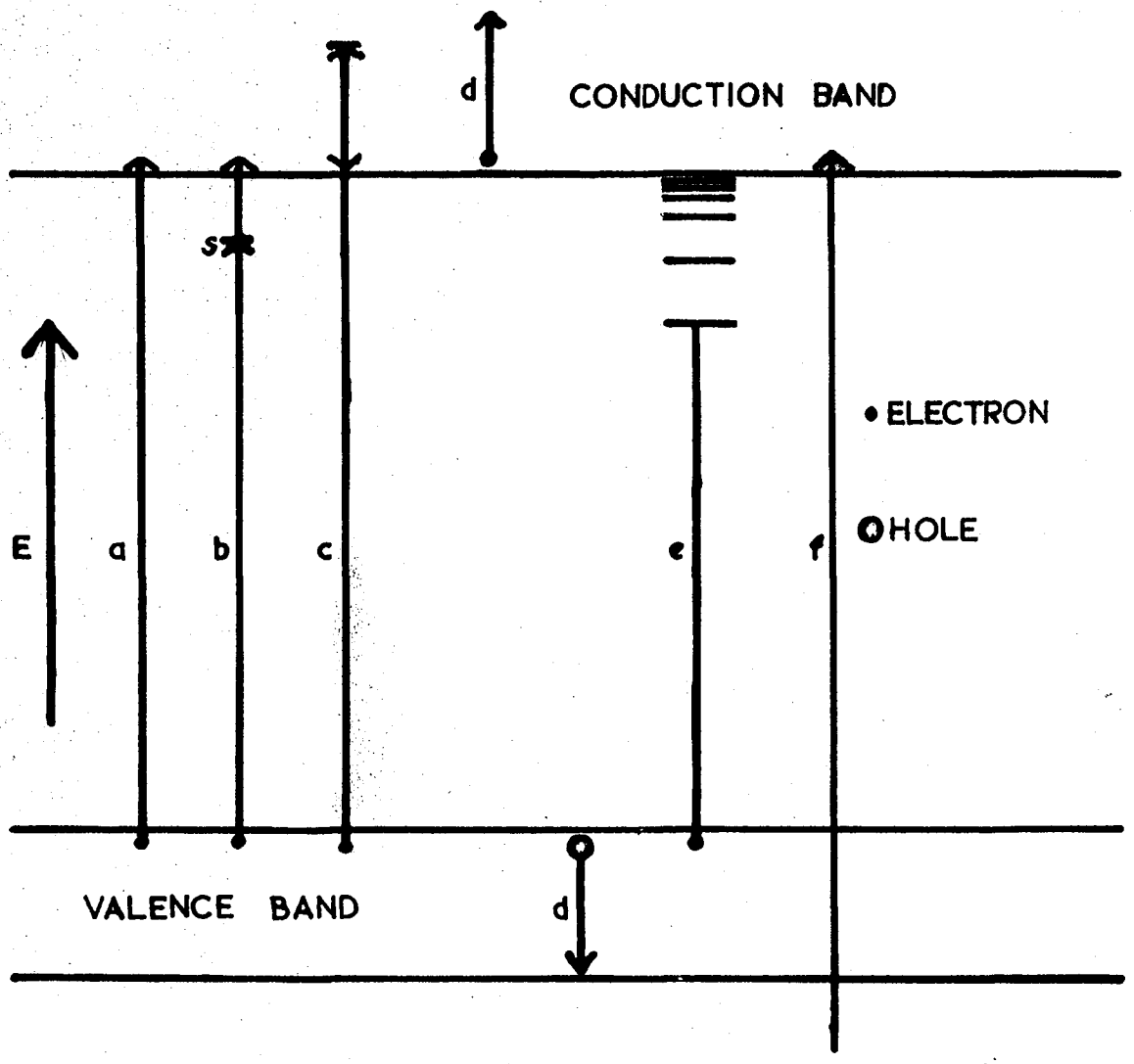

a Direct Band to Band Absorption
b Phonon Absorptive Indirect Absorption (see figure 2.1)
c Phonon Emissive Indirect Absorption
d Free Carrier Absorption
e Exciton Absorption
f Inner Shell Electron Absorption

FIGURE 2.2

THE ABSORPTION OF RADIATION IN AN INTRINSIC SEMICONDUCTOR

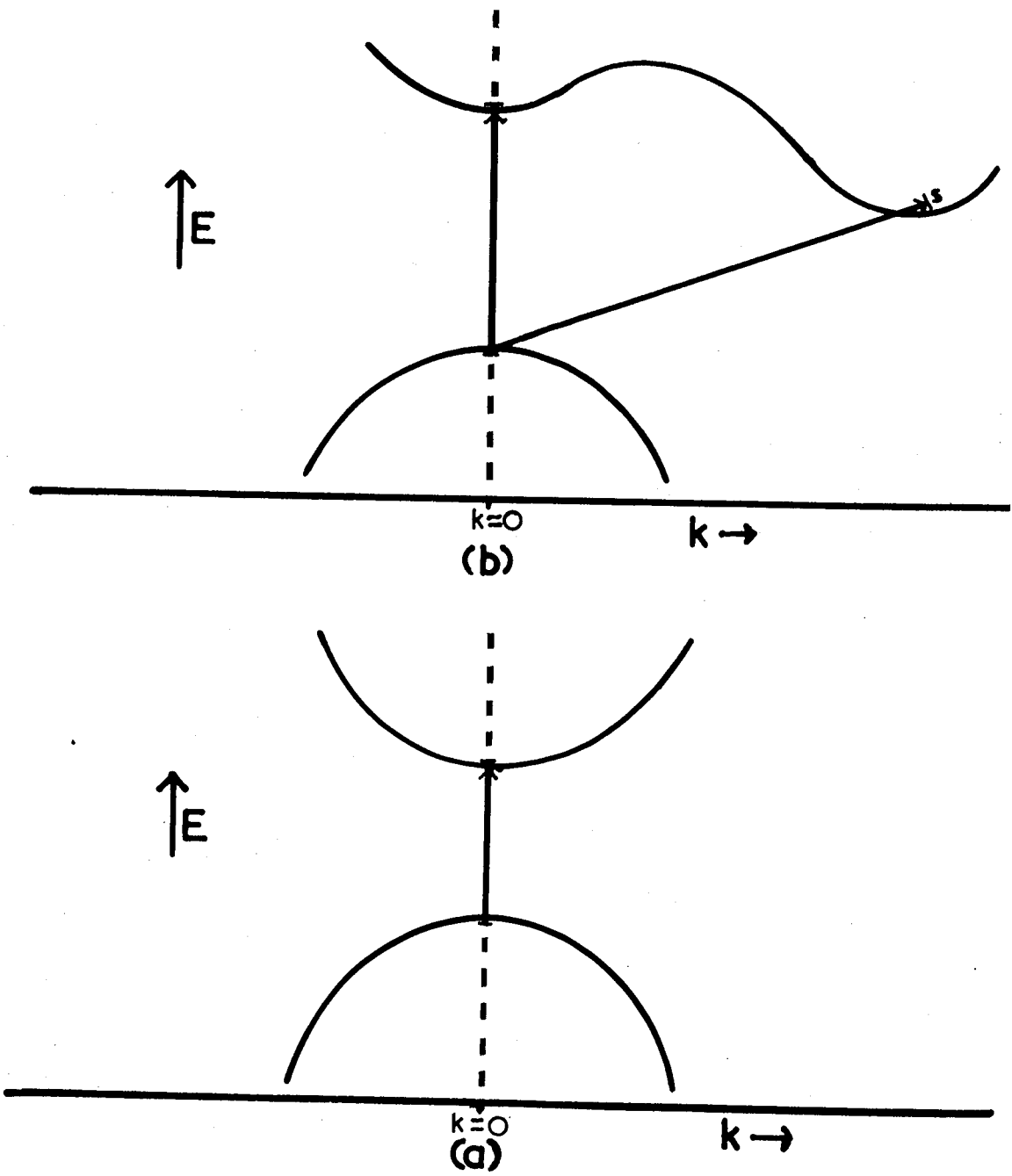

FIGURE 2.1

TYPICAL ENERGY BANDS

FOR A MANY-VALLEY SEMICONDUCTOR

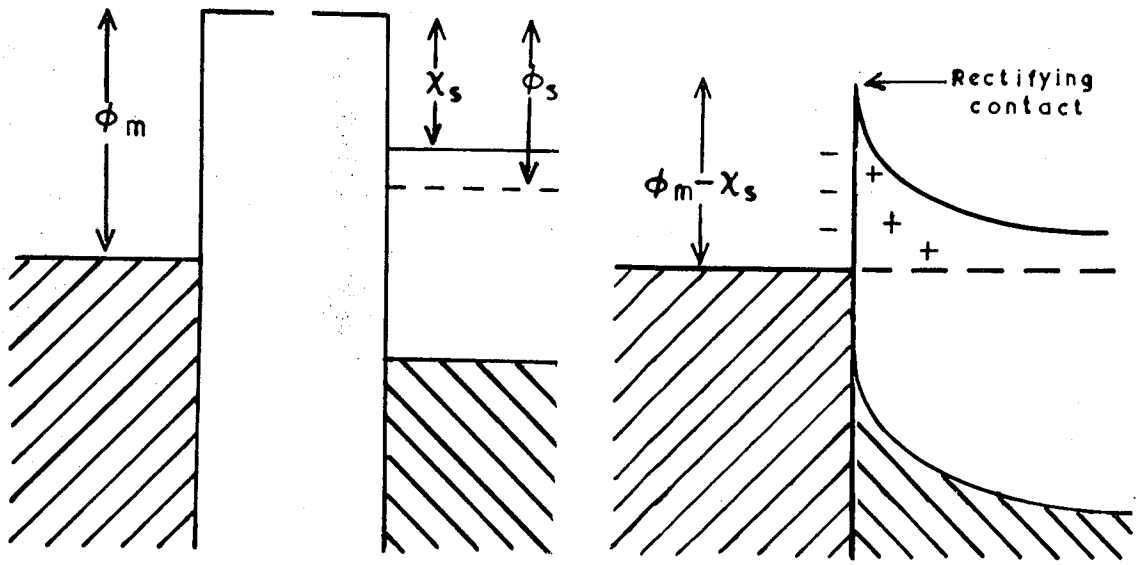

FIGURE 1.5

n-TYPE SEMICONDUCTOR – METAL CONTACTS

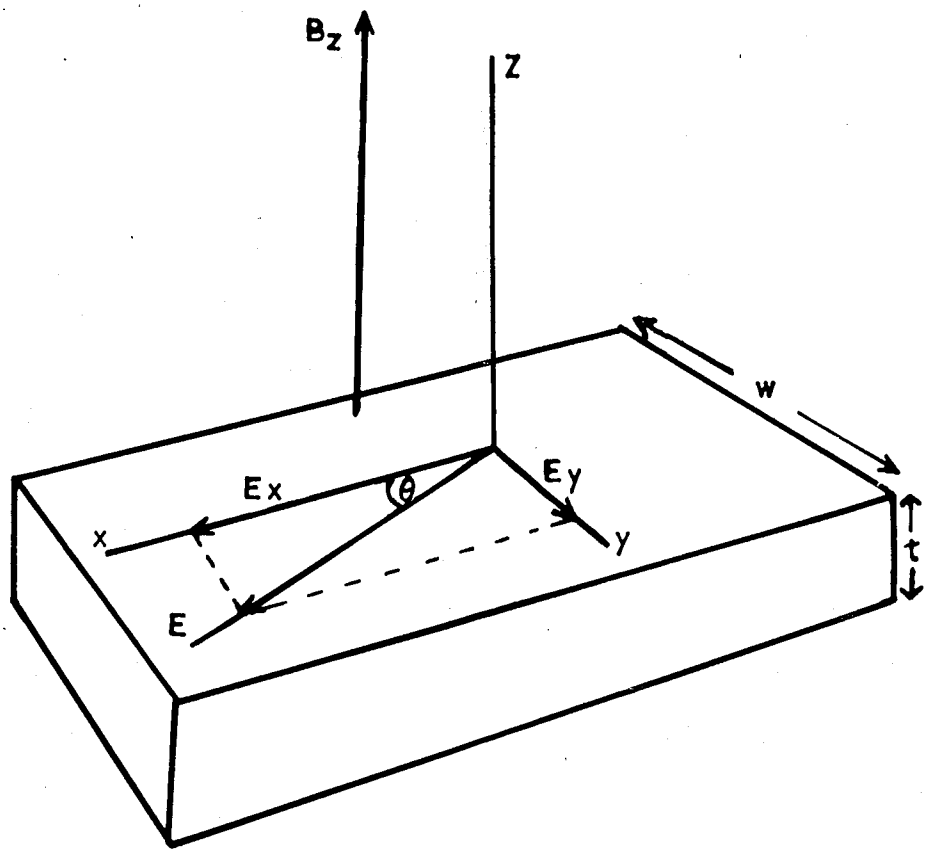

FIGURE 1.4

THE HALL EFFECT

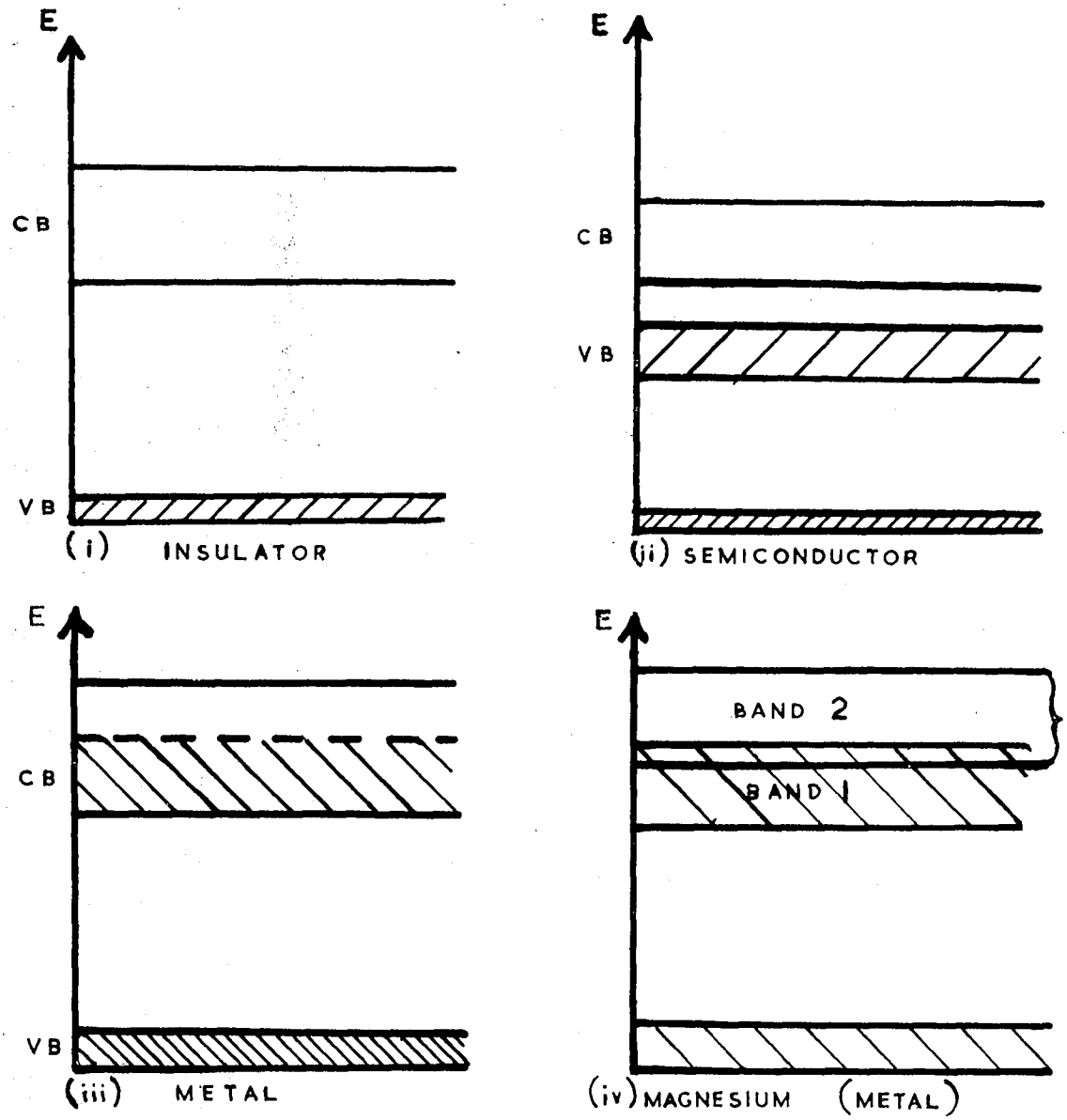

FIGURE 1.3

ELECTRON DISTRIBUTIONS IN SOLIDS

(SHADING INDICATES STATES FULL AT 0°K)

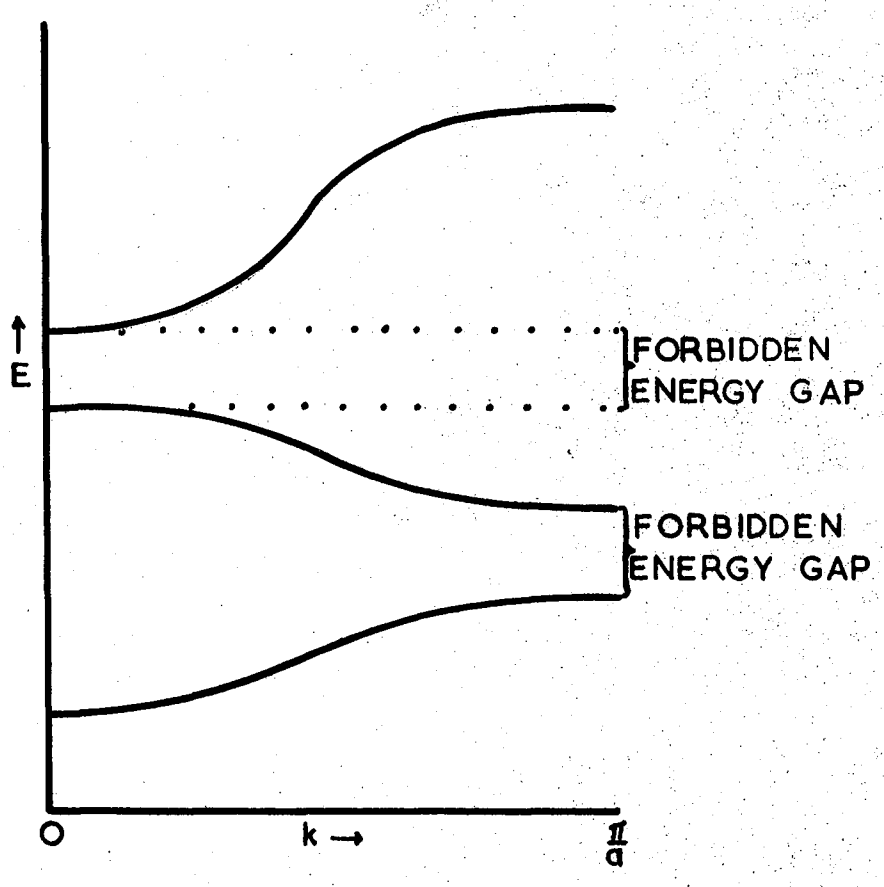

FIGURE 1.2

REDUCED REPRESENTATION OF

ENERGY BANDS

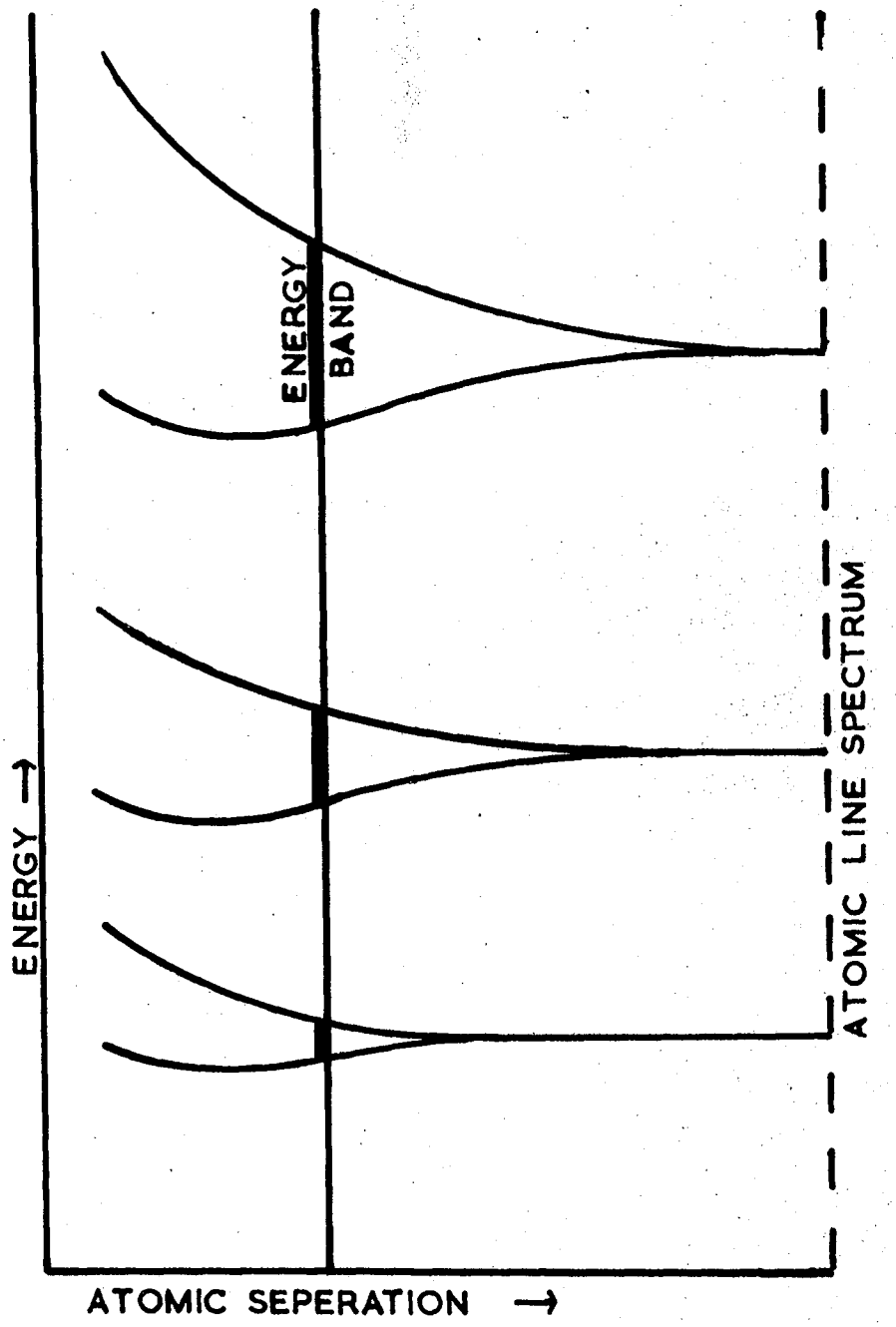

FIGURE 1.1

THE EFFECT OF LATTICE SPACING ON THE ELECTRONIC ENERGY LEVELS IN A CRYSTAL

TABLE 11.2 (0.41 eV)

Crystal	S4	S5	S2	S3	P2	$S3_V$	$S5_V$	V1	P3	P2	R1	$S2_V$	$S6_V$	Ave.
Conditions	a.l.	a.l.		a.l.	a.l.		a.l.	a.l.	a.l.	a.l.	a.l.		a.l.	a.l.
T*	260	270	270	270	280	280	290	320	320	330	340	370	300	300
E_B	0·49 ±0·01	0·49 ±0·01	0·41 ±0·01	0·53 ±0·01	N.M.	0·45 ±0·02	0·50 ±0·01	0·49 ±0·01	N.M.	N.M.	0·65 ±0·05	N.M.	N.M.	0·47 ±0·07
E_G	0·78 ±0·02	0·95 ±0·10	≈0·86	0·83 ±0·06 0·42 ±0·08	0·46 ±0·04	N.M.	0·82 ±0·03	0·42 ±0·03	0·58 ±0·04	0·70 ±0·20	0·72 ±0·04	N.M.	0·93 ±0·03	0·42 ±0·03
E_L	0·64 ±0·04	0·75 ±0·02	≈0·74	0·26 ±0·06 0·40 ±0·08 POOR	0·41 ±0·02	N.M.	0·75 ±0·10	0·76 ±0·44	0·48 ±0·03	≈0·28 POOR	0·80 ±0·07	N.M.	0·84 ± 0·04	0·44 ±0·03
E_{FK}	0·57 ±0·04	0·70 ±0·02	≈0·68	0·25 ±0·01 0·40 ±0·09 POOR	0·37 ±0·03	N.M.	0·76 ±0·10 POOR	BAD	≈0·45 POOR	BAD	0·78 ±0·07	N.M.	0·80 ± 0·09	0·41 ±0·08
E_{HB}	0·87 ±0·06	0·70 ±0·15	N.M.	≈0·85 ≈0·45	0·44 ±0·05	N.M.	0·84 ±0·03	0·37 ±0·05 POOR	N.M.	0·80 ±0·20	N.M.	N.M.	0·94 ±0·04	0·44 ±0·05
E_{GG}	0·41 ±0·01	0·39 ±0·03	0·45 ±0·04	0·42 ±0·02	0·21 ±0·02 POOR	0·42	0·75 ±0·10 POOR	0·39 ±0·01	0·46 ± 0·02	N.M.	0·45 ±0·04	0·48 ±0·02	0·83 0·40 ±0·04 ±0·01	0·41 ±0·01
E_{HR}	0·7 ±0·1	0·76 ±0·15	N.M.	0·49 ±0·05	0·5 ±0·2	0·8 ±0·1	0·5 ±0·1	0·47 ±0·06	N.M.	0·4 ±0·1	N.M.	N.M.	0·8 ± 0·2	0·47 ±0·07
E_{HA}	1·0 ±0·2 POOR	0·45 ±0·25 POOR	N.M.	BAD	0·6 ±0·2	0·78 ±0·09	0·82 0·44 ±0·03 ±0·02	JOINT GRAPHS WITH $S6_V$	N.M.	0·53 ±0·15	N.M.	N.M.	0·3 ±0·2 POOR	0·44 ±0·01
E_τ	0·40 ±0·04	N.M.	≈0·8	0·45 ±0·04	0·41 ±0·02	N.M.	0·80 0·48 ±0·05 ±0·05	N.M.	N.M.	0·78 ±0·03	N.M.	N.M.	0·44 ±0·03	0·42 ±0·02
S_G	N.M.	N.M.	N.M.	2×10^{-20}	3×10^{-20}	N.M.	N.M.	5×10^{-22}	2×10^{-19}	N.M.	N.M.	N.M.	N.M.	10^{-20}
S_τ	7×10^{-21}	N.M.	N.M.	3×10^{-21}	6×10^{-21}	N.M.	N.M.	N.M.	N.M.	N.M.	N.M.	N.M.	10^{-22}	5×10^{-21}